Decreasing Bladed Disk Response with Dampers on a Few Blades: Optimization Algorithms, Linear and Nonlinear Applications

by

Raghavendra Narasimha Murthy

A Dissertation Presented in Partial Fulfillment
of the Requirements for the Degree
Doctor of Philosophy

Approved November 2012 by the
Graduate Supervisory Committee:

Marc Mignolet, Chair
Subramaniam Rajan
Jeff Lentz
Aditi Chattopadhyay
Hanqing Jiang

ARIZONA STATE UNIVERSITY

December 2012

ABSTRACT

The focus of this investigation is on the optimum placement of a limited number of dampers, fewer than the number of blades, on a bladed disk to induce the smallest amplitude of blade response. The optimization process considers the presence of random mistuning, i.e. small involuntary variations in blade stiffness properties resulting, say, from manufacturing variability. Designed variations of these properties, known as intentional mistuning, is considered as an option to reduce blade response and the pattern of two blade types (A and B blades) is then part of the optimization in addition to the location of dampers on the disk.

First, this study focuses on the formulation and validation of dedicated algorithms for the selection of the damper locations and the intentional mistuning pattern. Failure of one or several of the dampers could lead to a sharp rise in blade response and this issue is addressed by including, in the optimization, the possibility of damper failure to yield a fail-safe solution. The high efficiency and accuracy of the optimization algorithms is assessed in comparison with computationally very demanding exhaustive search results.

Second, the developed optimization algorithms are applied to nonlinear dampers (underplatform friction dampers), as well as to blade-blade dampers, both linear and nonlinear. Further, the optimization of blade-only and blade-blade linear dampers is extended to include uncertainty or variability in the damper properties induced by manufacturing or wear. It is found that the optimum achieved without considering such uncertainty is robust with respect to it.

Finally, the potential benefits of using two different types of friction dampers differing in their masses (A and B types), on a bladed disk are considered. Both A/B pattern and the damper masses are optimized to obtain the largest benefit compared to using identical dampers of optimized masses on every blade. Four situations are considered: tuned disks, disks with random mistuning of blade stiffness, and, disks with random mistuning of both blade stiffness and damper normal forces with and without damper variability induced by manufacturing and wear. In all cases, the benefit of intentional mistuning of friction dampers is small, of the order of a few percent.

To my parents B N Narasimha Murthy and Manjula N Murthy,

& my sister Brinda N Murthy

ACKNOWLEDGEMENTS

I would like to thank, first and foremost, my advisor Dr. Marc Mignolet for his patient guidance and continuous support throughout this project, and my study at Arizona State University.

I would also like to thank Dr. Aditi Chattopadhyay, Dr. Hanqing Jiang, Dr. Subramaniam Rajan, and Mr. Jeff Lentz, for their participation and willingness to serve as members of my graduate supervisory committee.

The support of this work by the GUIde Consortium is gratefully acknowledged. In addition, I would also like to thank Professor C. Pierre, Dr. M. P. Castanier, and Dr. R. Bladh from the University of Michigan, for the use of both REDUCE and the blisk example geometry.

The invaluable collaboration of Dr. Javier Avalos, and the encouragement and support of Dr. Xiaoquan Wang, Dr. Ricardo Perez, and Mr. Andrew Matney is much appreciated. Thanks also go out to the ASU Advanced Computing Center (A2C2) whose Saguaro computing cluster proved invaluable for the large number of simulations carried out in this work.

TABLE OF CONTENTS

Page

LIST OF TABLES

LIST OF FIGURES

Figure Page

Figure Page

Figure Page

Figure Page

Figure Page

1 – INTRODUCTION

1.1 Motivation

Increasing the high cycle fatigue life of blades typically implies reducing the amplitude of their response in some particular resonant condition. A standard approach to achieving this reduction is to increase blade damping through dedicated devices such as underplatform dampers. However, blade designs that do not exhibit platforms, e.g. impellers and blisks, cannot typically benefit from such dampers and one may then have to rely on more complex and expensive damper solutions, such as coatings, constrained layers, etc. which have been proposed in the past. To mitigate the cost of following this approach, Avalos and Mignolet [1] assessed the possibility of damping the response of the disk using dampers on only a fraction of the blades on the disk. They demonstrated that dampers positioned on well-chosen blades could indeed notably reduce the response of the entire bladed disk. However, the effect of random mistuning, small variations in the blade properties occurring due to manufacturing or in-service wear, may be quite detrimental by localizing the response and preventing the flow of energy around the disk to the dampers. In such cases, it was found that introducing intentional mistuning using 2 different types of blades, denoted as A and B, increases the robustness to random mistuning of the bladed disk with a few dampers. However, for either of these strategies, i.e. dampers on a few blades with or without A/B intentional mistuning, it is of key importance to optimize the locations of the dampers and, as appropriate, the intentional mistuning pattern for these methods to be effective.

Since the focus of [1] was on introducing and assessing the concepts, a "brute force" optimization strategy was adopted in which all combinations of damper locations and intentional mistuning patterns were considered. The best one was then simply identified as the one giving the smallest maximum blade response on the disk. Such an approach, referred to in the sequel as the "exhaustive search", is however not feasible in practice as the optimization problem is combinatorial in nature, i.e. the number of cases to be considered grows near exponentially with the number of blades on the disk. Moreover, the dampers considered in [1] were assumed to be:

(i) linear while in fact novel dampers proposed in the literature often exhibit a definite/strong nonlinearity e.g. coatings, impact dampers, and particle dampers; see [2] for a nonlinear modeling of coatings. Further, the hard nonlinearity of friction dampers is well recognized, see [28-35].

(ii) pure dashpots, i.e. the model ignored any stiffness component that may be present in the damper model which induces an intentional mistuning effect when dampers are present on blades. This issue would be encountered for a series of damper designs, such as constrained layer systems, e.g. see [3-6], as well as coatings, see [2, 7-10].

(iii) acting on single blade, i.e. blade-alone dampers. Such an assumption is not appropriate for example with friction dampers which typically couple two consecutive blades.

(iv) all identical with well-established properties. However, uncertain variations in these properties from one damper to another are expected due

to in-service wear and/or manufacturing limitations, e.g. variations in thickness of coatings, differences in mass of friction dampers.

Accordingly, the focus of the present investigation is on extending the work of [1] by:

(1) introducing dedicated, fast optimization algorithms for the selection of the damper locations and, when appropriate, intentional mistuning pattern leading to the smallest amplitude of blade response on the disk,

(2) extending the optimization algorithm of (1) to allow for a nonzero probability of failure of the dampers to achieve a fail-safe damper placement strategy,

(3) assessing the sensitivity of the optimum damper placement, intentional mistuning pattern (as necessary), and performance to uncertainty on the damper properties, and

(4) validating the concepts on linear blade-blade dampers as well as dampers with nonlinear characteristics.

Chapters 2 and 3 of this document are focused on the development and validation of dedicated optimization algorithms, i.e. objectives (1) and (2) above, focusing on linear blade-only dampers. Chapter 4 then focuses on the application of the optimization algorithms developed in Chapter 2 to nonlinear dampers (more specifically to underplatform friction dampers) as well as to the consideration of blade-blade dampers, linear or nonlinear. Additionally, the optimization of blade-only and blade-blade linear dampers is extended to include uncertainty/variability in the damper properties that arise during the

manufacturing and/or in-service. It is found that the optimum achieved without considering such uncertainty/variability is robust with respect to this uncertainty.

Finally, Chapter 5 investigates the potential benefits resulting from using two different types of friction dampers on a bladed disk, i.e. intentional mistuning using friction dampers. In this scenario, every blade or platform is equipped with a damper of either type A or type B, with these two types differing in their masses. The benefit of this strategy is measured in comparison to using identical dampers of optimized mass on every blade/platform, and is dependent on the pattern of A/B dampers around the disk as well as the damper masses. It is accordingly desirable to optimize both the pattern and the damper masses to obtain the largest benefit. As a discovery effort, this optimization is accomplished here through an exhaustive search for all patterns and on a large grid of values of the two damper masses. Owing to the large computational cost of this effort, only single degree of freedom per blade models are assumed with both blade-blade and blade-ground dampers and only small blade counts are considered (6 and 12 blade models). Three particular situations are considered: disks tuned except for the arrangement of A/B dampers, disks that also exhibit random mistuning of the blades' stiffness, and, finally, disks exhibiting random mistuning of both blades' stiffness and of the normal forces of the dampers. This latter situation is considered to include the variability induced by manufacturing and wear. In all cases considered, the benefit of this intentional mistuning of friction dampers is either zero or small, of the order of a few percent, consistently with a single data point reported in the literature, see [48].

1.2 Cyclic Symmetry, Unintentional and Intentional Mistuning

Bladed disks found in turbomachinery rotors have the property of rotational symmetry, i.e. a rotation of the system by an angle $n\varphi_0$ will leave the system unchanged, where $\varphi_0 = \frac{2\pi}{N}$ and N is the number of blades in the system. The modes of vibration of such a system consist of constant amplitude harmonic waves travelling forward and backward around the disk. The amplitude of vibration of two different blades at a certain resonance will be equal but will be out of phase with each other. Such a system is called a tuned system, and a series of analyses of a single sector can be used to obtain all the information that can be got from an analysis of the complete assembly (see [37]).

However, manufacturing variability and in-service wear leads to small difference in blade to blade properties of these bladed disk systems. These small variations of the geometrical and structural properties of blades (e.g. mass, stiffness, natural frequencies, and mode shapes) are known as unintentional or random mistuning. Although this random mistuning may be relatively "small" (of the order of a few percent), it has been shown in the literature (see [38-42]) that the effect of these small variations on the forced response of the blades can be quite large, and can lead to a localization of the response on a few blades, whose amplitude of response would then be much larger than their tuned counterparts. This increase in response can lead to a significant decrease in the fatigue life of bladed disks. Since the presence of random mistuning also results in the breaking

of the symmetry of the structure, a sector analysis can no longer be used, and the fully assembled structure will have to be analyzed.

In order to mitigate the undesirable effect of random mistuning, it has been proposed to intentionally design bladed disks not to be tuned, see [14]. The term intentional mistuning is typically used to refer to such a bladed disk design. It has been shown that intentionally mistuning a bladed disk can reduce the magnification of the forced response due to unintentional mistuning. Typically, the introduction of intentional mistuning would involve two types of blades with significant differences in properties (e.g. A and B blades with $+5\%$ and -5% difference in stiffnesses or Young's modulus when compared to the tuned stiffness) arranged in some, perhaps harmonic pattern around the bladed disk.

2 – FORMULATION AND VALIDATION OF DEDICATED OPTIMIZATION ALGORITHMS

2.1 Bladed Disks Considered

The optimization problem characteristics and algorithms discussed and implemented here are valid for any bladed disk model and any damper design, e.g. a full finite element model or reduced order model, with blade-alone or blade-blade, linear or nonlinear dampers. Here, their exemplification is carried out on the two bladed disk models shown in Figure 1 and Figure 2. More specifically, the parameters of the single degree of freedom per sector model of Figure 1 were selected to be $k_t = 430300\ N/m$ (the tuned or baseline value of the blade stiffness k_j), $c = 0.143\ Ns/m$ (leading to a damping ratio of approximately 0.1% on all modes), and $m = 0.0114\ kg$. Further, the blade to blade coupling stiffness was chosen to be $k_c = 10000\ N/m$ which falls within the transition of weak to strong coupling in which regime the peak of the response amplification due to mistuning occurs. Finally, the disk was assumed to support $N = 12$ blades in all computations.

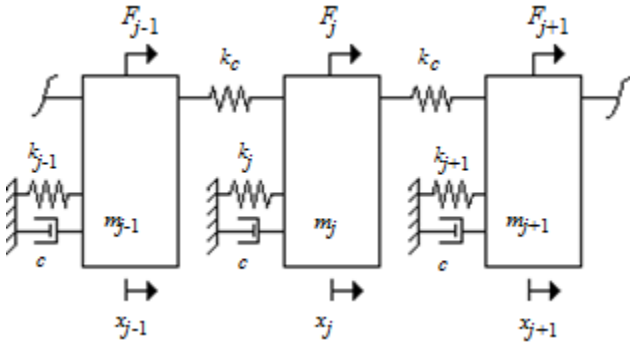

Figure 1. Single degree of freedom per sector bladed disk model (all m_j are equal)

Equally considered was the REDUCE reduced order model (see [11]) of the blisk shown in Figure 2. Note that this model is a modification of the one considered in [12], obtained by reducing of the number of blades from 24 to 12. This reduced order modeling technique is based on a component mode approach. The disk motions are described by the finite element modes of the disk with massless blades, and the blade motions are described by the summation of the blade deflections of these disk modes plus the finite element cantilever blade modes with the blade fixed at the disk-blade interface. The first 8 cantilevered blade modes and a set of 60 disk modes were selected to build the reduced order model which thus involved $60 + 12 * 8 = 156$ degrees of freedom. The damping in the bladed disk was assumed to be structural damping providing a damping ratio of approximately 0.1% on the modes of interest. Further, each blade was subject to two forces of unit magnitude, one in the axial direction and the other in the tangential direction at a 30 degree phase angle to the axial one at a node on the blade tip. Both of these forces exhibited the same frequency which was swept in the range of $[4775, 7958]Hz$ and the distribution of the force magnitudes around the disk was assumed in the form of engine orders 1 or 2. Finally, for simplicity, the response of each blade was quantified by the 2-norm of the 8 corresponding generalized coordinates of the reduced order model. The consideration of a different measure of the blade response (e.g. norm of the physical displacements, maximum response, or maximum stress) is readily accomplished.

The consideration of specific resonances in the blisk example was guided by the blade disk coupling index (see [1, 13]). This index is defined as

$$ci = 1 - \frac{\omega_r(1+\delta E) - \omega_r(1)}{(\sqrt{1+\delta E} - 1)\omega_r(1)} \tag{1}$$

where $\omega_r(1)$ and $\omega_r(1+\delta E)$ denote the r nodal diameter natural frequencies of the tuned bladed disks with blade Young's modulus equal, respectively, to its design value and to this value multiplied by the factor $(1+\delta E)$. Note that the increment of Young's modulus affects only the blades and not the disk. Then, a coupling index $ci = 0$ indicates a purely blade alone mode while $ci = 1$ corresponds to a disk mode with rigid blades. A plot of the natural frequencies and coupling indices as function of the nodal diameter are shown in Figure 2(c) for the 12 blade disk of Figure 2(a) and (b).

Unless otherwise specified, the linear blade-alone dampers used were assumed to provide a damping equivalent to 9 times the naturally existing damping in the blades. Thus, the combined damping ratio of the blades with dampers is 1%. Further, while considering intentional mistuning in blade stiffness, A and B denote blades which have natural frequencies 5% lower and 5% higher, respectively, than those of the tuned disk. Finally, unintentional mistuning was introduced as a 1% standard deviation in stiffness/Young's modulus of the blade.

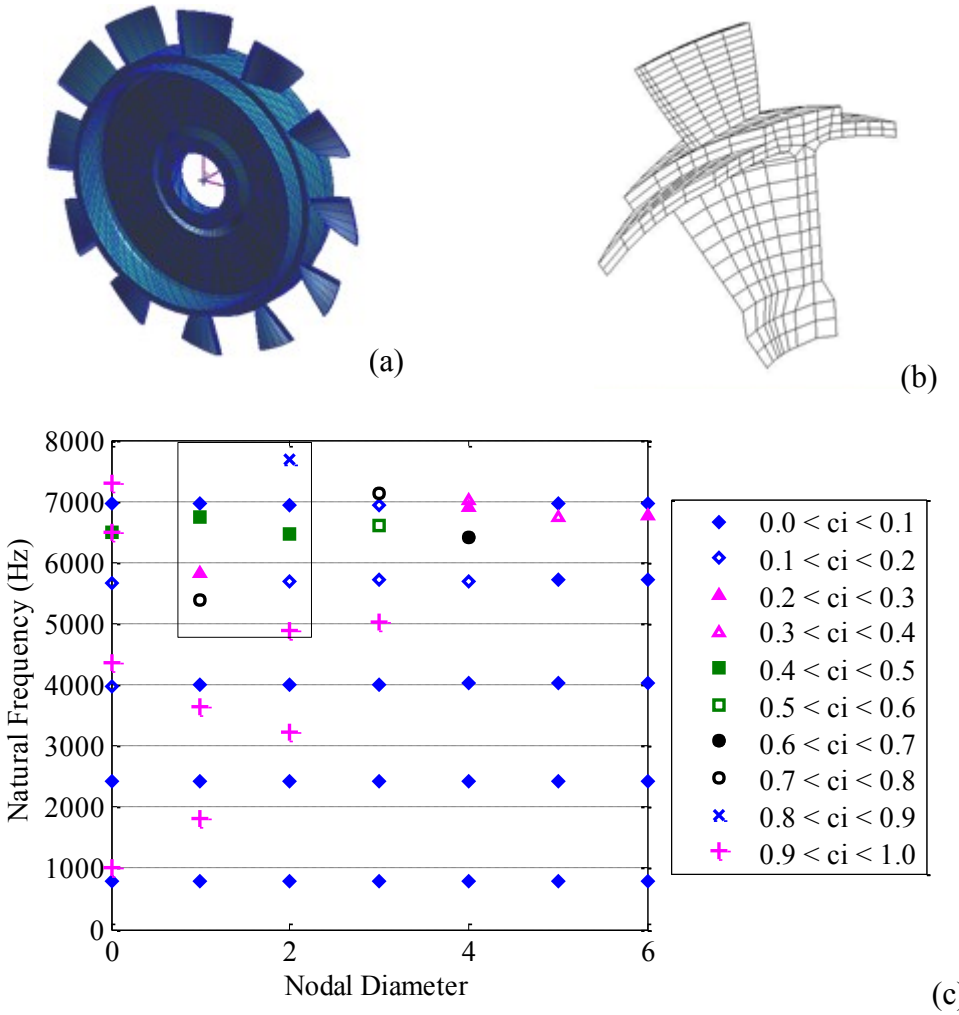

Figure 2. Blisk example: (a) blisk view, (b) blade sector finite element mesh, and (c) natural frequencies and coupling indices vs. nodal diameter plot (box showing frequency range of sweep).

2.2 The Three Optimization Problems

The present investigation focuses on three particular optimization problems, referred to as the P1, P2, and P3 problems. They correspond to the placement of dampers on tuned or intentionally mistuned bladed disk with or without considering the effects of involuntary random mistuning. More specifically,

- P1 Problem: optimization of the location of N dampers on a tuned disk to minimize the largest blade response on the disk in a frequency sweep without random mistuning.
- P2 Problem: optimization of the location of N dampers on a tuned disk to minimize a specific response statistic when random mistuning is present. Here, the minimization of the 95th percentile of the maximum amplitude of blade response on the disk in sweep was selected.
- P3 Problem: optimization of the location of N dampers and the A/B intentional mistuning pattern to minimize a specific response statistics when random mistuning is present. Here also, the minimization of the 95th percentile of the maximum amplitude of blade response on the disk in sweep was selected.

The location of blade-alone damper will be denoted by using the blade number on which the dampers acts and the location of a blade-blade damper will be denoted by the lowest blade number of the two blades joined by the damper.

The optimization problem can be summarized as below, with the primary design variables being the locations of the dampers on the bladed disk and the intentional mistuning pattern when necessary.

The objective is then the minimization of the 95th percentile of the maximum blade response amplitude in a frequency sweep (as determined by the resonance and excitation conditions on the bladed disk) in the presence of random mistuning.

Design Variables

(1) Locations of N dampers $d_i \quad i = 1, 2, \ldots N$

(2) Intentional mistuning pattern $b_i = 0 - blade\ type\ A \quad i = 1, 2, \ldots M$

$b_i = 1 - blade\ type\ B$

Objective

$$\min_{\substack{d_i \\ b_i}} 95\text{th percentile} \left\{ \max_{\omega \in \Omega} \left[\max_{j} \left(\text{response of blade } j \text{ at freq } \omega \right) \right] \right\}$$

Constraints

(1) Frequency range of interest $\Omega_{lower} \leq \Omega \leq \Omega_{upper}$

Ω_{lower} and Ω_{upper} defined according to resonance excitation condition on bladed disk

2.3 Optimization Problem Characteristics

The three optimization problems, P1, P2, and P3, defined above are all combinatorial in nature, i.e. they involve a finite number of possible solutions that

rapidly grow with the number of blades on the disk. Considering first the placement of the N dampers on a M bladed disks, there exist in general

$$\binom{M}{N} = \frac{M!}{N!\,(M-N)!} \tag{2}$$

different combinations of damper positions. When the base bladed disk is tuned, there exist rotationally equivalent configurations of dampers which can be eliminated by enforcing that a damper be always located on the first blade. Accordingly, the number of combinations is reduced to

$$\binom{M-1}{N-1} = \frac{(M-1)!}{(N-1)!\,(M-N)!} \tag{3}$$

Even the lower value given by Eq. (3) grows very rapidly with the number M of blades: it is linear in M for 2 dampers, quadratic in this parameter for 3 dampers, and so on. Further, using Stirling's formula, for a constant fraction q of blades with dampers, i.e. $N = qM$, one obtains the equation below which grows exponentially with the number of blades on the disk.

$$\binom{M}{N} = \frac{\alpha^M}{\sqrt{2\pi q(1-q)M}} \quad where \quad \alpha = \frac{1}{q^q(1-q)^{1-q}} \tag{4}$$

$$for\ q \in (0,1)$$

The consideration of intentional mistuning leads to an increase in the number of solutions by a factor approximately equal to the number of blade patterns, not considering the occasional existence of a few solutions that are rotationally equivalent. For the two blade type intentional mistuning considered here, this latter number has been estimated in [14] as $2^M/M$.

Given the very large number of possible configurations of dampers, and A/B blade pattern when considering intentional mistuning, it is generally not feasible to optimize the placement of the dampers through an exhaustive search. Thus, a numerical optimization algorithm will need to be employed. In assessing which specific algorithm should be considered, it is useful to estimate the cost of a function evaluation and the complexity of the design space.

The evaluation of a particular configuration of dampers, and intentional mistuning pattern when appropriate, requires the estimation of the corresponding 95th percentile of the maximum amplitude of blade response in a frequency sweep which is obtained considering random mistuning in the system. Thus, a Monte Carlo simulation (1,000 samples were used for the blisk model and 10,000 for the single degree of freedom model) of the full bladed disk must be carried out for each damper/blade pattern configuration. A convergence analysis was carried out, see Appendix A, and this number of Monte Carlo simulations was found to be adequate to characterize the response of the system well. Per se, one or a few such computations is now considered routine using reduced order modeling techniques but as a function evaluation within an optimization code, this qualifies as "expensive". In this regard, depending on the reduced order modeling strategy selected, the reduced order model modal matrices of the entire disk may need to be recomputed for each dampers/blade pattern configuration. This is not necessary with the approach selected here (as with other methods, e.g. see [15]), and only a reassembly of stiffness and damping matrices was necessary for each dampers/blade pattern configuration before the response was evaluated.

Another key factor in the selection of a particular optimization algorithm is the complexity of the design space, i.e. the number of local extrema present and their respective values. This information is, in general, very difficult to estimate accurately unless exhaustive search results are available. Fortunately, such data has been generated (partially in [1]) for a few conditions of the bladed disks of Figure 1 and Figure 2. In this data, a local optimum was recorded when any shift by one blade of any single damper or the flip of any blade A into blade B or vice versa led to an increase in the amplitude of blade response considered (maximum over the disk for the P1 problem and the 95th percentile of this maximum for the P2 and P3 problems). The results of this analysis are shown in Figure 3 and provide both the number of local minima (curves labeled "Num. Min.") and this number as a fraction of the number of possible configurations (curves labeled "Frac. Min.") averaged over a set of P1, P2, and P3 analyses. For further clarity, the same results are shown in Figure 4 providing both the number of local minima (curves labeled "Num. Min.") and the total number of possible configurations (curves labeled "Total Cases") averaged over the same set of P1, P2, and P3 analyses. Note the logarithmic Y-axis in Figure 4(c).

While the number of these local minima (which includes rotationally equivalent optima for the P1 and P2 problems) is already significant for the P1 and P2 problems, e.g. up to 140 on the blisk, it is even larger for the P3 problem due to the increased complexity of intentionally mistuned disks. Note from Figure 3(b) and Figure 3(c) that the number of local minima may depend significantly on the resonant condition and the bladed disk model considered. To complete this

perspective, it is necessary to assess the penalty associated with reaching a local-only minimum. To support this assessment, shown in Figure 5 are the minimum, average, and maximum amplification factors obtained for the P1, P2, and P3 problems as a function of the number of blades. Clearly, reaching a local-only minimum may lead to a large penalty, e.g. an increase in amplitude of blade response up to 50%, although it is often a much smaller penalty.

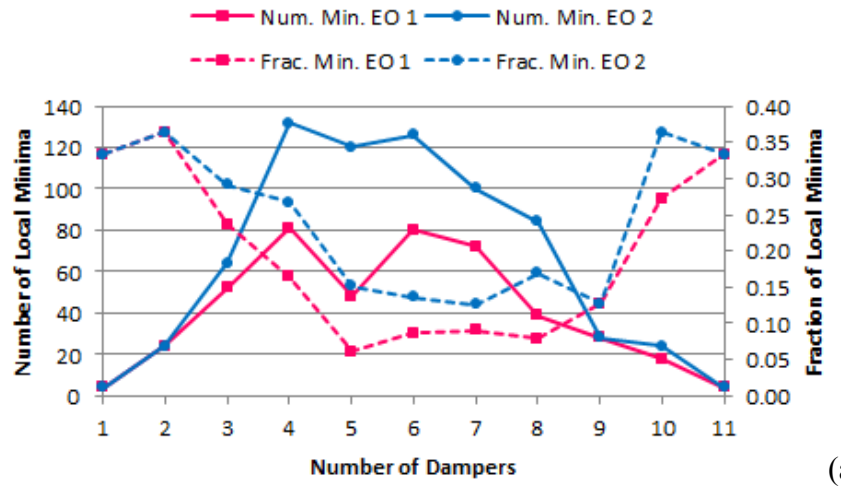

(a)

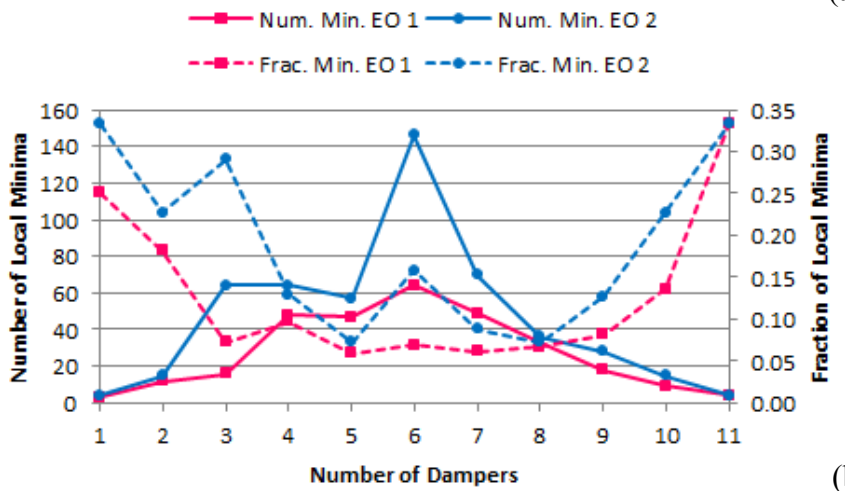

(b)

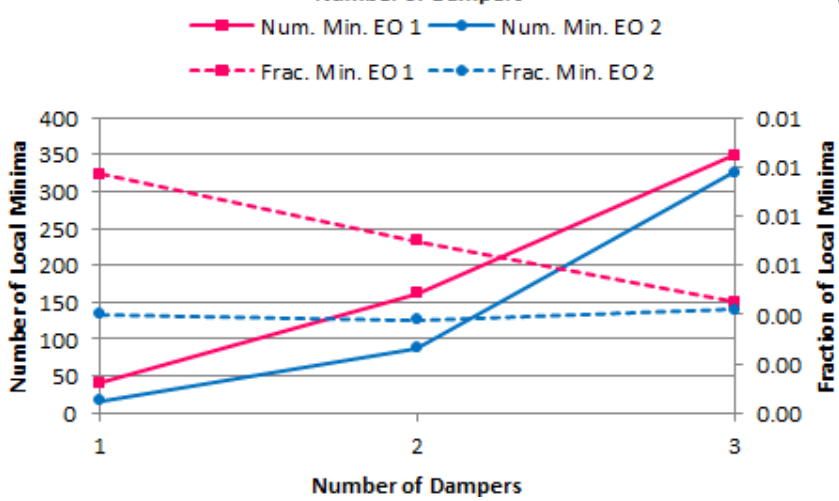

(c)

Figure 3. Number of local minima vs. number of dampers on (a) a tuned disk (P1 problem), (b) a randomly mistuned disk (P2 problem), and (c) an intentionally mistuned disk (P3 problem). Blisk reduced order model, raw number of minima ("Num. Min.") and fraction of the total number of possible combinations ("Frac. Min.").

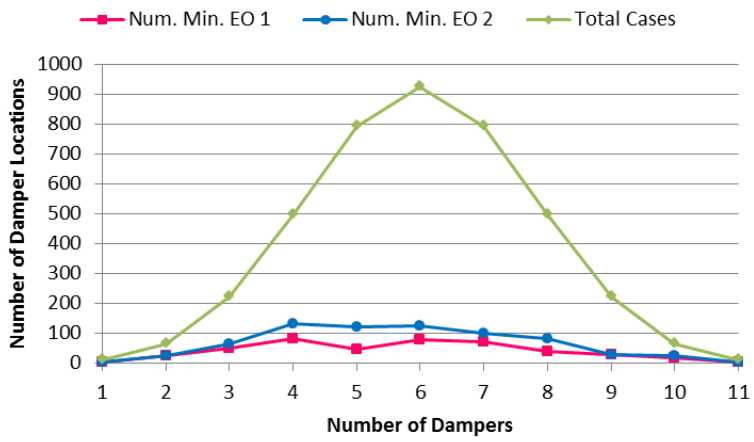

(a)

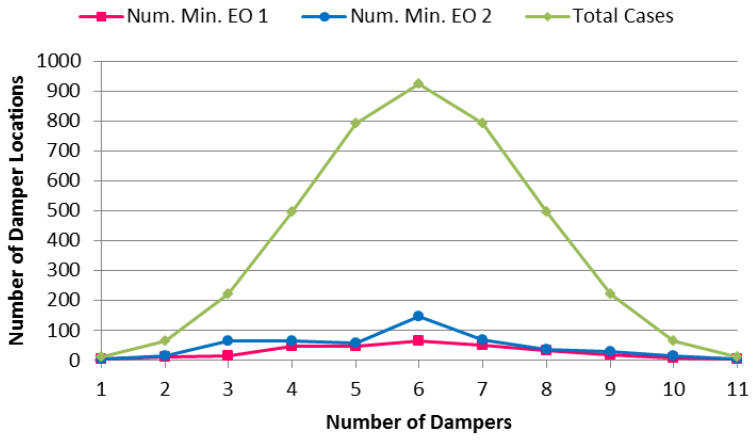

(b)

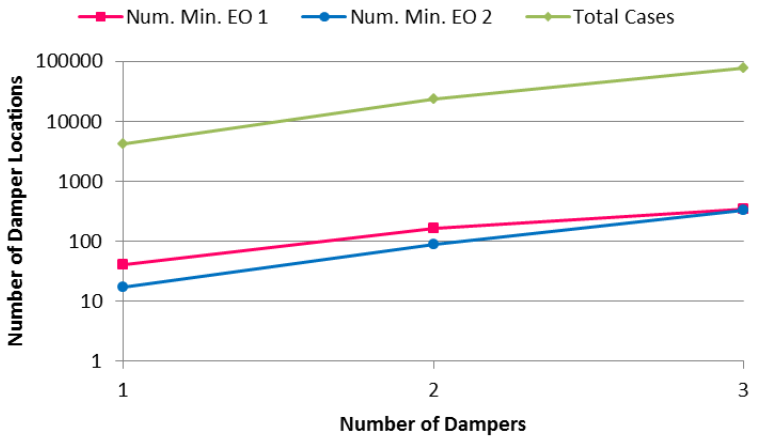

(c)

Figure 4. Number of local minima vs. number of dampers on (a) a tuned disk (P1 problem), (b) a randomly mistuned disk (P2 problem), and (c) an intentionally mistuned disk (P3 problem). Blisk reduced order model, raw number of minima ("Num. Min.") and total number of possible combinations ("Total Cases").

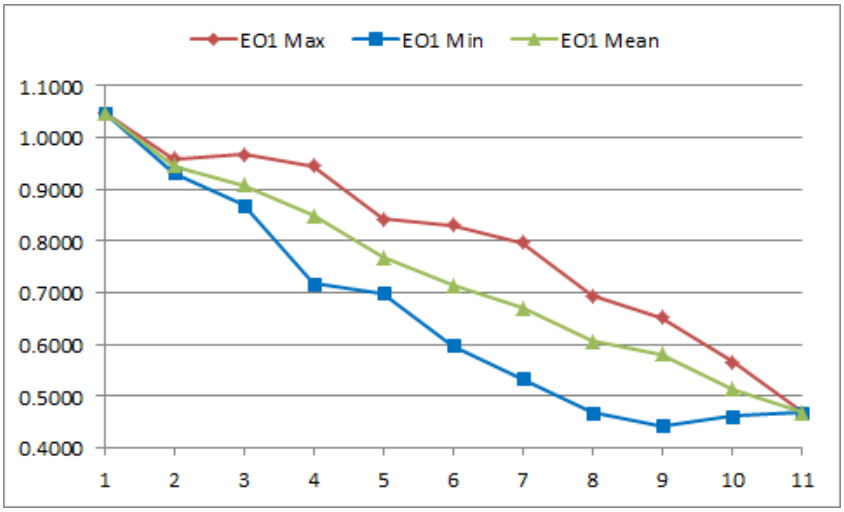

(a)

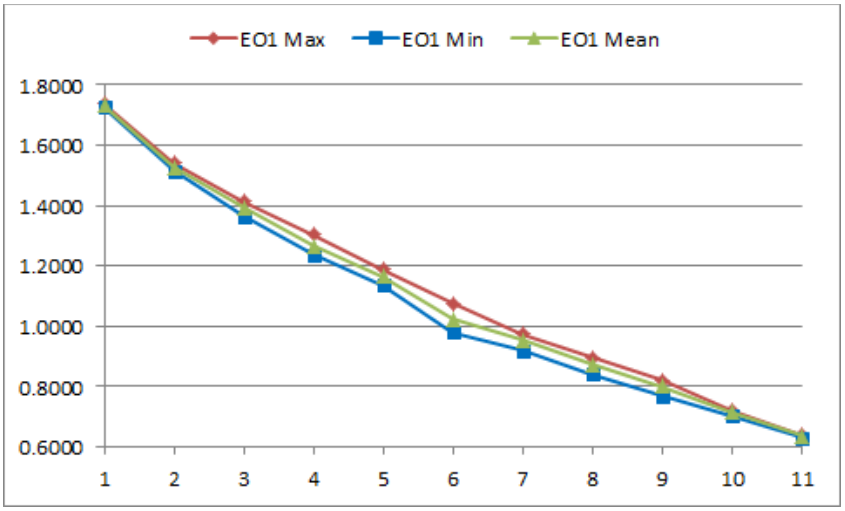

(b)

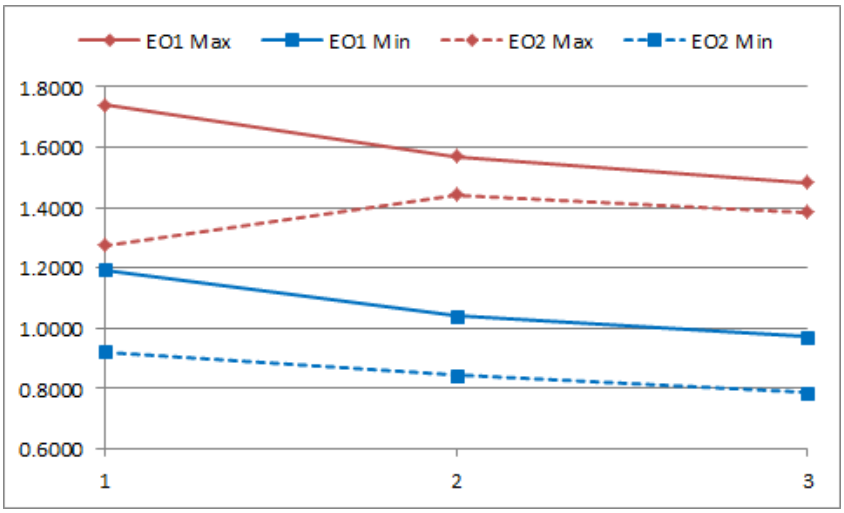

(c)

Figure 5. Minimum, average, and maximum amplification factors of local minima vs. number of dampers on (a) a tuned disk (P1 problem), (b) a randomly mistuned disk (P2 problem), and (c) an intentionally mistuned disk (P3 problem). Blisk reduced order model.

2.4 Basic Optimization Strategy

The discussion of the previous section has demonstrated that:

(1) there is a large number of local optima to each P1, P2, and P3 optimization problem with largely different amplitudes of blade response.

(2) the cost of a function evaluation is large for the P2 and P3 problems owing to the Monte Carlo simulations they involve.

The property (1) indicates that local search algorithms, e.g. steepest difference, will typically not be successful unless they are started at initial conditions close enough to the global optimum. Otherwise, they will converge to one of the many local optima. There are a series of algorithms, e.g. simulated annealing, genetic algorithms, which are known to perform well in the presence of multiple local optima but all of these require many function evaluations. In view of property (2), they are thus poorly suited for the present task as they are too computational expensive, at least for the P2 and P3 problems. In this light, the present optimization problems would benefit from dedicated approaches. Hence, a two-step algorithm was developed for the solutions of the P1, P2, and P3 problems in which:

- Step 1: solve a similar yet simpler optimization problem using standard algorithms.
- Step 2: proceed with a local search through a steepest descent strategy from a set of initial conditions resulting from the first step.

In this light, the first step of the algorithms aims at producing "good" initial conditions, i.e. "close" to the optimum solution. The local search is accomplished

by assessing the change in amplitude of blade response induced by a shift by one blade of any single damper or the flip of any blade A into blade B or vice versa. The steepest difference is then the one leading to the largest decrease in blade response of all shifts and flips. This process is repeated until a minimum is reached for every initial condition selected and the best (lowest maximum response) of the converged optima is chosen as the desired solution. To minimize the computational effort, random mistuning, when present, was considered only in step 2.

The details of the corresponding algorithms for the P1, P2, and P3 problems are given in the ensuing sections in which validations with available exhaustive search data has also been carried out.

2.5 P1 and P2 Two Step Optimization: Formulation and Validation

The validation is summarized by two key numbers: the percentage of cases in which the optimization algorithm correctly converged to the global minimum and the average relative error for the cases in which the global minimum was not reached.

The first step of the P1 optimization algorithm (see Figure 6 for flowchart) is the construction of one or several tentative configurations of the N dampers around the disk. More specifically, a sequential construction of these configurations is proposed. Assuming that a good or optimum configuration of $N-1$ dampers is known, it was suggested that a tentative initial condition for the N damper problem be obtained from one of the following rules:

(1) Rule 1: place the new damper on the blade that has the highest response without it but with the other dampers.

(2) Rule 2: place the damper on the blade that leads, after its insertion, to the lowest highest blade response on the disk.

(3) Rule 3: place the damper on the blade that leads, after its insertion, to the lowest average blade response on the disk.

A key advantage of the sequential construction of the solutions is that it eliminates the combinatorial increase of the search space with the number of dampers. In fact, the computational effort associated with the placement of one additional damper decreases with increasing number of dampers. Its drawback is clearly that if the predicted configuration of $N-1$ dampers is poor, it is likely that the one deduced from it for N dampers will also be poor.

This issue has been addressed here by performing the second step of the algorithm not simply when the desired number of dampers N has been reached but rather more often – for every $D < N$ dampers. That is, position D dampers sequentially according to rule 1, 2 or 3, then proceed with a local search with this solution as initial condition. The optimum solution with D dampers thus obtained serves as initial condition to the sequential construction of $D+1, D+2, \ldots, 2D$ dampers. Proceed with a local search with the solution at $2D$ dampers as initial condition and use the optimum solution thus obtained as the initial condition to the sequential construction of $2D+1, 2D+2, \ldots, 3D$ dampers and so on.

To obtain several initial conditions for the local search of step 2, each of the 3 rules was considered in the P1 problem leading to 3 solutions processed

through local search in step 2. The predicted arrangement of dampers is then, of the three converged solutions, the one which yields the lowest highest blade response

The above algorithm was applied here to both models of Figure 1 and Figure 2 with both $D = 1$ and $D = N$ and the results, see Table 1, clearly demonstrate that the algorithm consistently finds either the global minimum or a local one with a value very close to it. Note that the updating scheme, i.e. using $D = 1$, does not always lead to a better solution, e.g. in the blisk case, after the local search is performed.

The first step of the P2 optimization algorithm (see also Figure 6 for flowchart) is identical to the one of P1 problem as random mistuning is only considered in the second step, i.e. the local search. Thus, the initial conditions selected here were the optimum solution obtained for the P1 problem with the same number of dampers, i.e. the sequential construction with possible updating discussed above is only applied to the P1 problem. Its application to both the single degree of freedom per sector and blisk reduced order models consistently gave an excellent prediction of the global optimum, see Table 1. To support the benefits of the proposed P1 and P2 algorithms, the computational cost, i.e. the number of response evaluations, was determined for all cases analyzed as absolute numbers but also as percentages of the exhaustive search. The results of this analysis without considering updating, i.e. with $D = N$, are presented in Figure 7, averaged over all cases analyzed. Note in both of these figures that the number of response evaluations does increase with increasing number of dampers (up to

$N = M/2$) but much less rapidly than the exhaustive search, see Eq. (3), leading to a rapid reduction of the cost as a percentage of the exhaustive search. As N increases past $M/2$, the computational costs, both of the algorithm and of the exhaustive search, decrease as the number of combinations becomes smaller finally reaching 1 for $N = M$.

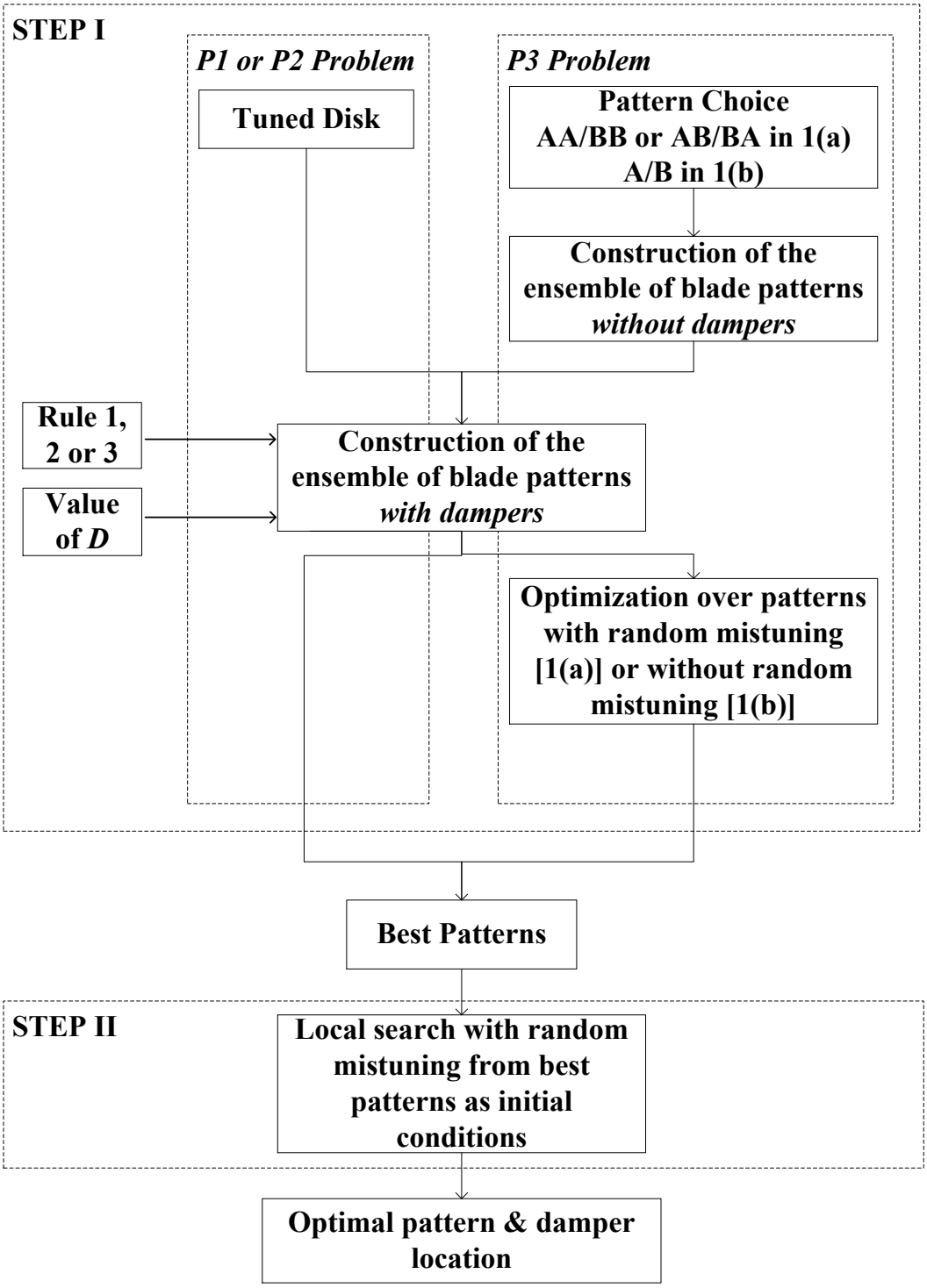

Figure 6. Flowchart of the optimization problems.

Table 1. Performance of the optimization algorithms.

		P1 D=1	P1 D=N	P2 D=1	P2 D=N	P3 D=1	P3 D=N
SDOF	Percentage of time the global min found	100%	85%	100%	100%	67%	50%
	Average error when local min not found	-	4.9%	-	-	1.5%	2%
	Maximum error when local min not found	-	9.7%	-	-	2.2%	3%
BLISK	Percentage of time the global min found	91%	94%	85%	79%	66%	50%
	Average error when local min not found	5.5%	3.1%	1.9%	2%	1%	0.3%
	Maximum error when local min not found	10%	4.2%	5.8%	5.8%	1.6%	0.9%

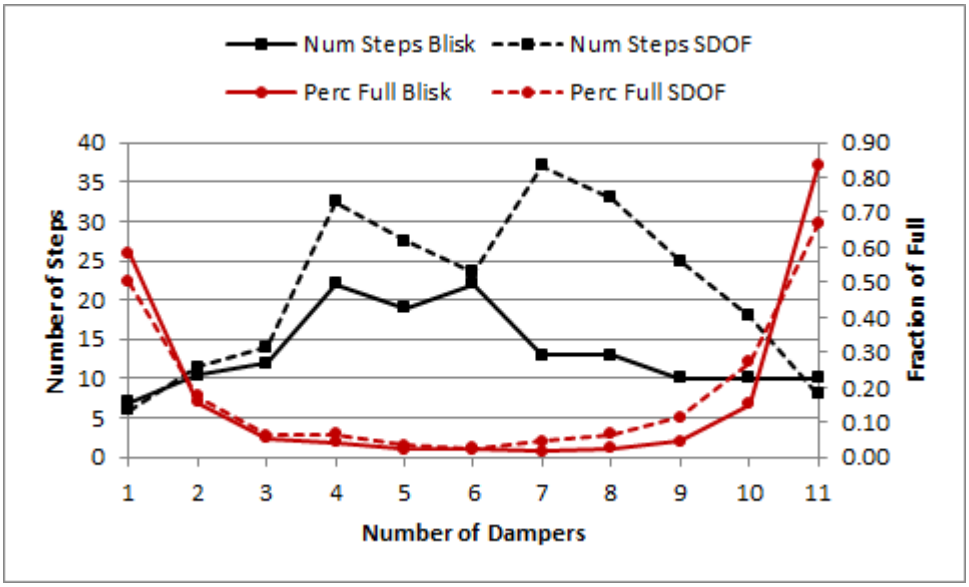

(a)

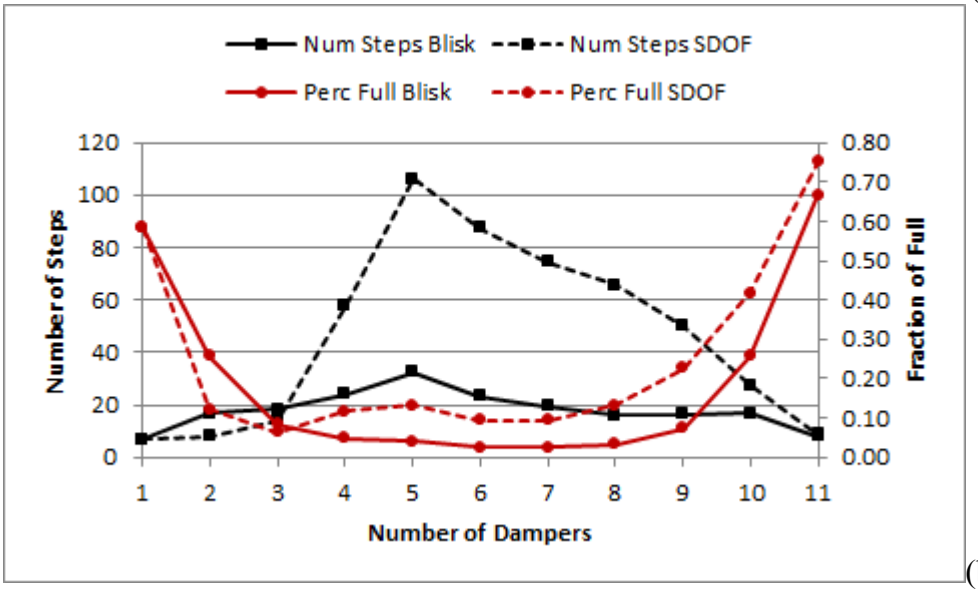

(b)

Figure 7. Computational cost of the (a) P1 and (b) P2 optimization algorithms vs. number of dampers, blisk and single degree of freedom per sector models. Cost measured by the raw number of steps and its fraction of the exhaustive search.

2.6 P3 Two Step Optimization: Formulation and Validation

In addition to the three rules proposed in the previous section for the tentative placement of dampers, the first step of the P3 algorithm requires the selection of one or several intentional mistuning patterns. Such a problem has been addressed in [14] which focused on the selection of the best intentional mistuning without any dampers. In fact, a two-step approach was formulated and validated there that is similar to the one proposed here in which the second step is a local search.

As first step in [14], two different options referred to in the sequel as step 1(a) and step 1(b) were suggested. In step 1(a), leading to the so-called subspace algorithm, two or more consecutive sectors were constrained to vary in relation with each other. For example, two consecutive sectors could be restricted to be the same, either both A (AA) or B (BB). Alternatively, they could be constrained to be different generating the choices AB and BA. This approximate problem is similar to the one to be solved (the full problem) but with a smaller number of blades/sectors. This reduction in the number of sectors leads to a dramatic reduction in the computational cost which is approximately proportional to $2^R/R$ where R is the number of sectors, i.e. $R = M/2$. The initial conditions to the full problem are thus the best solutions to the one with the constrained patterns which can be obtained by an exhaustive search. If the number of sectors is still too large to permit an exhaustive search, 3 or more blades can be linked leading to choices AAA/BBB, $AAAA/BBBB$, ABA/BAB, etc.

In step 1(b), random mistuning is not included and thus the computational cost is reduced by not carrying out the Monte Carlo simulation, performing only one computation per intentional mistuning pattern. If necessary, the solution to this problem can be obtained by a two-step approach based on the subspace algorithm thereby combining the two approaches for an even more efficient strategy. Given the very successful validation of these two algorithms in [14], they were considered here to obtain the intentional mistuning pattern and the location of the dampers. They were used as described above only for the intentional mistuning pattern. The placement of the dampers was obtained, for each pattern of the subspace for step 1(a) or full space for step 1(b), sequentially by placing one damper first, then a second, third, etc. according to rules 1, 2, or 3 above. Further, updating every D dampers can also be performed; see Figure 6 for flowchart.

Two minor variations were further considered. In the "ordered" variation, the best 5 intentional mistuning patterns obtained in step 1 were used as initial conditions while in the "no neighbor" variation, the best 5 patterns which are not direct neighbors were used. In this context, two solutions are direct neighbors if they differ by a switch of either one blade or the shift of one damper by one blade.

These algorithms were validated in comparison with the exhaustive search data of [1] available for 1, 2, and 3 dampers for both models of Figure 1 and Figure 2; see Table 1 for the subspace method (step 1(a)). These results were obtained using the best solutions obtained by using the step 1 results of both AA/BB and AB/BA subspaces, so that 10 initial conditions were effectively

used. Further, only rule 2 was applied for the positioning of the dampers, it was found to be consistently better than rule 1. Finally, the "no neighbor" option was used as it led to a better final solution, almost consistently so, than the ordered one.

Having successfully validated the step 1(a) based approach it was of interest next to assess its computational cost measured by the total number of function evaluations carried out (averaged over the all cases treated for each number of dampers). This cost is displayed in Figure 8 both in absolute numbers and as a fraction of the cost involved in the exhaustive search. This ratio can be considered as the computational efficiency of the approach. For 3 dampers, the approach leads to a reduction of the computation by a factor of over 100. In fact, this approach permits the consideration of a much large number of blades and dampers than was considered in [1] and some of these results are presented in the next few sections.

Having validated and assessed the two-step algorithm based on step 1(a), it is now desired to proceed similarly with step 1(b), that is the algorithm in which the initial conditions used for the steepest descent search are obtained from the solution of the full problem but without random mistuning. The computational effort associated with this preliminary solution is thus smaller than the one for the full problem by the number of simulations used to capture the random mistuning effects, which is typically of the order of 100-1,000. When the number of blades on the disk is large, the subspace approach will typically lead to a larger saving because the reduction of the number of sectors, from M to $R = M/2$, will

provide a reduction of computations larger than 1,000. Nevertheless, this second approach for the optimization of the intentional mistuning pattern and damper location achieves generally good results but not as good as those obtained with the subspace approach used previously.

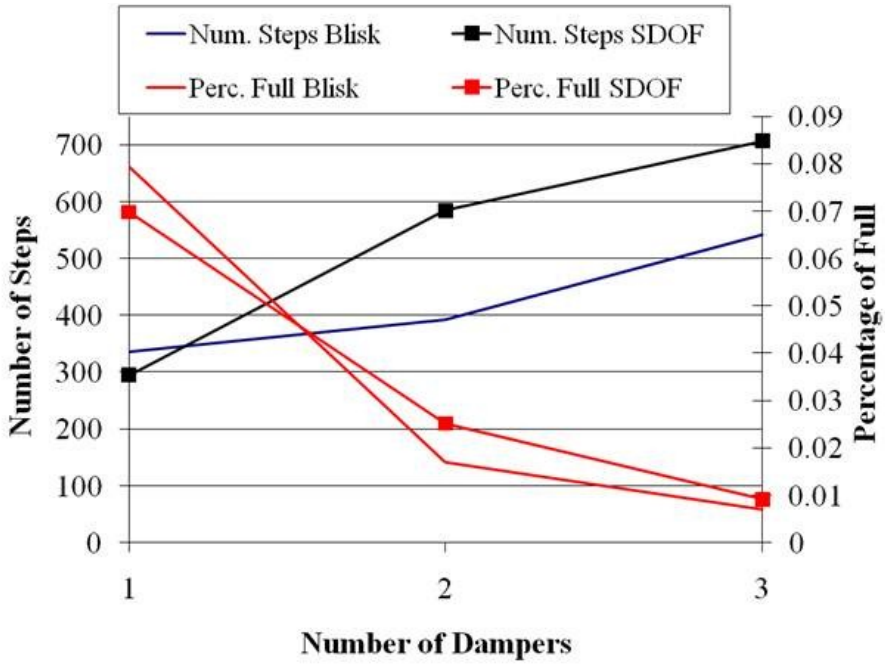

Figure 8. Computational cost of the subspace method based on step 1(a) vs. number of dampers, blisk and single degree of freedom per sector models. Cost measured by the raw number of steps and its fraction of the exhaustive search.

3 – APPLICATION TO LINEAR BLADE-ONLY DAMPERS

The availability and reliability/accuracy of the optimization algorithms presented in the previous chapter permits the extension of the results presented in [1] to a larger number of dampers than three and to assess the benefits of introducing the dampers but also of the benefits of using intentional mistuning. The corresponding results are discussed below.

3.1 P3 Problem with More Than Three Dampers

It was first desired to extend the P3 problem to a number of dampers larger than three which was the maximum that could be carried out with the exhaustive search. To this end, the subspace algorithm based on step 1(a) was used for both the blisk and single degree of freedom model. Shown in Figure 9 and Figure 10 are typical plots of the 95th percentiles of the amplification factor divided by the corresponding value obtained without any damper for the single degree of freedom per sector model and the blisk respectively. Also shown on these figures are the solutions of the P1 and P2 problem reported in [1] also normalized by their own values (maximum amplitude for P1 and 95th percentile of max response for P2) obtained without dampers. Note that the solutions for the P3 problems are normalized with respect to the 95th percentile of maximum response of the P2 problem without dampers.

The steady decrease of the response with increasing number of dampers is clearly shown on these figures for all options, intentionally tuned or mistuned. The benefits of using intentional mistuning can be seen by comparing the red

lines with the crosses. In the single degree of freedom per sector model, only a small improvement is achieved by varying the blade properties by choosing A/B patterns. However, when analyzing the blisk model, a large improvement is observed when using intentional mistuning. This finding suggests that the benefits of using intentional mistuning in addition to optimized damper locations may be case dependent. The availability of the fast optimization approach developed and validated here makes the assessment of this benefit easier.

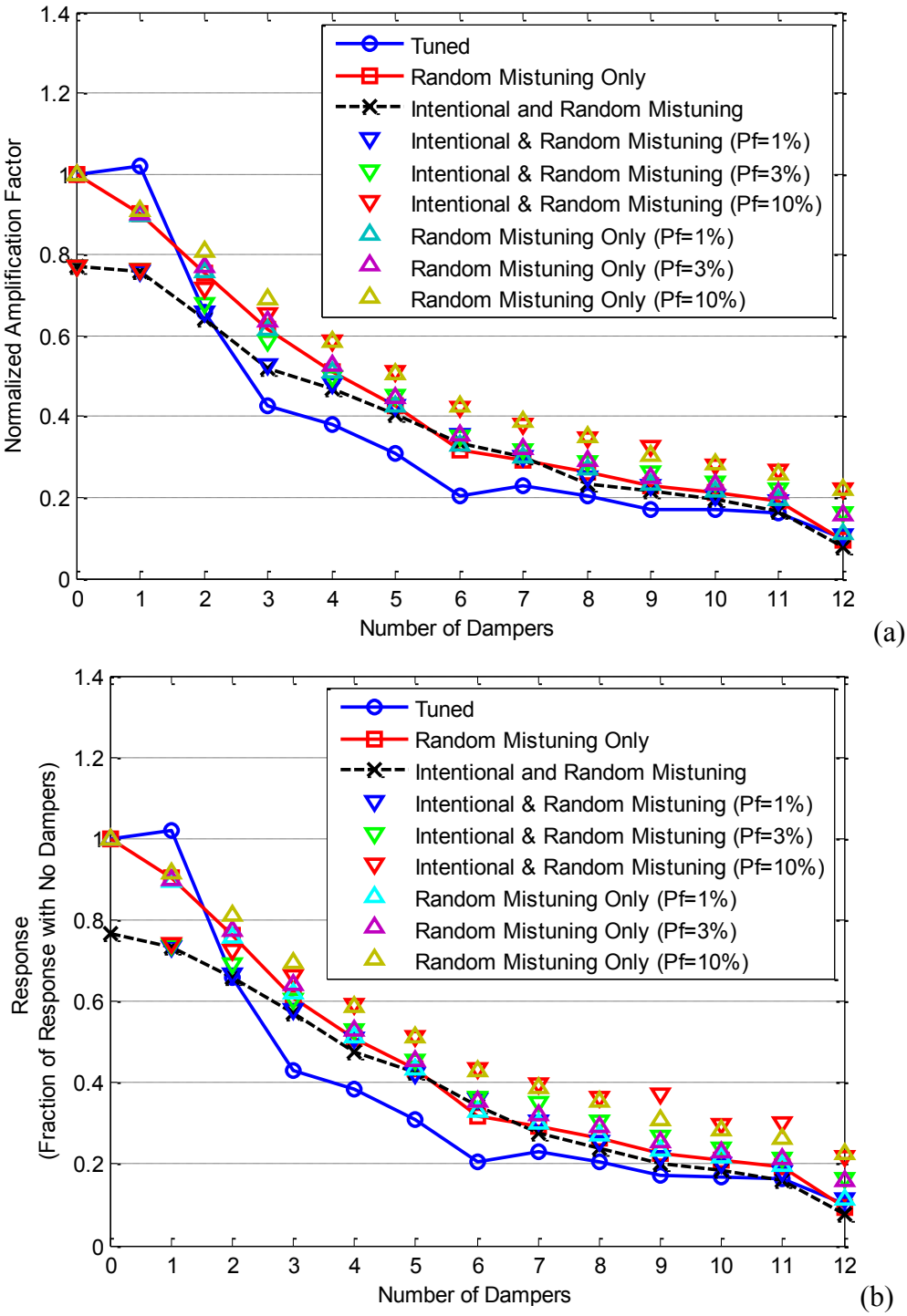

Figure 9. Normalized peak response vs. number of dampers for different options, single degree of freedom per sector model, (a) engine order 2 excitation, (b) engine order 4 excitation.

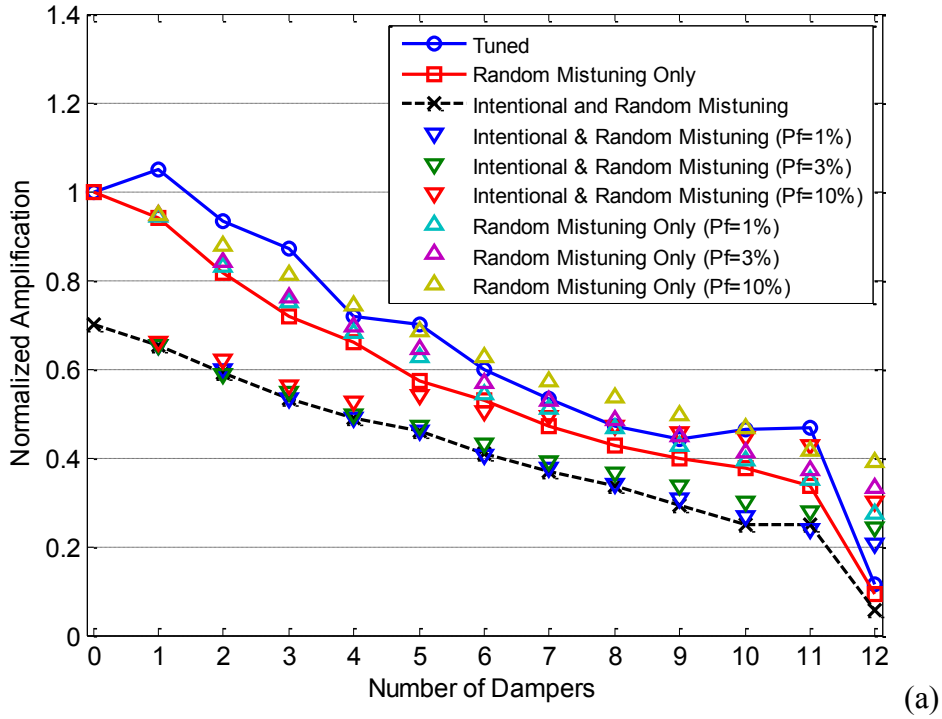

(a)

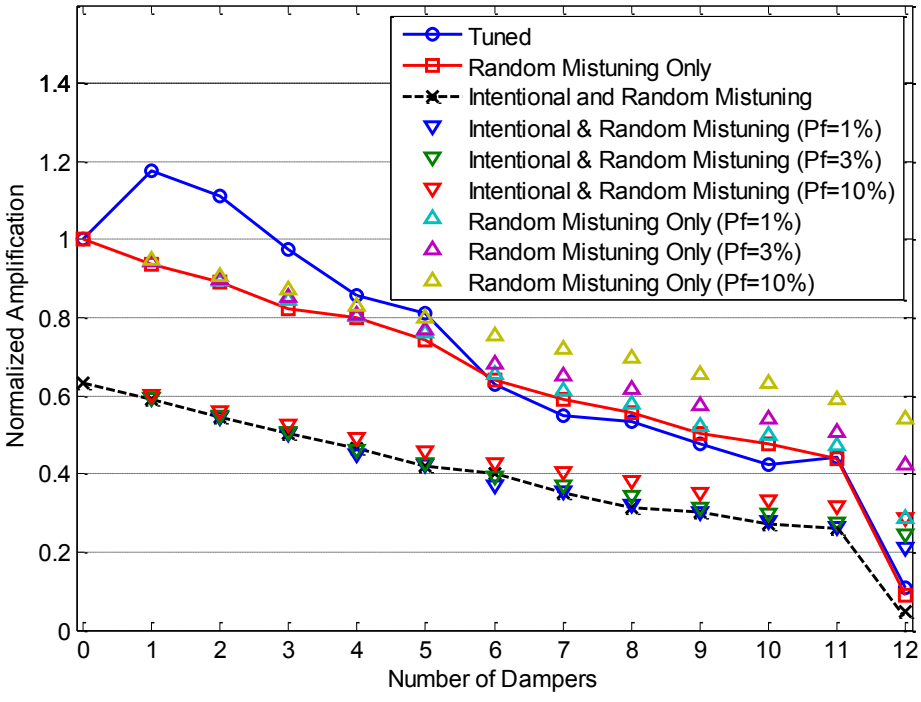

(b)

Figure 10. Normalized peak response vs. number of dampers for different options, blisk model, (a) engine order 1 excitation, (b) engine order 2 excitation.

3.2 P2 Problem for Various Coupling Stiffnesses

To assess the benefits of using dampers on only a few blades of intentionally tuned but randomly mistuned disks, it was desired to extend the investigation of this issue conducted in [1] focusing more specifically on the number of dampers needed to achieve a specific reduction in the peak response. Here the 95th percentile of the maximum amplitude of blade response on the disk in sweep was considered with a Monte Carlo analysis used to quantify random mistuning.

Clearly, the level of blade-to-blade coupling in the system around the resonance of interest is a key factor in the number of needed dampers. The stronger the coupling is, the smaller the number of dampers should be. The single degree of freedom per sector model was first considered here for different values of the coupling stiffness. To help in the modeling of a particular family of modes by such a model, the natural frequency vs. number of nodal diameter plot was first generated, see Figure 11. Then, an exhaustive search was conducted to place 1, 2, 3, etc., dampers on the disk to minimize the peak response without intentional mistuning and the ratio of the peak response to the one obtained for the disk without damper was computed. This process was repeated for the set of k_c values of Figure 11 and for engine orders 2 and 4. Shown in Figure 12 are the contour plots of the reduction in amplitude obtained vs. coupling stiffness and number of dampers obtained for engine order 2 and 4. It can be observed that these two engine orders behave quite similarly. The same data is also shown in Figure 13 in a format similar to that of Figure 9 and Figure 10. These results

confirm and quantify the expectation that the number of dampers needed reduces as the blade-blade coupling level increases.

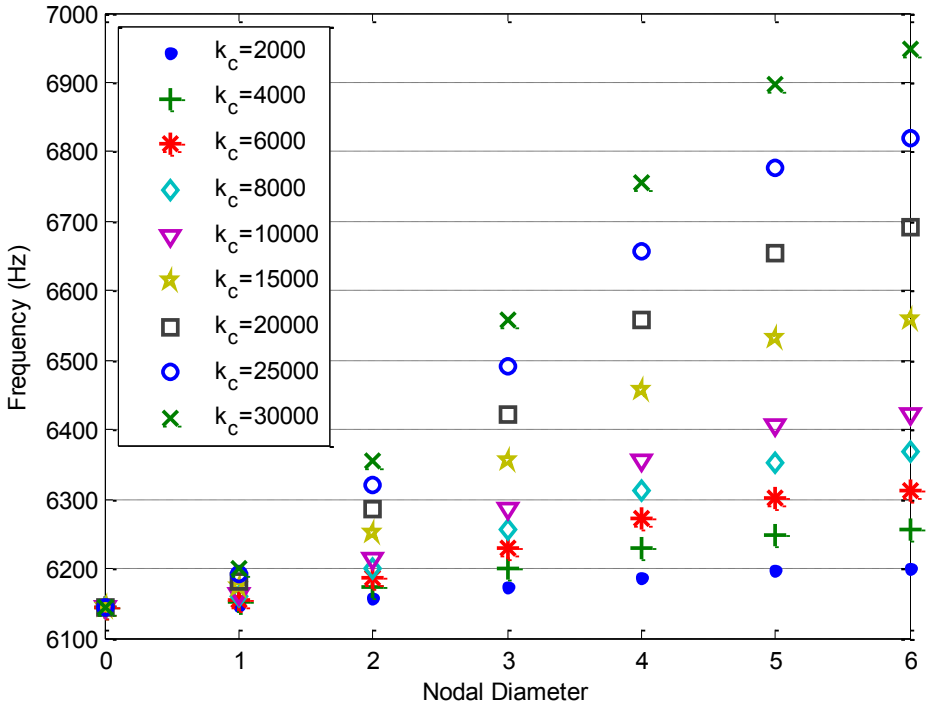

Figure 11. Frequency vs. nodal diameter plot, single degree of freedom per sector model for various coupling stiffnesses k_c.

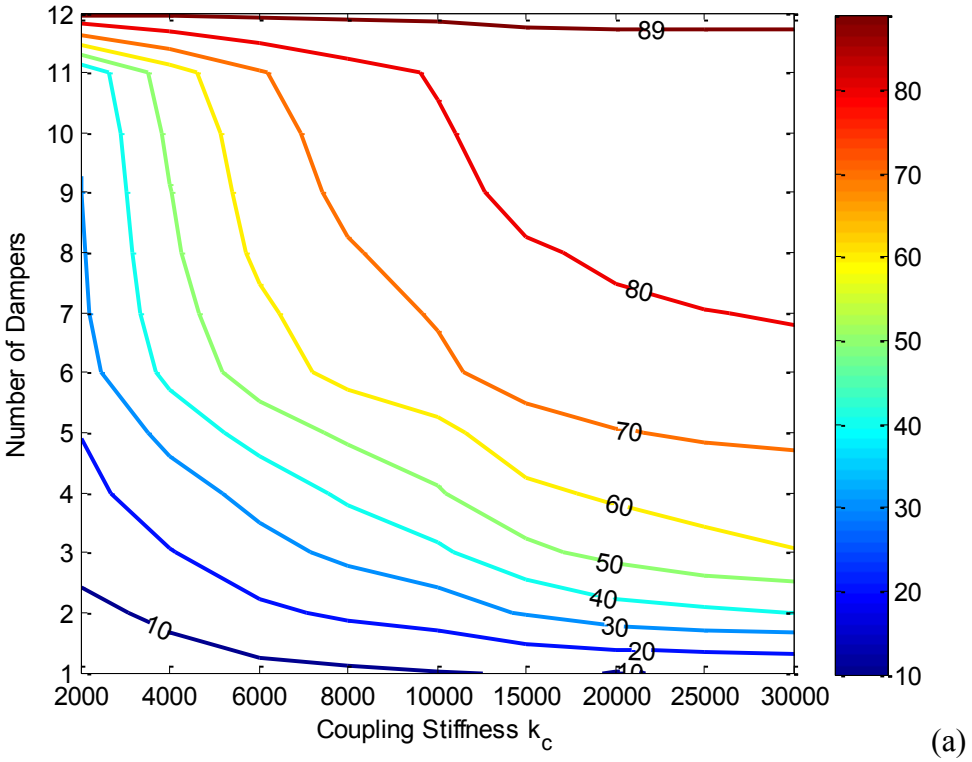

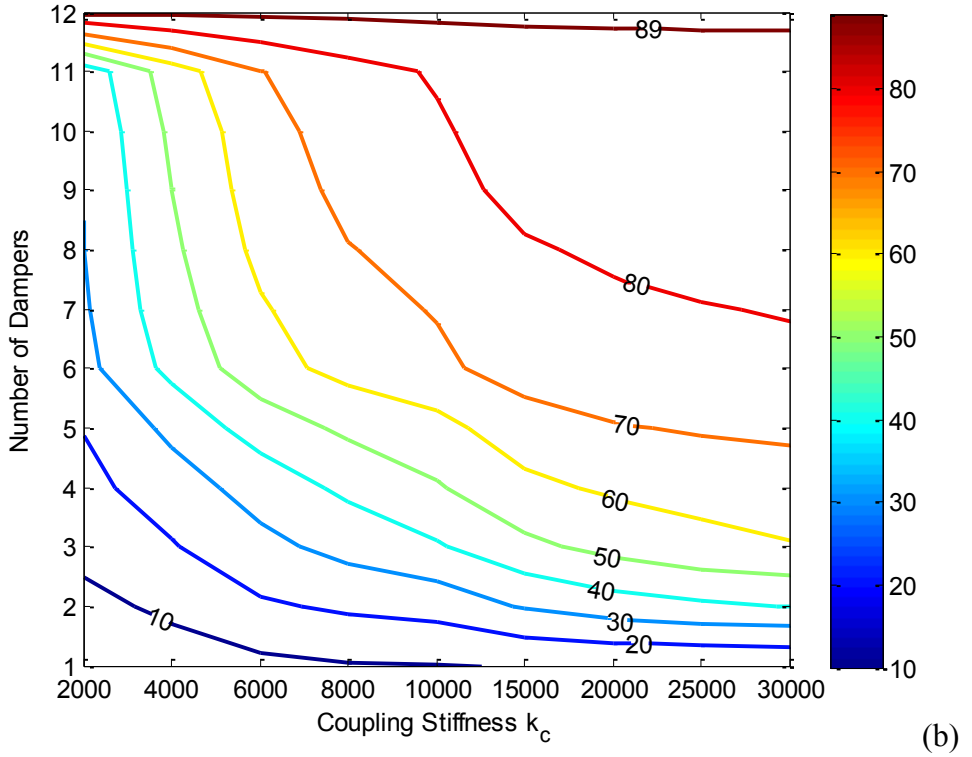

Figure 12. Reduction in peak response (in percentage) vs. number of dampers and coupling stiffness, single degree of freedom per sector model, (a) engine order 2, (b) engine order 4 excitation.

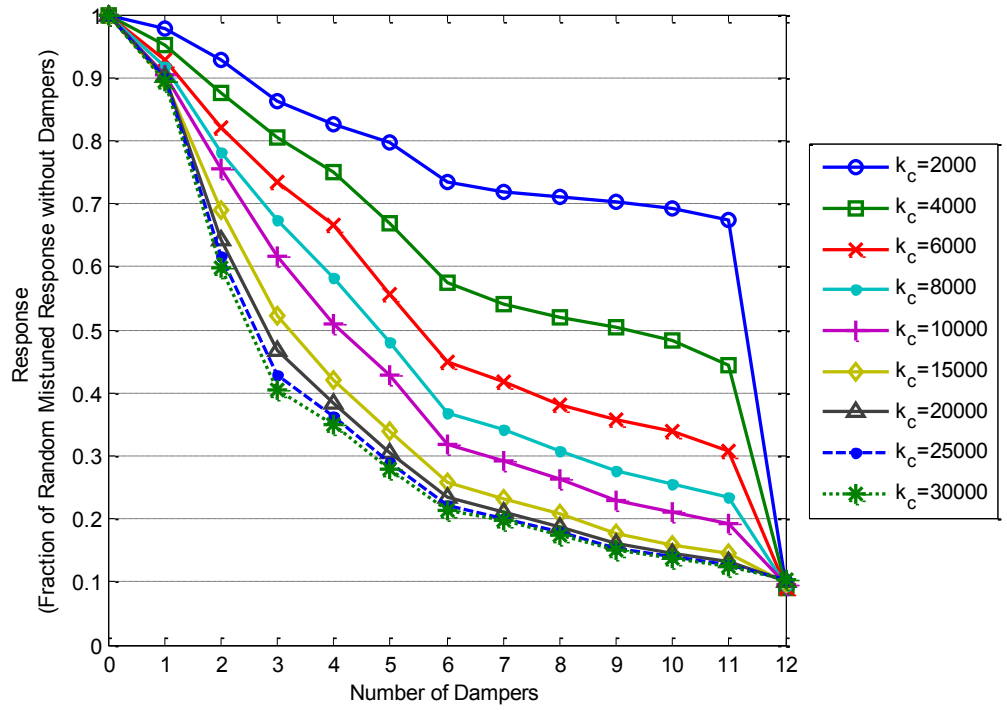

(a)

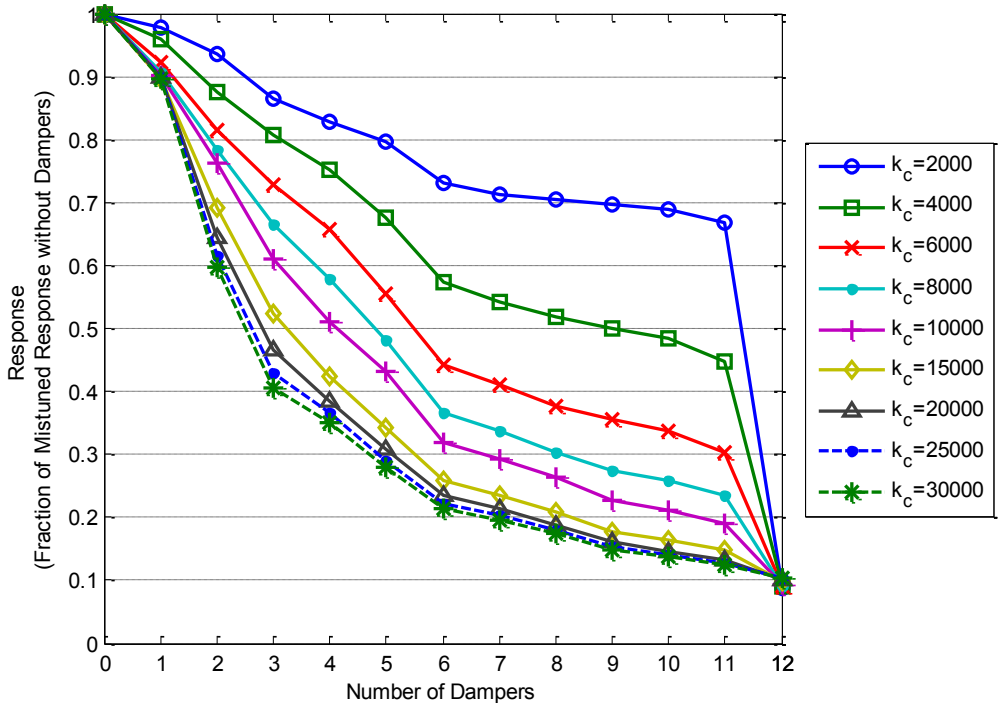

(b)

Figure 13. Normalized peak response vs. number of dampers for different values of coupling stiffness, single degree of freedom per sector model, (a) engine order 2, and (b) engine order 4 excitation.

3.3 Damper Efficiency as a Function of its Damping Level

The original discussion of [1] demonstrated the existence of an optimum value of the damping coefficient of the damper for the reduction of the blade response. This optimum resulted from two effects of the damper the first of which is positive and it is the dissipation of energy. The second one, is negative, and is the localization of the response induced by the non-uniform distribution of dampers which thus reduces the energy transfer around the disk necessary to decrease the response of all its blades. The combination of these effects had been studied in [1] by analyzing the reduction of the maximum amplitude of response, as a function of the ratio C/c of the single degree of freedom per blade sector model. Owing to the computational demand associated with the exhaustive search for the P2 and P3 problems, this analysis had been carried out in [1] only for the P1 problem, see Figure 14. These results can now be extended to the P2 and P3 problems as well, see Figure 15 for the latter case.

It can be noted that the appearance of the curves shown in Figure 14 and Figure 15 (for $k_c = 10{,}000\ N/m$) are very similar, they both exhibit a rapid drop at the beginning to plateau at a rather large value of C/c which appears to be quite similar, approximately 20, for both problems and for 1, 2, or 3 dampers present. A key difference between them however is the ratio in amplitude achieved at the optimum C/c which is notably smaller for the P1 problem than it is for the P3, e.g. 0.4 for the P1 problem vs. 0.77 for the P3 one for 3 dampers. This result is however expected as random mistuning was shown in [1] to decrease the efficiency of using only a few dampers on the disk.

This discussion tentatively suggests that the problem of placement of dampers on an otherwise tuned disk (P1 problem) may be used to assess the efficiency of placing dampers on selected blades, even though mistuning would in general be present.

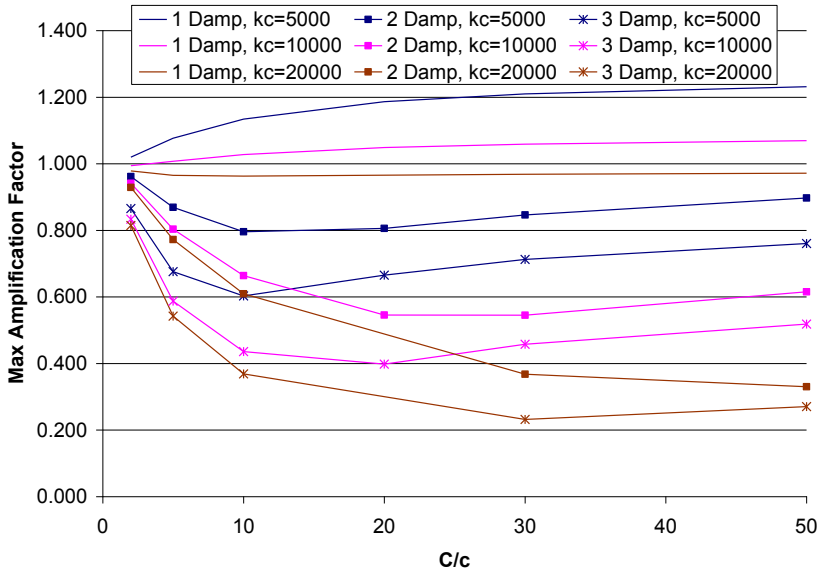

Figure 14. Amplification factor of the maximum blade response vs. damper coefficient, C/c, single degree of freedom per sector model, and for 1, 2, and 3 dampers of optimized locations. P1 problem, $r = 4$ (from [1]).

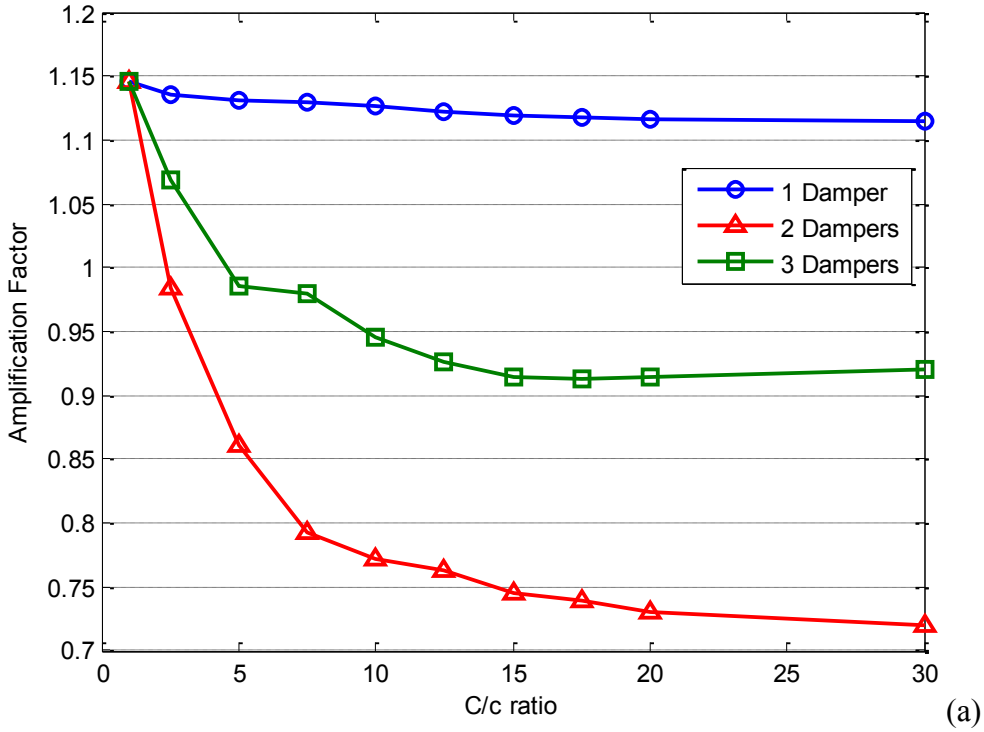

(a)

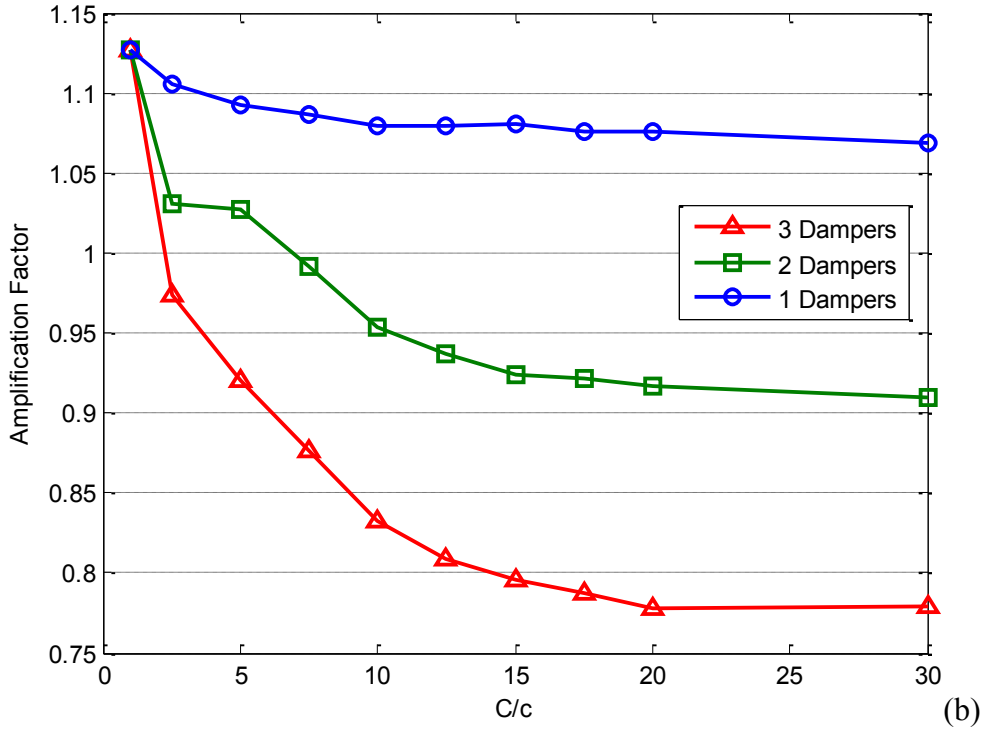

(b)

Figure 15. 95th percentile of the amplification factor of blade response vs. damper coefficient, C/c, single degree of freedom per sector model, and for 1, 2, and 3 dampers of optimized locations. P3 problem, (a) $r = 2$, (b) $r = 4$.

3.4 Optimization with Nonzero Probability of Damper Failure

The results presented in the previous section suggest that a significant reduction in the forced response of bladed disks may be expected as a result of the combination of intentional mistuning and selected dampers. Then, it could be argued that the reverse also holds, i.e. that if the failure of a damper occurred, a significant increase in response would take place and that the safe operation of the bladed disk might be at risk. To avoid such an outcome, it was proposed here that the optimization process account for the possibility of one or multiple failures and the associated increase in blade response. More specifically, a probabilistic optimization strategy similar to the one carried out in [17] for the optimal positioning of strain gages on blades will be formulated. This strategy proceeds as follows.

The failure of a damper is a random event that affects the distribution and magnitude of blade amplitudes around the disk. Thus, the maximum amplitude of response corresponding to a particular design (i.e. a given intentional mistuning pattern and specified locations of the dampers) can be viewed as a random variable the value of which depends on the state, failed or intact, of the dampers. Accordingly, it is no longer appropriate to proceed with a minimization of the maximum amplitude of response in the absence of failure. Rather, one should minimize some statistics of the random maximum amplitude of response that encompasses all situations, failure or lack thereof of the dampers.

Two approaches can be followed to implement such a concept. The first is to include the failure potential as part of the simulation process necessary to

account for the random mistuning. That is, in addition to generating random properties of the blades, the state of the dampers, failed or intact, will also be simulated according to the stated probability of failure, and the corresponding response will be evaluated. Then, the usual statistics, i.e. the 95th percentile here, of the response can be evaluated and their minimization performed with respect to the location of dampers and intentional mistuning pattern.

Another, similar but not quite identical, approach is to recognize that the potential failure of the dampers creates a series of scenarios differing by how many and which dampers remain active. A probability can be associated with each scenario and the expected value over the ensemble of scenarios of a cost function $C(A)$ of the random amplitude A can be determined. Then, denoting by the probability of failure of a damper and assuming that the state (failed/intact) of different dampers are statistically independent random variables, it can be shown that

$$\begin{aligned} E[C(A)] \;=\; & (1-P_f)^p \; C\left(A^{(p)}\right) + P_f \; (1-P_f)^{p-1} \left[\sum_{l=1}^{p} \; C\left(A_l^{(p-1)}\right) \right] \\ & + P_f^2 \; (1-P_f)^{p-2} \left[\sum_{\substack{k,l=1 \\ k \neq l}}^{p} C\left(A_{kl}^{(p-2)}\right) \right] + \cdots \end{aligned} \tag{5}$$

where $E[\cdot]$ is the expected value operator. Further, $C\left(A^{(p)}\right)$ denotes the cost function in the absence of any damper failure. Similarly, $C\left(A_l^{(p-1)}\right)$ is its value but for the disk in which the lth damper has failed. Next, $C\left(A_{kl}^{(p-2)}\right)$ is the cost function after the kth and lth dampers have failed, and so on.

It should be noted that Eq. (5) has been obtained under the assumption of an equal probability of failure for all dampers but it is readily extendable to the situation where this probability varies with damper, e.g. is dependent on either the blade (A or B) on which it is installed.

The application of Eq. (5) is limited to well specified cost functions $C(A)$, although not necessarily moments, but for $C(A) = A$ it would yield the mean and for $C(A) = A^2$ the mean square value. Using these two quantities, one can then easily obtain the mean plus twice or thrice the standard deviation which could be used as the representative amplitude for the optimization process.

Each of the above two options to incorporate the probability of damper failure in the optimization process has its advantages and drawbacks. The incorporation of the probability of failure directly in the Monte Carlo simulation is convenient and permits the estimation of any statistics of the amplitude of blade response, e.g. mean, 95th percentile. Unfortunately, it is more challenging to use, e.g. larger number of samples to be considered, when the probability of damper failure becomes very small. This is not an issue with the formulation based on Eq. (5) in which the dependence on P_f is explicit. However, Eq. (5) is not applicable to the 95th percentile of the amplitude, used so far, as this quantity cannot in general be expressed as an expected value of a function of the random amplitude.

For the probabilities of damper failure considered here, 0.01 or higher, the capture of failure events has not been found to be a problem with the simulation option and thus this approach has been followed as it permits the consideration of

the 95th percentile and thus a direct comparison with prior results. Then, shown in Figure 9 and Figure 10 is the 95th percentile of the maximum blade response obtained for the models of Figure 1 and Figure 2 respectively for probabilities of dampers failure of 0.01, 0.03 and 0.10, plotted with the results obtained without damper failure. As expected, an increase in the 95th percentile of the response is obtained when dampers can fail. The significance of this increase is however variable, noticeable for the one-degree-of-freedom per blade model but quite small for the blisk model. In fact, it seems the effect of the damper failure is correlated with the importance of the intentional mistuning effect: when the latter is strong (i.e. the blisk case), the damper failure only affects minimally the response. This observation seems to indicate the robustness of the intentional mistuning pattern.

The probability of damper failure may be difficult to estimate in practical situations and thus it is of interest to assess how well the solution optimized without considering the possibility of this event performs when failure does take place. This analysis was performed first for the single degree of freedom per sector model, see Figure 16. Clearly, there is a notable increase in 95th percentile of response that results from an unexpected/unaccounted for probability of failure, compare the curves in blue to those in red. In such a situation, it seems important to account for the possibility of damper failure.

In the case of the blisk model, however, the optimum solutions obtained with or without the possibility of failure were found to be same when this probability is small. This result is not unexpected in view of the close matching of

the results of Figure 10 for different probabilities of failure (0, 0.01, 0.03, and 0.10). For this model, it was decided to plot the evolution with the probability of failure of the optimum solution, see Figure 17. Note on these figures that the regular dots correspond to the solution obtained without damper failure. The solutions associated with the circled dots exhibit the same intentional mistuning pattern as the solution without damper failure but with different locations of dampers. Finally, the solutions associated with the squared dots are different in both intentional mistuning pattern and damper location from the one obtained without damper failure. It is seen that for a probability of failure below 0.15, the damper failure affects neither the optimum intentional mistuning pattern nor the optimum locations of the dampers. These locations appear to be the first one to be affected by the probability of failure.

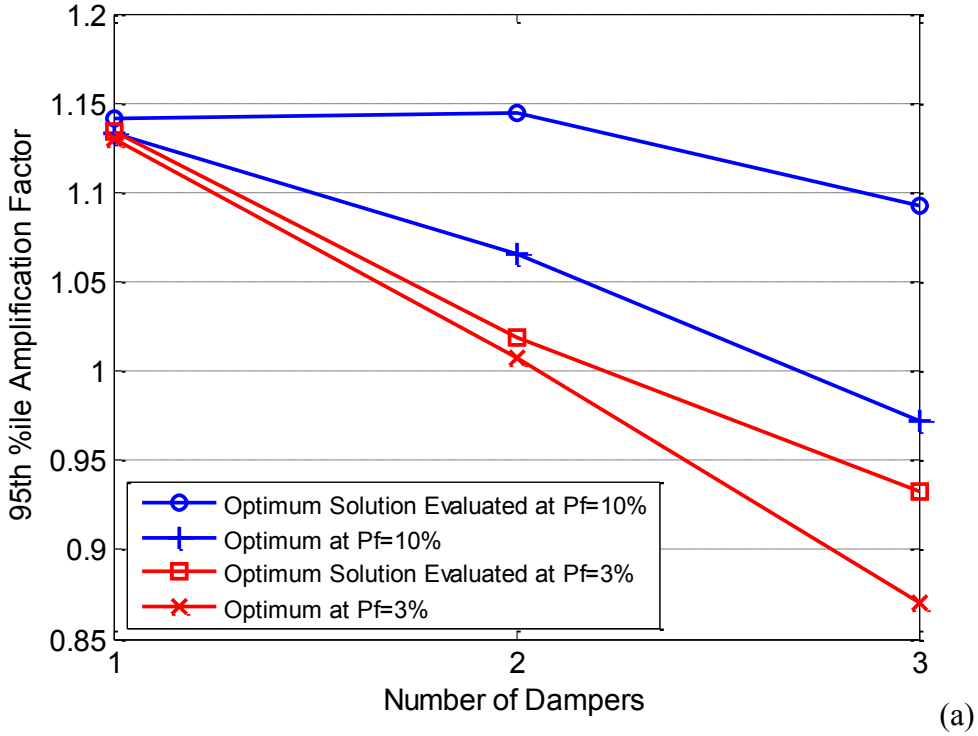

(a)

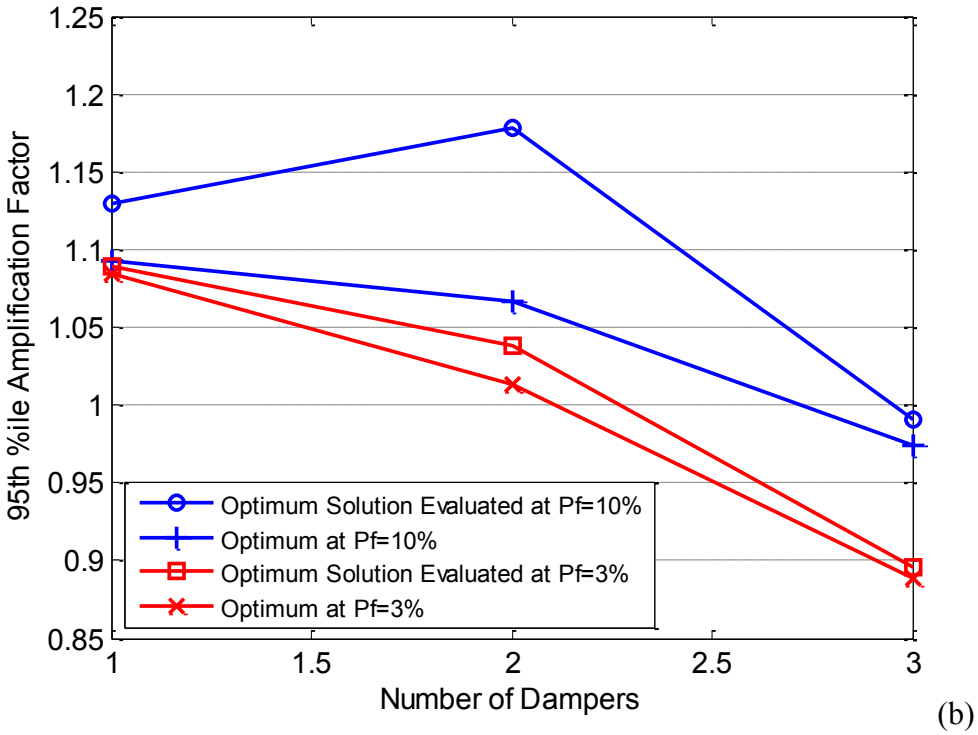

(b)

Figure 16. Comparison of solutions vs. number of dampers, single degree of freedom per sector model, (a) engine order 2 excitation, and (b) engine order 4 excitation.

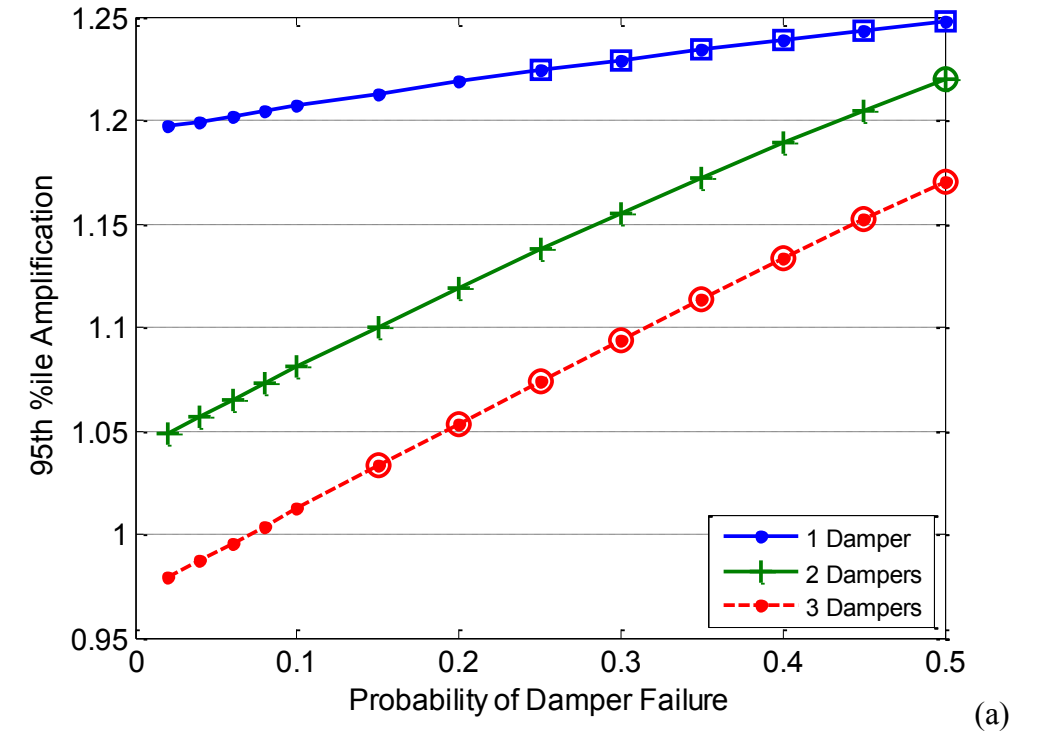

(a)

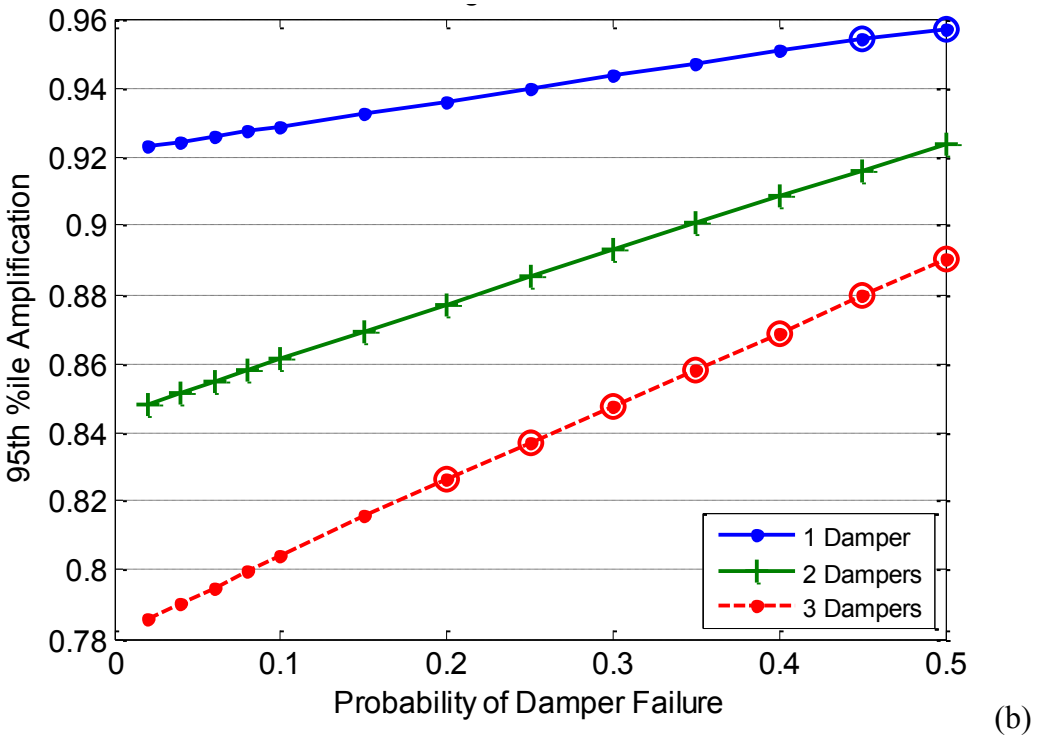

(b)

Figure 17. Comparison of solutions vs. number of dampers, blisk reduced order model, (a) engine order 1 excitation, and (b) engine order 2 excitation.

3.5 Validation of Optimization Algorithms on Larger Bladed Disk Models

Bladed disks used in industry typically carry a larger number of blades than the models that were used in the previous sections. Therefore, in order to assess the validity of the developed optimization algorithm on bladed disks with larger number of blades, four further validation cases were considered. The assessment was done in two parts, one to test the validity of the algorithm in finding the correct/optimum intentional mistuning pattern/s, and the other to test the validity of the algorithm in finding the correct/optimum damper locations on the disk.

The algorithm was first applied to an industrial 17 blade impeller, and an optimization of the intentional mistuning pattern was carried out both without and with random mistuning present in the system. This impeller shows a different geometry and hence a different level of blade to disk coupling than the two systems considered previously and is a good test case for the algorithm.

The identification of the best intentional mistuning pattern without the presence of random mistuning was considered first. To aid in the comparison, an exhaustive search of the 7712 intentional mistuning patterns of the 17 blade impeller was carried out and the best five patterns obtained are tabulated in Table 2 that follows. The optimization algorithm was then applied using the subspace strategy with a constraint on two consecutive sectors. Table 2 shows also the results of the subspace strategy. It can be observed that the subspace strategy is successful in converging to the optimum solution as found by the exhaustive search. In fact, the algorithm converges successfully to one of the top five

optimum patterns in a large number of cases, and in the cases where it does not converge to the top five solutions, the error margin between the solution found and the optimum is reasonably small (of the order of a few percent for most cases).

Table 2. Performance of optimization algorithms on 17 blade industrial impeller

Full Search		AB/BA Subspace		AA/BB Subspace	
Pattern	Amp. Factor	Pattern	Amp. Factor	Pattern	Amp. Factor
C6A2C3A CAC2A	0.8566	C6A2C3A CAC2A	0.8566	3C5A2C7 A	0.8886
3C7A2CA C2A	0.8640	CAC2AC AC3ACA C3A	0.8848	3C5A2C7 A	0.8886
CAC2AC AC3ACA C3A	0.8848	CAC2AC AC3ACA C3A	0.8848	C4A3C3A 5CA	0.9451
3C5A2C7 A	0.8886	C2AC2A CA2CAC AC3A	0.9372	4C7A2C4 A	0.9615
2C6AC4A CACA	0.8887	C3A2CA C2A4C3A	0.9789	17C	1.0000

The optimization algorithm was then used to optimize the intentional mistuning pattern to lead to the minimum blade response in the presence of random mistuning (here considered as a 2 percent standard deviation on the Young's Modulus of the blade). The five best intentional mistuning patterns without random mistuning were considered as initial conditions for the algorithm, and the random mistuning was then included as part of the local search. The

results of the optimization are shown in Figure 18, which shows the amplification factor versus the level of mistuning. Also shown in the figure is the tuned system as well as the best three intentional mistuning patterns without random mistuning. It can be observed that the converged solutions of the optimization with random mistuning show higher response when there is no random mistuning in the system, but have a considerably smaller level of response at 2 percent of random mistuning where they were optimized. The results show the validity of the optimization algorithm in predicting the intentional mistuning patterns for models with a larger number of blades.

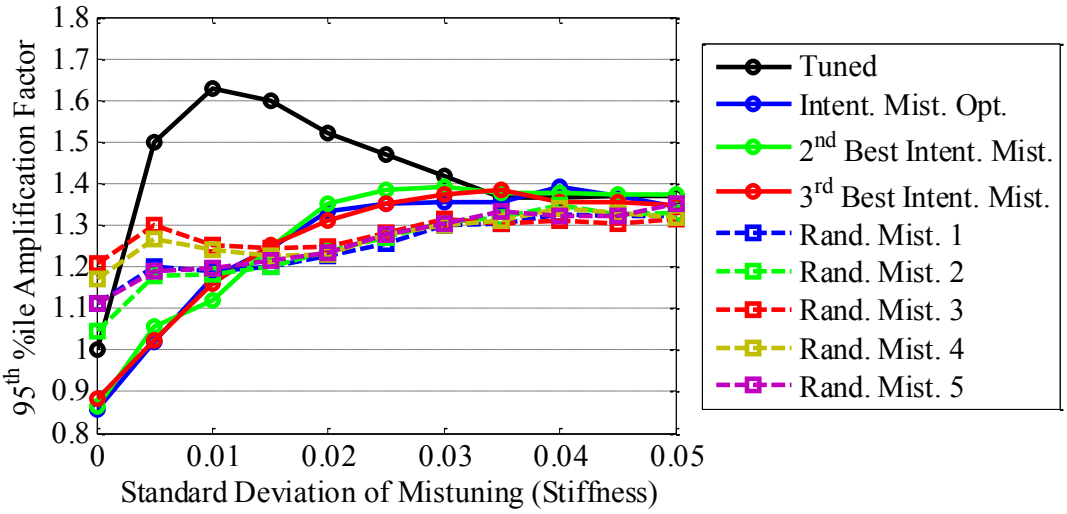

Figure 18. Normalized peak response vs. level of random mistuning, 17 blade industrial impeller model.

In order to test the validity of the optimization algorithm in finding the correct/optimum damper locations on larger bladed disk models, three validation cases were considered: a 24 blade blisk, a 37 blade blisk and finally a 49 blade blisk. Considered here was the REDUCE reduced order model (see [11]) of the blisk with a modification (an increment of the number of blades from 24 to 37 and 49) of the one considered in [12].

Shown below are the model and results of the performance of the optimization algorithm for the 24 blade blisk model. The results were compared, as before, to an exhaustive search of all possible damper locations on the bladed disk. Only the P1 and the P2 problems were considered for this effort, with a limited number of full exhaustive search validations, due to the computationally demanding nature of the problem. Similar computations were carried out with both the 37 and 49 blade models, but without a full exhaustive search in the interest of time. The results show expected trends, and support the validity of the application of the optimization algorithm developed on larger models.

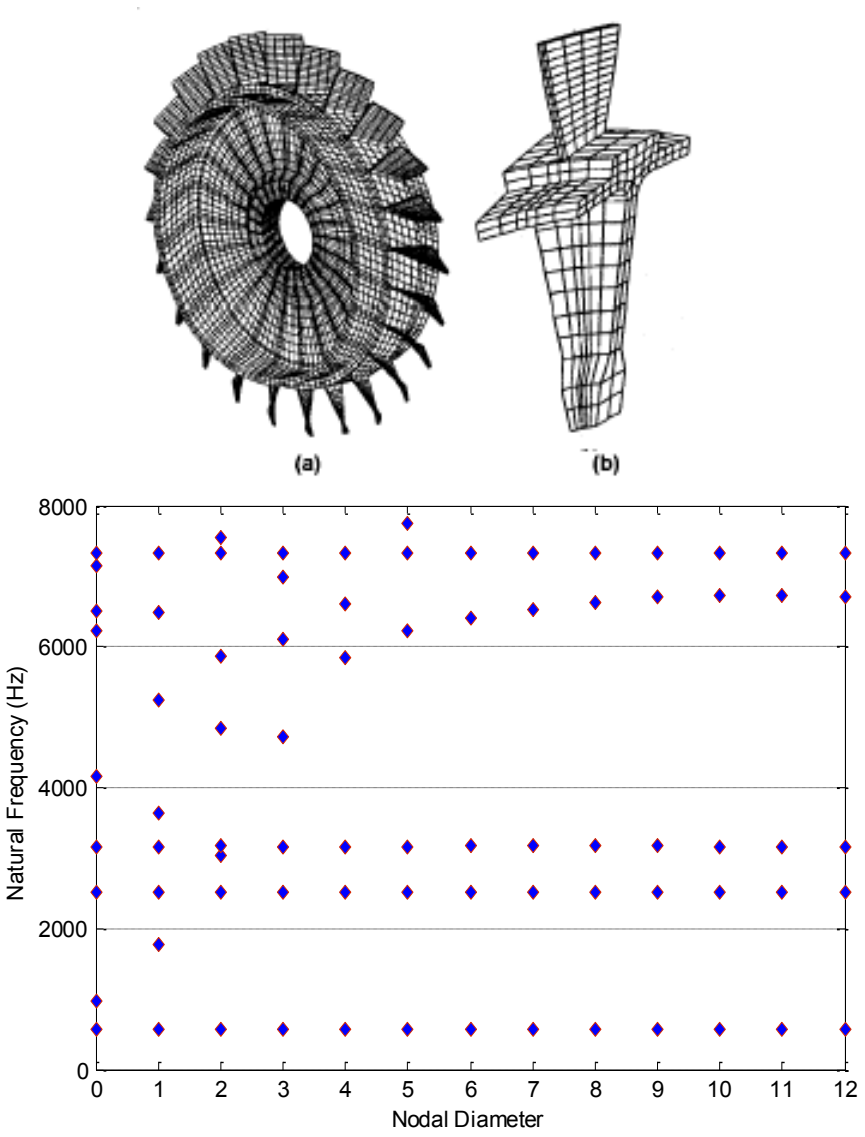

(c)

Figure 19. 24 blade blisk example: (a) blisk view, (b) blade sector finite element mesh, and (c) natural frequencies vs. nodal diameter plot (box showing frequency range of sweep).

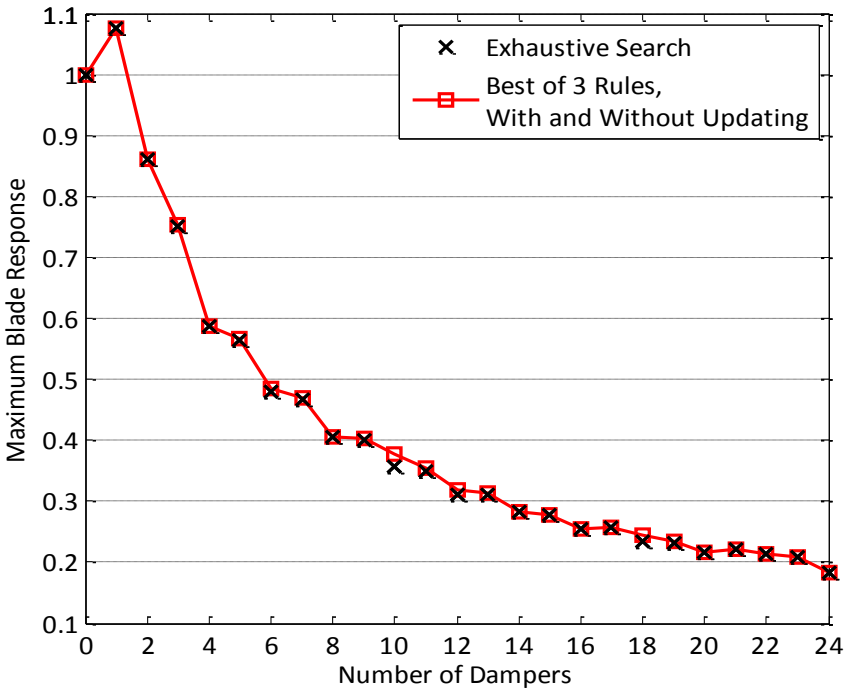

(a)

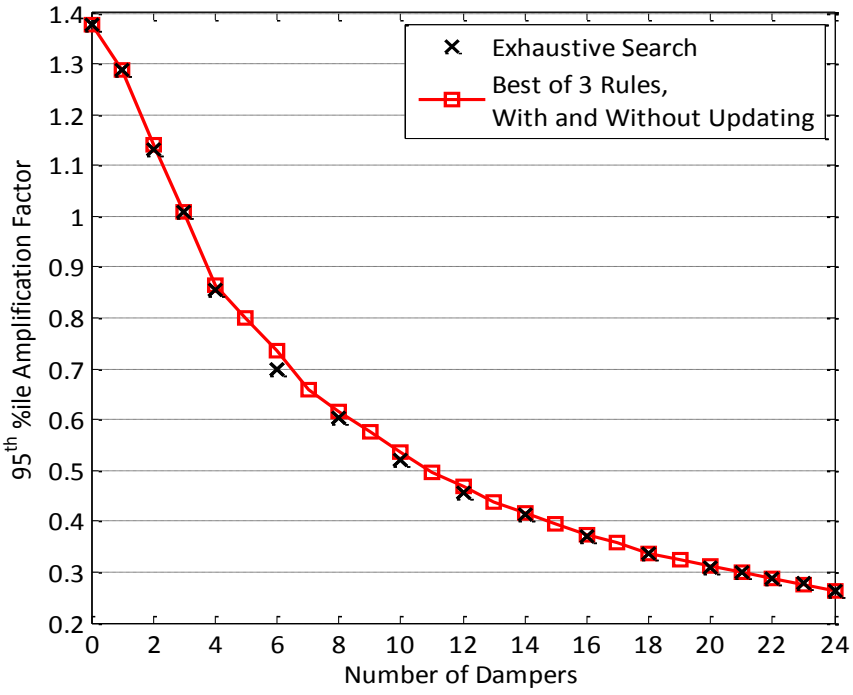

(b)

Figure 20. Normalized peak response vs. number of dampers for different options, 24 blade blisk model, (a) P1 Problem, (b) P2 Problem.

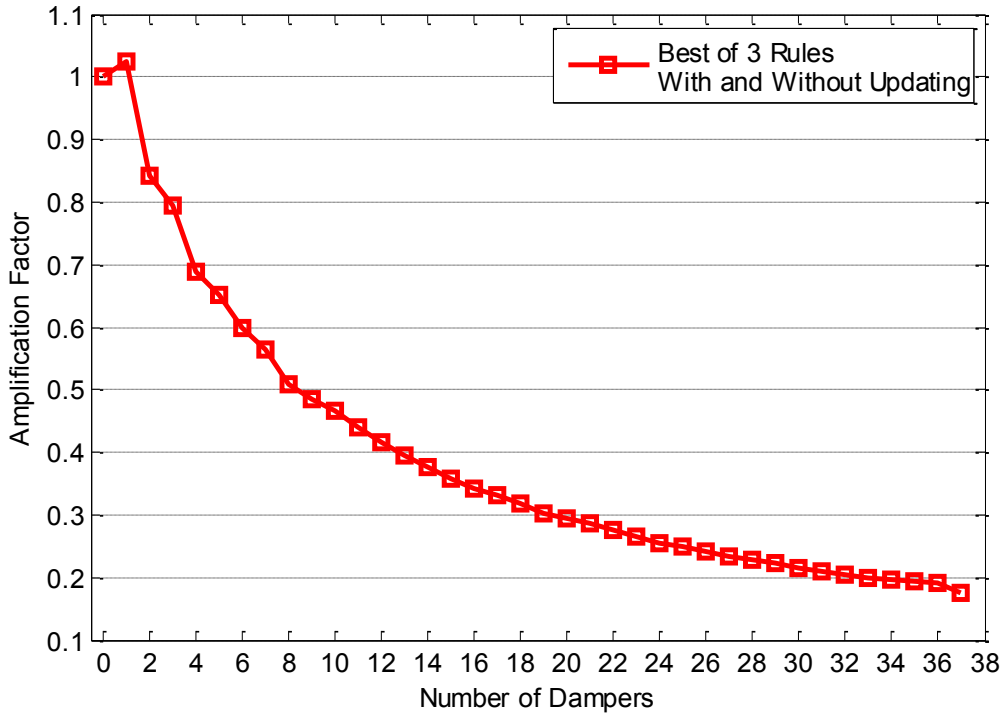

(a)

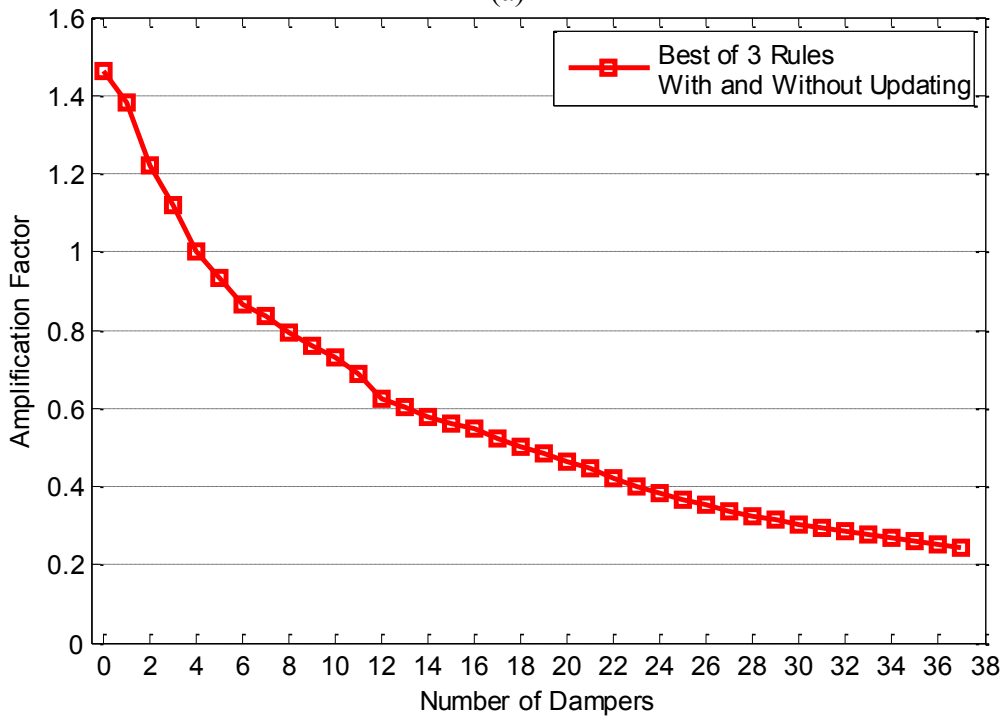

(b)

Figure 21. Normalized peak response vs. number of dampers for different options, 37 blade blisk model, (a) P1 Problem, (b) P2 Problem.

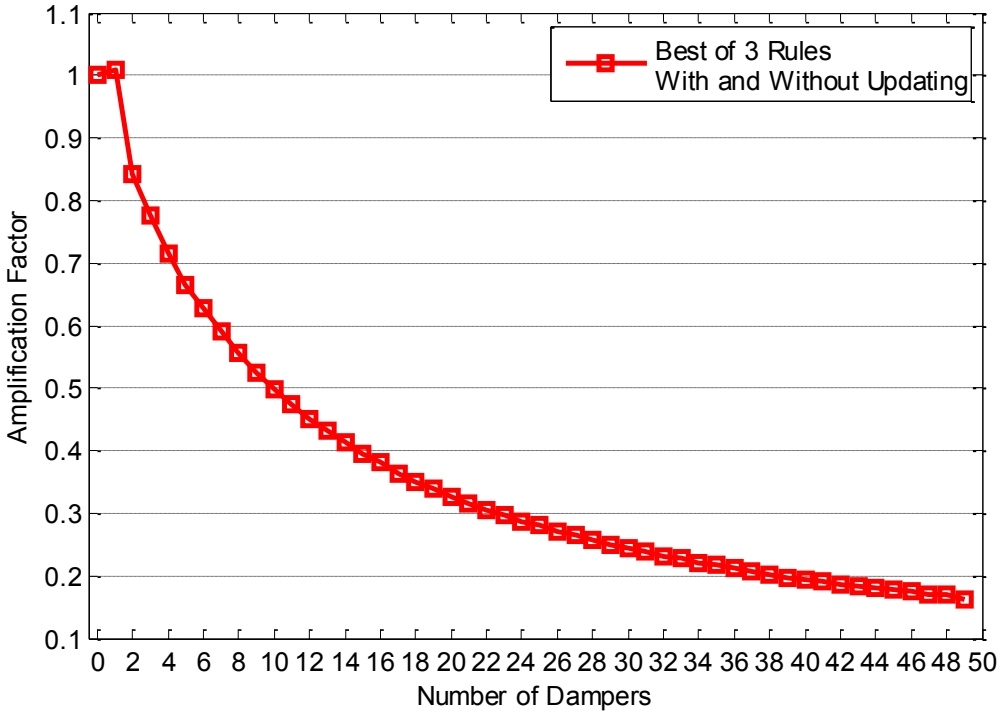

(a)

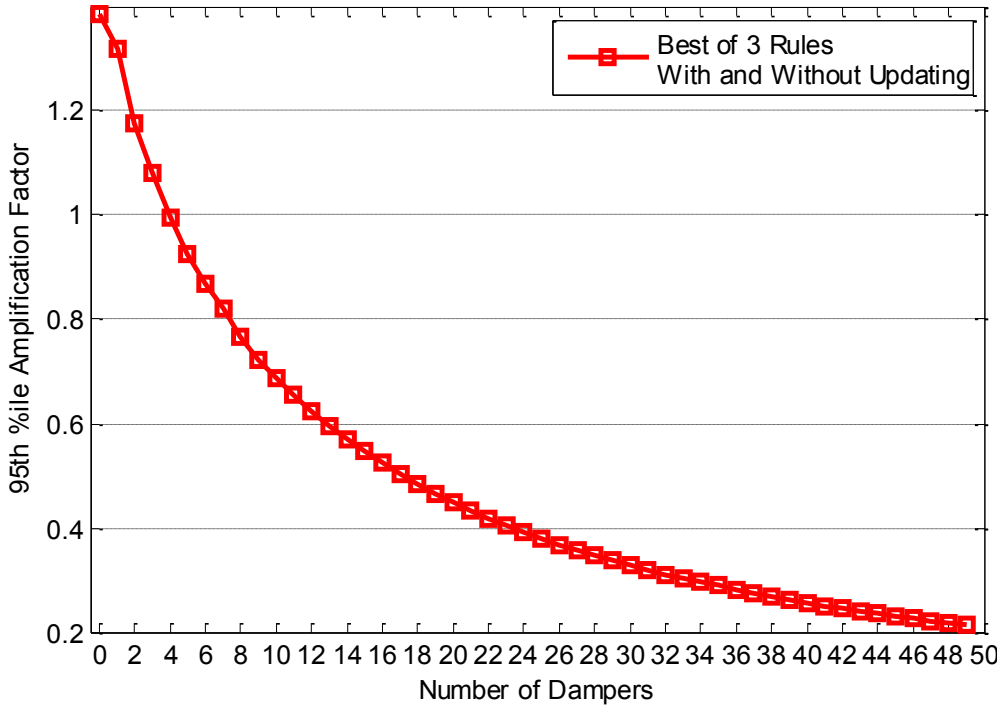

(b)

Figure 22. Normalized peak response vs. number of dampers for different options, 49 blade blisk model, (a) P1 Problem, (b) P2 Problem.

4 – APPLICATION TO LINEAR BLADE-BLADE AND NONLINEAR FRICTION DAMPERS

4.1 Linear Blade-Blade Dampers

The original effort of [1] and the results of the previous chapter all focused on dampers acting on single blades, i.e. blade-alone or blade-disk dampers. There are however dampers (friction dampers most notably) that act between two blades and the question arises whether similar results as obtained for blade-alone dampers would be observed for blade-blade dampers.

Accordingly, such dampers were considered and the first task was the determination of their performance in the absence of mistuning, both random and intentional, i.e. the "P1 problem" defined in the previous chapter and in [1]. In the absence of a physical model of a bladed disk with a blade-blade damper, the single degree of freedom per sector model of Figure 1 was again selected. Then, shown in Figure 23 is the maximum amplification factor obtained in the P1 problem as a function of the number of dampers used. The value of the damper coefficients was maintained at $C/c = 10$ (i.e. a blade in the tuned system with dampers would exhibit 10 times the damping it has without) to permit a comparison with the corresponding blade-disk dampers results, see Figure 24.

The comparison of these results suggests that the blade-blade dampers are as efficient in diminishing the amplitude of blade response as their blade-disk counterparts. This finding of the P1 problem also holds for the P2 and P3 problems, i.e. the 95th percentile of the maximum amplification of blade response

with random mistuning without or with intentional mistuning, see Figure 25, Figure 26, and Figure 27. In these figures, note that the single apostrophe ‘ following a blade type denotes the location of a blade-alone damper on the blade preceding it or a blade-blade damper between the two blades adjacent to the ‘. Further, the notation “Damp_Int_xx’ denotes the P3 problem (damper and intentional mistuning) with xx dampers. Finally, as in the previous blade-disk case, the optimization effort was carried out for a standard deviation of random stiffness mistuning equal to 1% of its mean value and blades B (respectively, A) had natural frequencies 5% higher (respectively, lower) than the tuned blades. The locations of the dampers for the various solutions shown in Figure 27 are presented in Table 2.

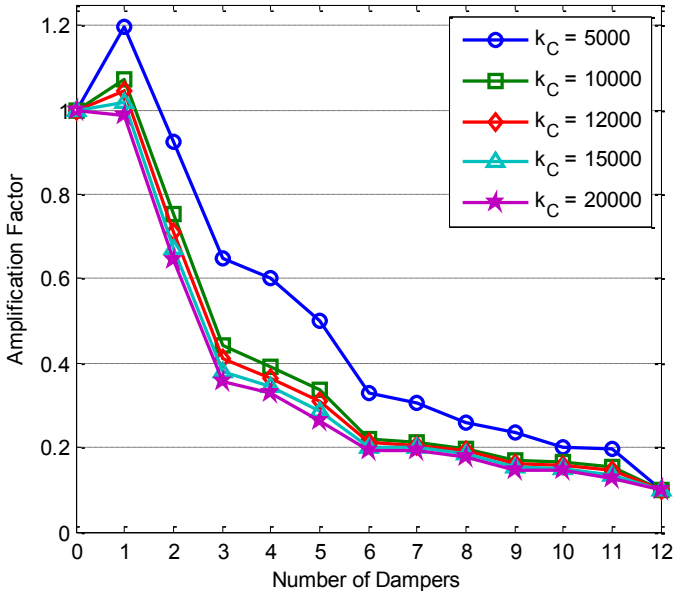

Figure 23. Amplification factor of the maximum blade response as a function of the number of optimized dampers for different values of k_c. P1 problem, blade-blade dampers, $r = 2$, and $C/c = 10$.

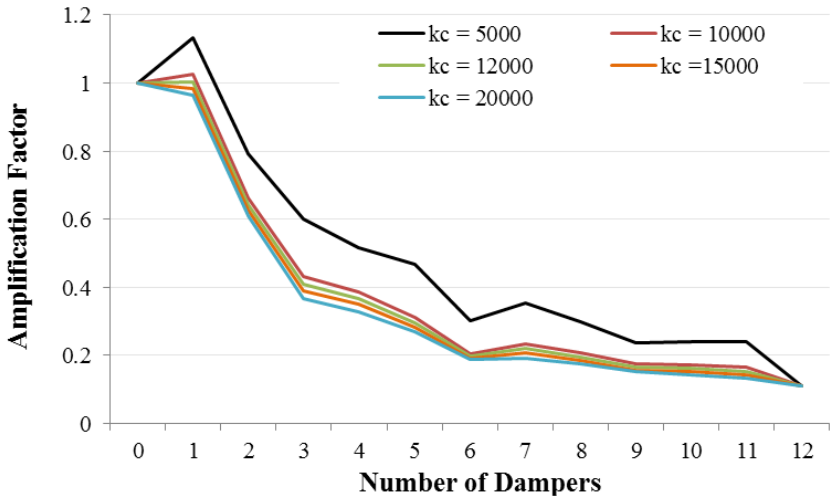

Figure 24. Amplification factor of the maximum blade response as a function of the number of optimized dampers for different values of k_c. P1 problem, blade-disk dampers, $r = 2$, and $C/c = 10$ (from [1]).

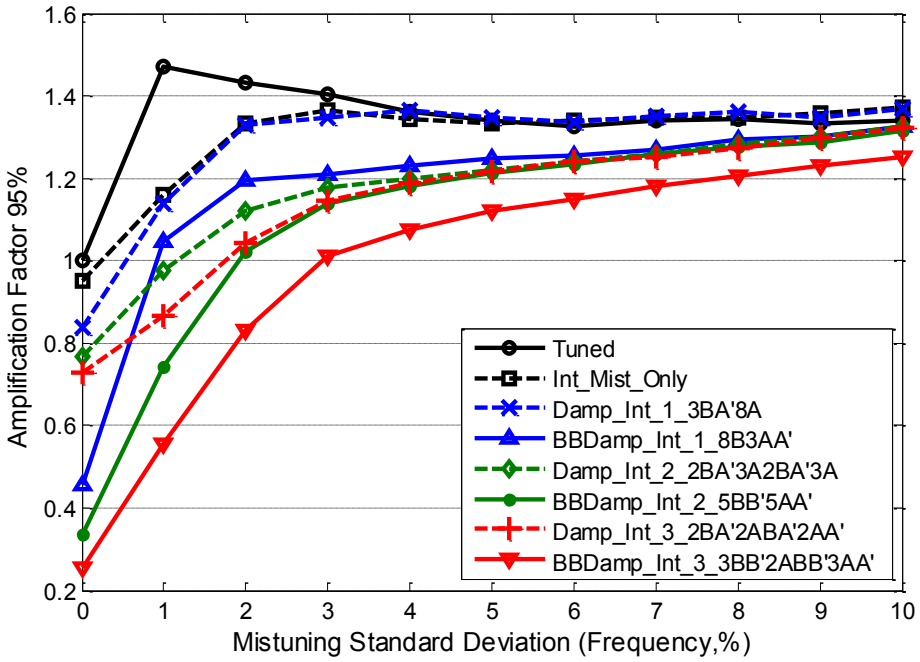

Figure 25. 95th percentile of the maximum blade response vs. standard deviation of random mistuning. Single degree of freedom per sector model, $C/c = 10$, optimization carried out at 1%, $r = 2$, with intentional mistuning level = 5%. Blade-disk (Damp) and blade-blade (BBDamp) dampers.

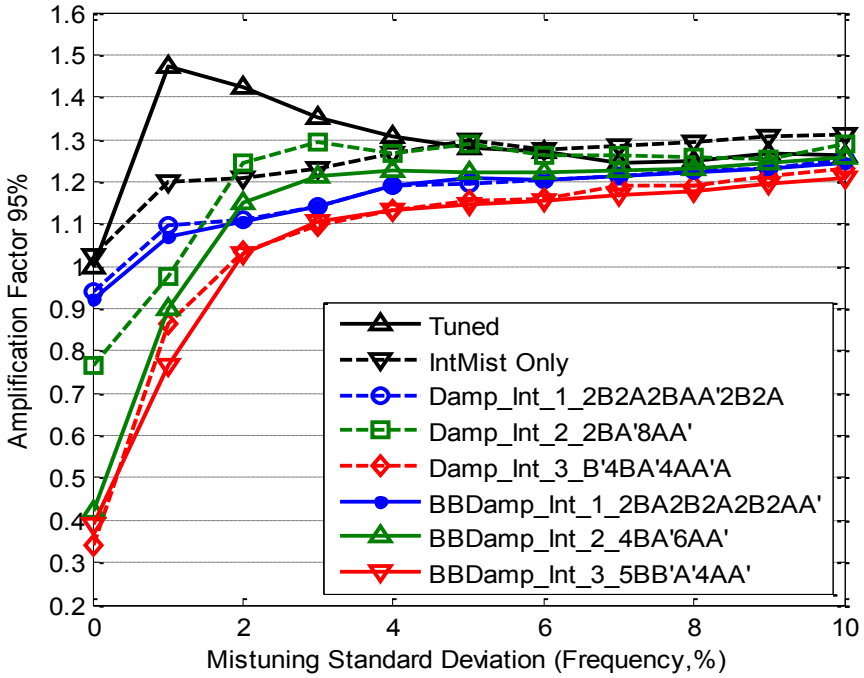

Figure 26. 95th percentile of the maximum blade response vs. standard deviation of random mistuning. Single degree of freedom per sector model, $C/c = 10$, optimization carried out at 1%, $r = 4$, with intentional mistuning level = 5%. Blade-disk (Damp) and blade-blade (BBDamp) dampers.

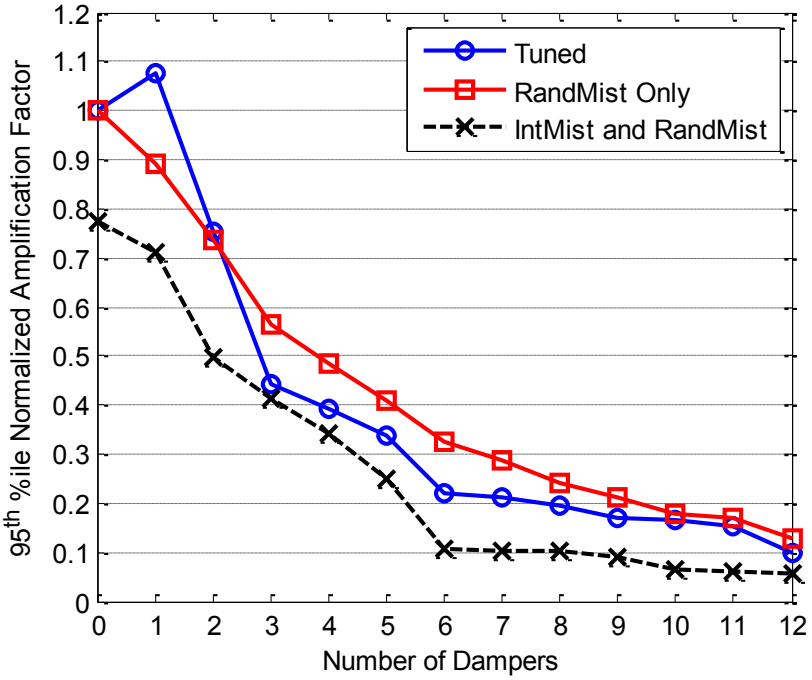

Figure 27. Normalized peak response vs. number of blade-blade dampers for different options, single degree of freedom per sector model, engine order 2 excitation.

Table 3. Optimum damper locations, system of Figure 27.

		Blade-Disk Dampers	Blade-Blade Dampers
1Damper	P1	1	1
	P2	1	1
	P3	3	11
	Pt	BBAAAAAAAABB	BBBBBBBAAAAB
2 Dampers	P1	1,3	1,5
	P2	1,2	1,6
	P3	2,11	3,9
	Pt	BAAAAAAAAAAB	BBBAAAAAABBB
3 Dampers	P1	1,3,5	1,6,8
	P2	1,3,5	1,2,5
	P3	2,8,10	2,6,10
	Pt	BAAAAAAABAAA	BBAABBAABBAA
4 Dampers	P1	1,3,5,7	1,3,4,9
	P2	1,2,7,8	1,2,7,9
	P3	1,2,6,8	3,9,6,12
	Pt	ABBBBBBAAAAA	BBBAAABBBAAA
5 Dampers	P1	1,3,5,7,9	1,2,6,8,10
	P2	1,3,5,8,10	1,3,6,7,11
	P3	2,4,6,10,12	1,3,5,8,10
	Pt	AAABBAAAAAAA	BABABAAABABB
6 Dampers	P1	1,2,4,6,9,11	1,2,5,6,9,10
	P2	1,3,4,6,8,11	1,3,5,7,9,11
	P3	2,4,6,8,10,12	2,4,6,8,10,12
	Pt	BAABBAABBAAB	BABABABABABA
7 Dampers	P1	1,2,3,5,7,9,11	1,2,4,6,7,9,11
	P2	1,3,5,7,8,9,11	1,2,3,6,7,9,10
	P3	1,3,5,7,8,10,12	1,2,4,5,7,9,11
	Pt	BBBBBBAAAAAA	BABBABABABAB
8 Dampers	P1	1,2,3,5,7,9,10,11	1,2,3,5,6,7,10,11
	P2	1,3,4,6,7,9,10,11	1,2,3,4,7,8,9,10
	P3	1,2,4,5,7,8,10,12	1,2,3,5,7,8,9,11
	Pt	BBBBBBAAAAAA	BAABABBAABAB
9 Dampers	P1	1,2,3,4,6,7,8,10,12	1,2,3,5,6,7,9,10,11
	P2	1,2,3,5,6,7,9,10,11	1,2,3,5,6,7,9,10,11
	P3	1,2,4,5,7,8,9,10,12	2,3,5,6,7,8,10,11,12
	Pt	BBBBBBBAAAAA	BBABABBABBAA
10 Dampers	P1	1,2,4,5,6,7,8,9,11,12	1,2,3,4,5,7,8,9,10,11
	P2	1,2,3,4,5,6,8,9,10,11	1,2,3,5,6,7,8,9,10,12
	P3	1,2,3,5,6,7,8,9,11,12	1,2,3,4,5,7,8,9,10,11
	Pt	ABBBBBABBBBB	BABBABBABBAB
11 Dampers	P1	1,2,3,4,5,6,7,8,9,10,11	1,2,3,4,5,6,7,8,9,10,11
	P2	1,2,3,4,5,6,7,8,9,10,11	1,2,3,4,5,6,7,8,9,10,12
	P3	1,2,3,4,5,7,8,9,10,11,12	1,2,3,4,5,6,8,9,10,11,12
	Pt	BBABBBBBAABA	BABABABBABAB

4.2 Optimization with Uncertainty on Dampers

The variability of the mass and stiffness properties from one blade to another have long been recognized to exist and be important and these observations have formed the basis for mistuning analyses. The variability of the blades damping coefficients has also been considered, although less frequently (e.g. see [17,18]), and increases in blade response have also been observed, albeit less dramatic than those created by blade to blade stiffness and mass variations. These observations suggest that a variability/uncertainty in the damper coefficients may result to a degradation of performance, i.e. an increase in the maximum blade response, and ought to be accounted for in the optimization process.

This inclusion was accomplished in a straightforward manner: random variations of the damper properties were included along with the random mistuning to obtain the 95th percentile of the response. Before proceeding with this revised process, it was first desired to perform a robustness analysis in which the optimum solutions obtained in [1] and the previous chapter was kept, but mistuning/variability in the damper properties was introduced. A comparison of the 95th percentiles of the response obtained in this manner with those obtained in [1] and the previous chapter would then provide an assessment of the robustness of the optimum solutions with respect to the damper properties variations. Shown in Figure 28, Figure 29, and Figure 30 are the results of this robustness analysis which suggest that the 20% variation introduced in the damper properties has only marginally affected the response.

This finding is rather surprising as it would seem that varying the damping level in the dampers should induce some difference in the overall response: an increase in these values should tend to decrease the largest blade response and similarly a decrease in the damper constant would be expected to lead to an increase in response of the entire disk. To better understand these results, the response of a particular configuration, the optimum solution of Figure 29 with three dampers with 3% standard deviation of random mistuning, was analyzed with several damper constants: C/c ranging from 8.2 to 11.8 (10 being the design point), see Figure 31. It is seen on this figure that the response of the highest responding blade (blade 9) is nearly independent of the value of the damper constant. It appears that the effect of the dampers is very much localized, affecting only the blades on which they are placed. This situation is not altogether unusual, as it was recognized in [1] that the dampers have a localization effect. Nevertheless, this situation is not the optimum which could have been expected in which a damper is affecting at least somewhat globally the disk, damping energy from several of its neighboring blades.

Since the optimum damper locations and mistuning patterns seem insensitive to variations in the damper constants, it is expected that an optimization effort as in the previous chapter and [1] but with variation of damper properties included in the prediction of the 95th percentile of the response would give very similar results to those obtained in [1]. The comparison of these two sets of optimization results are shown in Figure 32, Figure 33, and Figure 34, fully confirming this expectation.

For completeness, a similar analysis was also conducted for the blade-blade dampers. The results, shown in Figure 35, Figure 36, and Figure 37, demonstrate similar conclusion, i.e. that variations of the damper properties have only a marginal effect in the optimization process and that the sensitivity of the optimal solution to these variations is small.

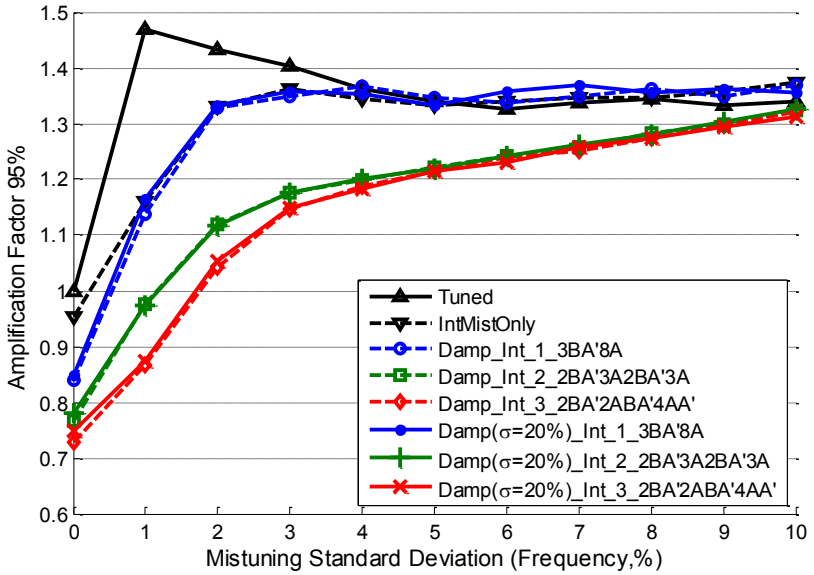

Figure 28. 95th percentile of the maximum blade response vs. standard deviation of random mistuning. Single degree of freedom per sector model, $C/c = 10$, optimization carried out at 1%, $r = 2$, with intentional mistuning level = 5%. Robustness Assessment. Shown without (dashed line) and with (solid lines) random variations in blade-only damper properties (coefficient of variation of 20%).

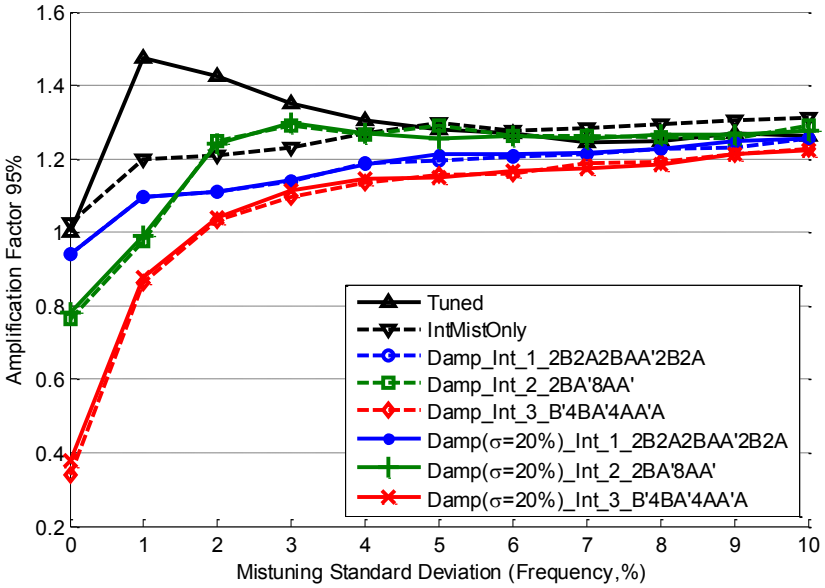

Figure 29. 95th percentile of the maximum blade response vs. standard deviation of random mistuning. Single degree of freedom per sector model, $C/c = 10$, optimization carried out at 1%, $r = 4$, with intentional mistuning level = 5%. Robustness Assessment. Shown without (dashed line) and with (solid lines) random variations in blade-only damper properties (coefficient of variation of 20%).

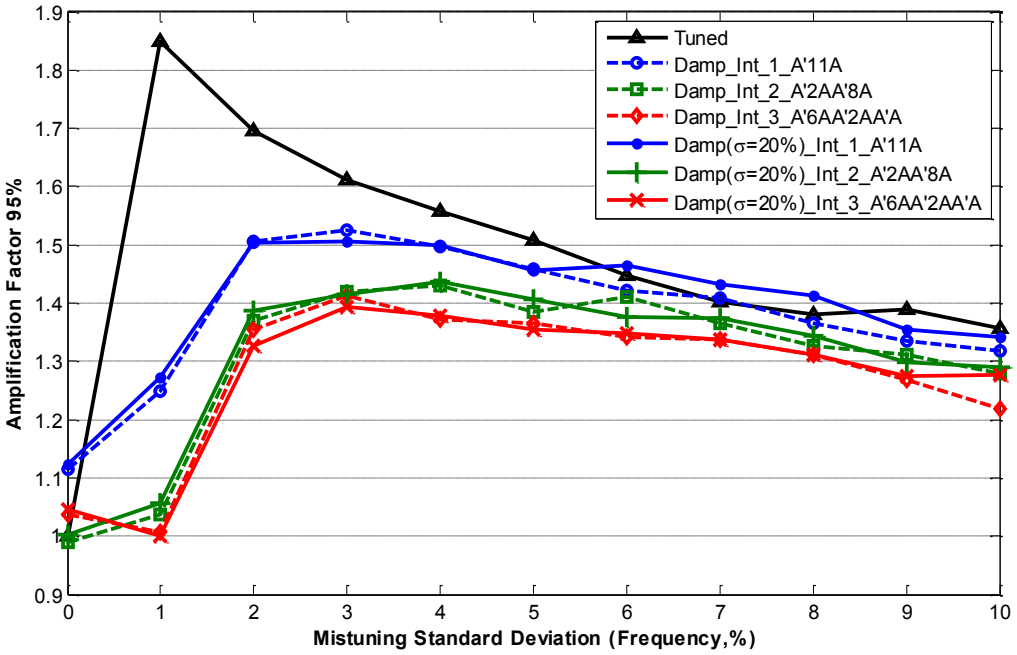

Figure 30. 95th percentile of the maximum blade response vs. standard deviation of random mistuning. Blisk reduced order model, $C/c = 10$, optimization carried out at 1%, $r = 1$, with intentional mistuning level = 5%. Robustness Assessment. Shown without (dashed line) and with (solid lines) random variations in blade-only damper properties (coefficient of variation of 20%).

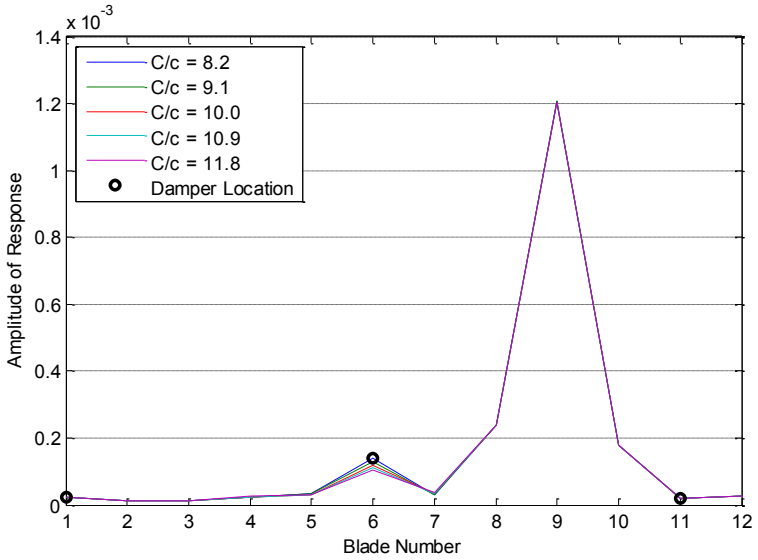

(a)

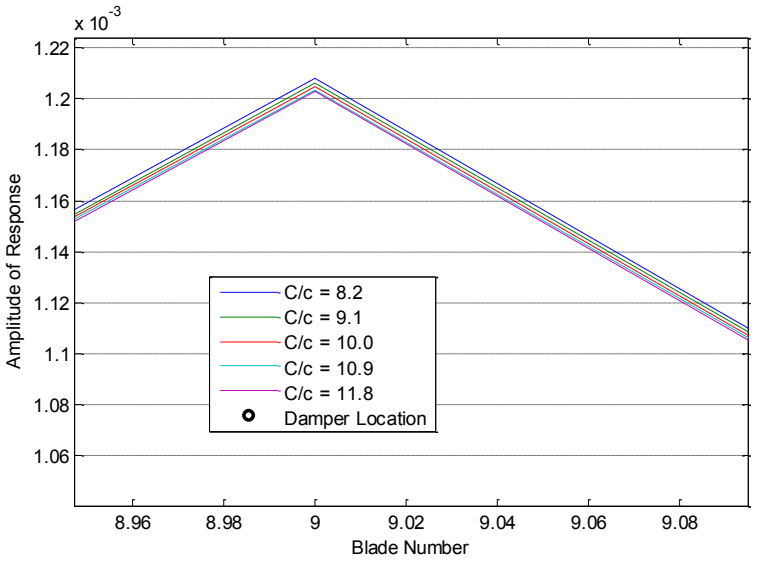

(b)

Figure 31. (a) Amplitude of response of the 12 blades of the disk and at the frequency that yielded the 95th percentile of the response of Figure 29 at 3% standard deviation of mistuning. (b) Same as (a), zoomed.

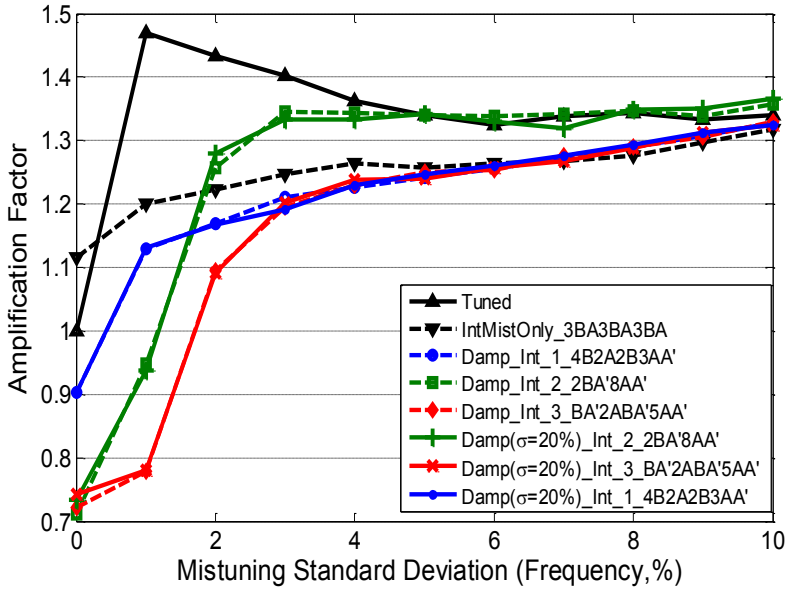

Figure 32. 95th percentile of the maximum blade response vs. standard deviation of random mistuning. Single degree of freedom per sector model, $C/c = 10$, optimization carried out at 1%, $r = 2$, with intentional mistuning level = 5%. Optimization without (dashed line) and with (solid lines) random variations in blade-only damper properties (coefficient of variation of 20%).

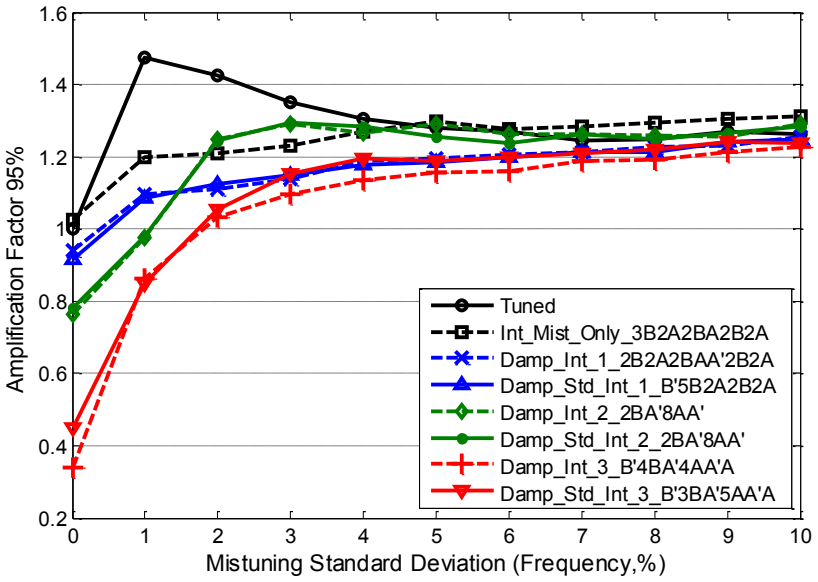

Figure 33. 95th percentile of the maximum blade response vs. standard deviation of random mistuning. Single degree of freedom per sector model, $C/c = 10$, optimization carried out at 1%, $r = 4$, with intentional mistuning level = 5%. Optimization without (dashed line) and with (solid lines) random variations in blade-only damper properties (coefficient of variation of 20%).

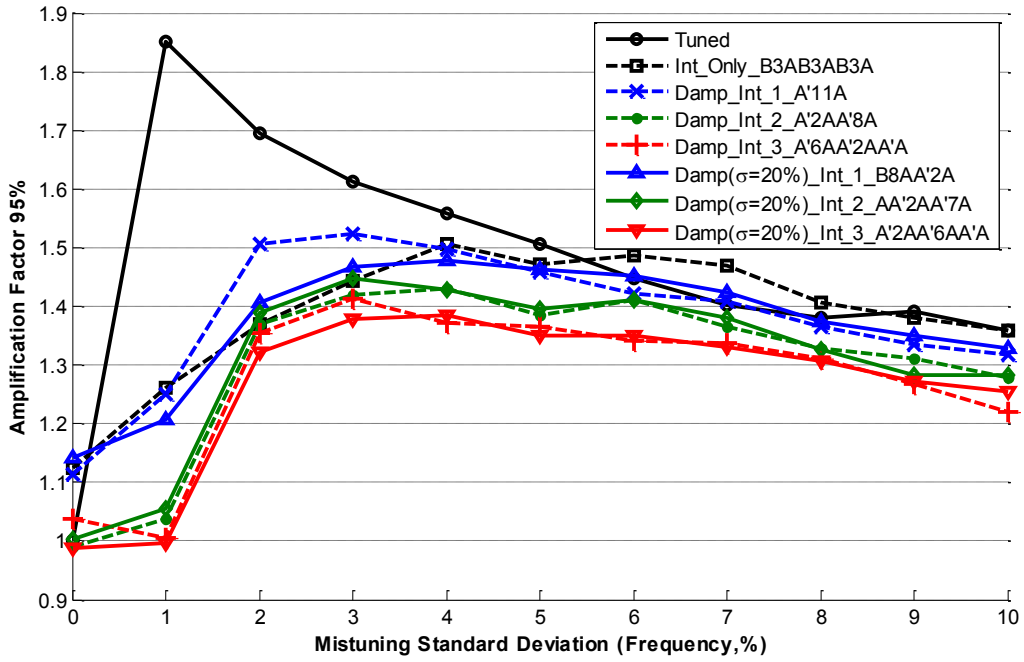

Figure 34. 95th percentile of the maximum blade response vs. standard deviation of random mistuning. Blisk reduced order model, $C/c = 10$, optimization carried out at 1%, $r = 1$, with intentional mistuning level = 5%. Optimization without (dashed line) and with (solid lines) random variations in blade-only damper properties (coefficient of variation of 20%).

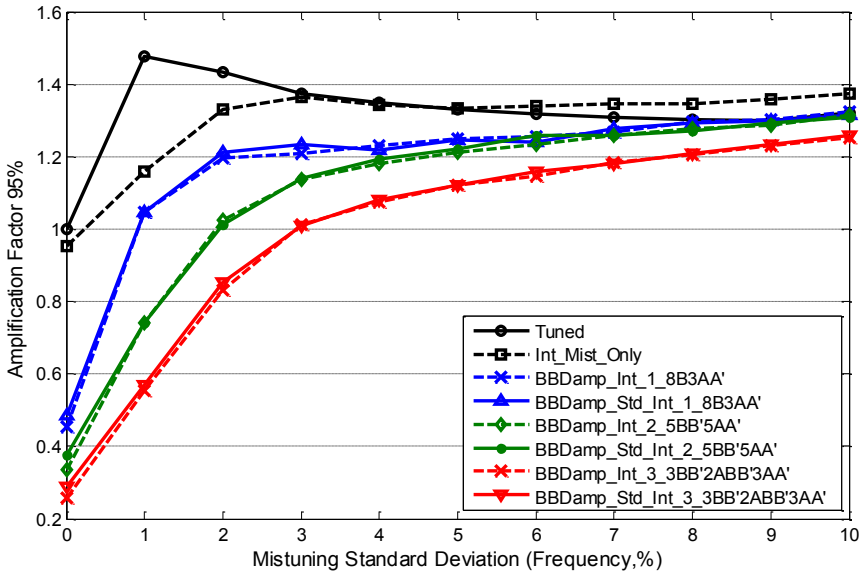

Figure 35. 95th percentile of the maximum blade response vs. standard deviation of random mistuning. Single degree of freedom per sector model, $C/c = 10$, optimization carried out at 1%, $r = 2$, with intentional mistuning level = 5%. Robustness Assessment. Shown without (dashed line) and with (solid lines) random variations in blade-blade damper properties (coefficient of variation of 20%).

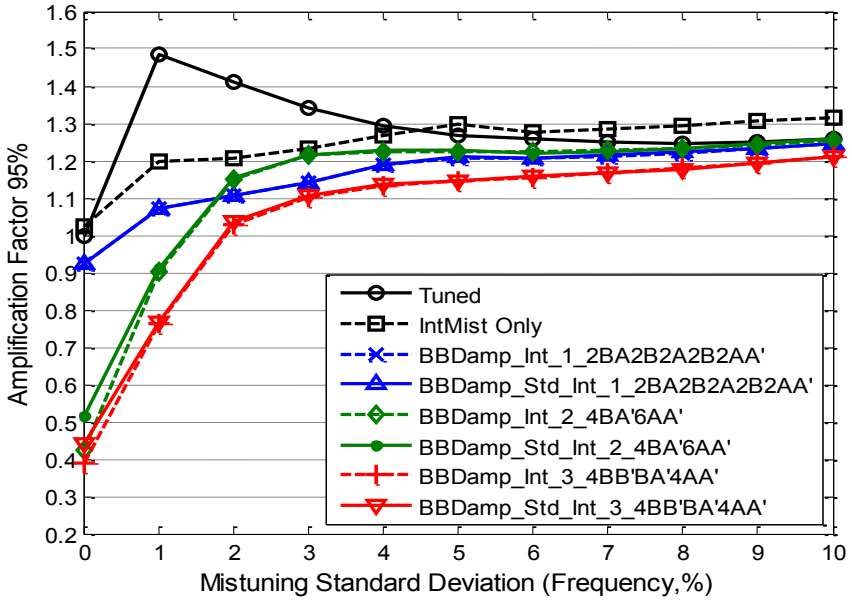

Figure 36. 95th percentile of the maximum blade response vs. standard deviation of random mistuning. Single degree of freedom per sector model, $C/c = 10$, optimization carried out at 1%, $r = 4$, with intentional mistuning level = 5%. Robustness Assessment. Shown without (dashed line) and with (solid lines) random variations in blade-blade damper properties (coefficient of variation of 20%).

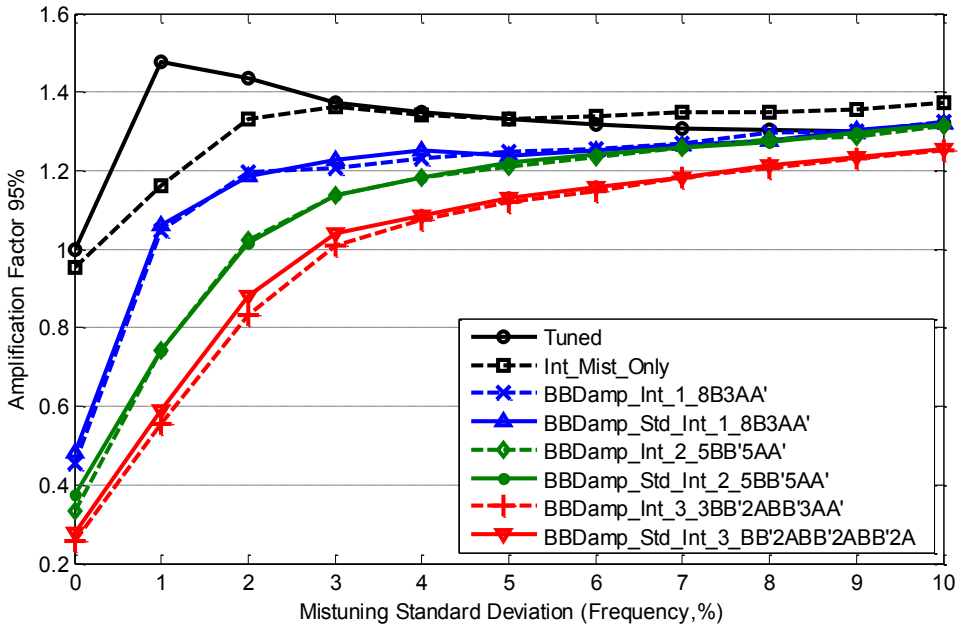

Figure 37. 95th percentile of the maximum blade response vs. standard deviation of random mistuning. Single degree of freedom per sector model, $C/c = 10$, optimization carried out at 1%, $r = 2$, with intentional mistuning level = 5%. Optimization without (dashed line) and with (solid lines) random variations in blade-blade damper properties (coefficient of variation of 20%).

4.3 Nonlinear Applications – Friction Dampers

Many novel damper designs (see [1] for a short review) are expected to exhibit nonlinear properties and thus it was of importance to assess the adequacy of the algorithm of Chapter 3 to this situation and to investigate the benefits of using only a few nonlinear dampers on the disk, as opposed to one on each blade. To exemplify these issues, friction dampers were selected as they are well characterized and are present in a variety of engines, see [19-35] for a sample of the published literature on the modeling and behavior of these dampers. As a first validation of this application, the single-degree-of-freedom model of Sinha and Griffin [19] with blade-ground dampers, see Figure 38, was selected with the properties of Table 3. The nonlinearity of friction dampers implies that the determination of the response of bladed disks including them necessitates appropriate analytical and/or numerical techniques and algorithms. In this regard, the present effort is based on the harmonic balance equations of [19] which are assumed to adequately model the bladed disk behavior but higher order approximations (e.g. see [24]) or direct integration of the equations of motion can used instead. Further, the numerical solution of the harmonic balance equations was accomplished with the MATLAB function *fsolve* (Levenberg-Marquardt algorithm [36]) in a frequency marching scheme through the sweep domain, i.e. the results obtained at one frequency were used as initial conditions for the next one. This algorithm accurately recovered a series of results presented in [22].

The damping obtained with the friction damper in a tuned system is approximately 1% vs. the 0.1% obtained with the present viscous damping. While

the parameters of Table 3 correspond to the optimum for a damper on each blade, they will not in general provide the optimum damping when fewer blades, e.g. if a single one is installed on the disk. Indeed, the damping provided by a friction damper depends on the level of response of the blade on which it is attached which will vary with the number of dampers on the disk. To provide a meaningful assessment of the benefit of using fewer dampers than blades, it is thus necessary to proceed with an optimization of the parameters of the dampers (the normal force was considered here), for each number of dampers on the disk.

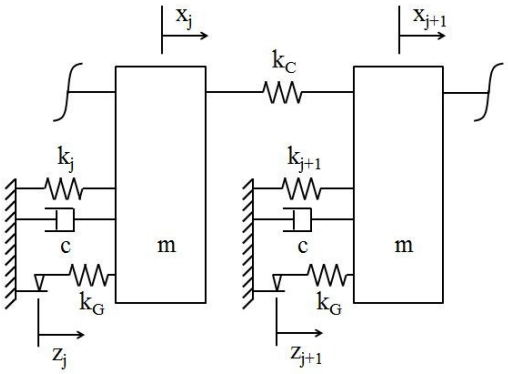

Figure 38. Model of bladed disk with blade-ground friction dampers (from [19]).

Table 4. Parameter values of the model of Figure 38.

Property	**Value**
Number of Blades (N)	12
Mass (m)	0.0114 Kg
Damping coefficient (c)	0.143 Ns/m
Blade-Disk Stiffness (k_i)	430300 N/m
Blade-Blade Coupling Stiffness (K_C)	10000 N/m
Blade-Disk Friction Damper Stiffness (K_G)	43000 N/m
Friction Damper Normal Force ($\mu_f F_N$)	1.505 N
Forcing Amplitude (F_0)	1 N

The optimization problem can be summarized as below, with the primary design variables being the locations of the dampers on the bladed disk and the intentional mistuning pattern when necessary. In this case of nonlinear friction dampers considered, the optimization process includes the optimization of the friction damper coefficient.

The objective is then the minimization of the 95th percentile of the maximum blade response amplitude in a frequency sweep (as determined by the resonance and excitation conditions on the bladed disk) in the presence of random mistuning.

Design Variables

(1)	Locations of N dampers	d_i	$i = 1, 2, \ldots N$
(2)	Intentional mistuning pattern	$b_i = 0 - blade\ type\ A$	$i = 1, 2, \ldots M$
		$b_i = 1 - blade\ type\ B$	
(3)	Optimum Friction Coefficient	μ_i	$i = 1, 2, \ldots N$

Objective

$$\min_{\substack{d_i,\mu_i \\ b_i}} 95\text{th percentile}\left\{\max_{\omega\in\Omega}\left[\max_{j}\left(\text{response of blade } j \text{ at freq } \omega\right)\right]\right\}$$

Constraints

(1) Frequency range of interest $\Omega_{lower} \le \Omega \le \Omega_{upper}$

Ω_{lower} and Ω_{upper} defined according to resonance excitation condition on bladed disk

This prior optimization was carried out through an exhaustive search without random or intentional mistuning, i.e. for the P1 problem. Specifically, the "bucket curve", i.e. maximum amplitude of blade response over the disk vs. slip distance $\mu_F F_N / K_G$ was established for every configuration of N identical dampers on the disk. The configuration and normal force yielding the lowest maximum amplitude of blade response over the disk was then retained as the optimum P1 solution for N dampers. Note that the normal force relates directly to the mass of the friction damper. This process was repeated for $N = 1,2,\ldots M$ and led to the family of optimal bucket curves shown in Figure 39. The corresponding optimal slip distances are shown in Figure 40 vs. the number N of dampers. The behavior of these curves is expected: as the number of dampers is increased, the overall response level of the blades decreases and a lower normal force (thus smaller slip distance) must be applied to achieve the optimum efficiency of the damper between its fully stuck and fully slipping operations. These changes in response and normal force with increasing number of dampers are particularly notable when only a few dampers are present. The very low value of the optimum slip distance for 1 damper is thought to be related to the observed localization induced by the presence of a single damper seen in [1], Chapter 3, e.g. Figure 9, and Figure 10, or in Figure 23, Figure 24, and Figure 27 above. It appears thus that the low slip distance arises to minimize the detrimental localization of the response.

Finally, shown in Figure 41 is the corresponding maximum amplitude of blade response obtained without either random or intentional mistuning the appearance of which is very similar to the one obtained with linear dampers.

Next, the assessment of the effects of random mistuning on this solution and the P2 problem was considered but without any change to the normal forces obtained in the P1 analysis. The corresponding 95th percentile of the amplification factor normalized by its value without any damper was obtained with the subspace algorithm of Chapter 2 and is also shown in Figure 41. Clearly, random mistuning leads to a reduction in the benefits of using only a few dampers, exactly as observed in connection with the linear damper analyses. Further, the introduction of intentional mistuning in addition to the friction dampers (the P3 problem) does increase the robustness against random mistuning and provides a reduction of the amplitude of blade response, see Figure 41.

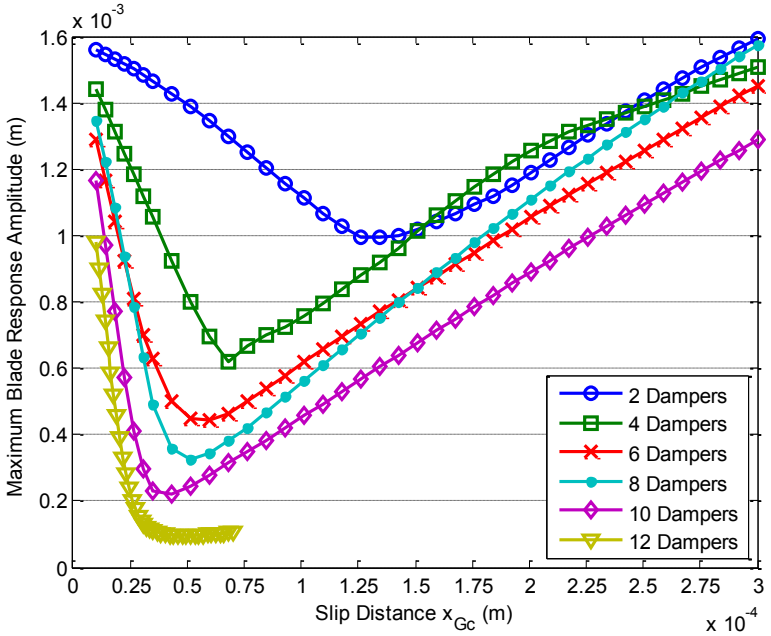

Figure 39. Optimum bucket curves as a function of the number of blade-ground friction dampers.

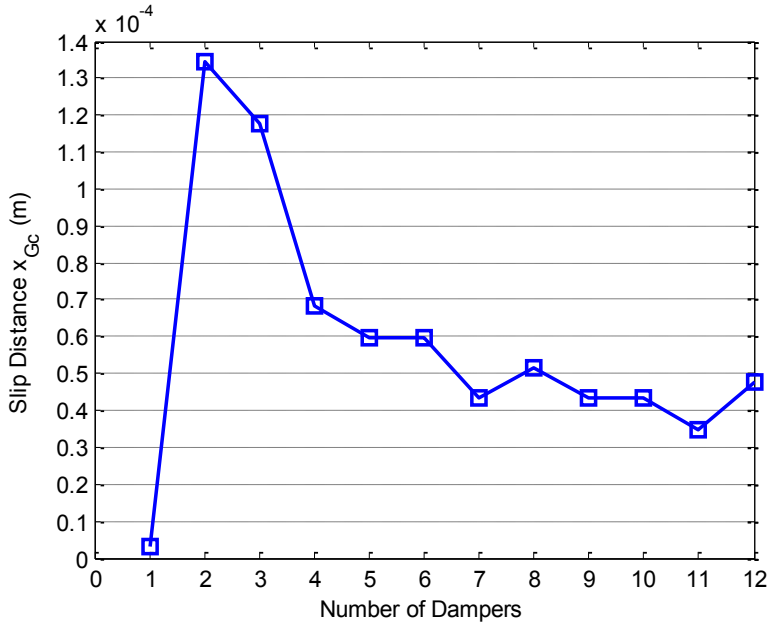

Figure 40. Optimum slip distance $\mu_F F_N / K_G$ as a function of the number of blade-ground friction dampers.

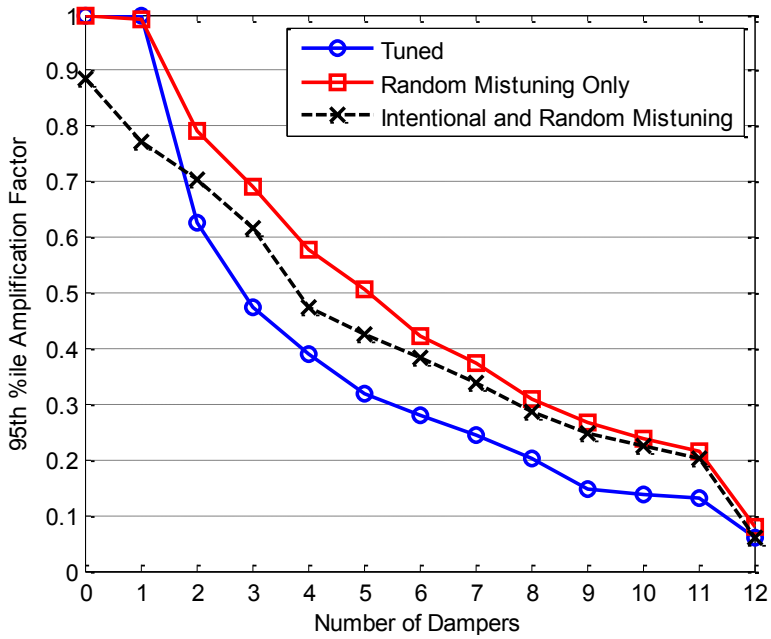

Figure 41. Normalized peak response vs. number of blade-ground friction dampers for different options, single degree of freedom per sector model, engine order 2 excitation.

Friction dampers are most often blade-blade devices and it was accordingly desired to repeat the above analysis with the blade-blade friction damper model of Figure 42 (see [19]) with the parameters of Table 3 with $K_B = K_G$. The optimization process of the normal force described above was repeated and led to the bucket curves and optimal slip distance $\mu_F F_N / K_B$ vs. number of dampers shown in Figure 43 and Figure 44. These curves are similar to their blade-ground counterparts with the notable difference in Figure 44 that the optimum slip distance appears to have converged for 7 dampers on the disk.

The maximum amplitude of blade response obtained with and without random mistuning (P1 and P2 problems) is shown in Figure 45(a). Also presented in this figure are a series of results for the P3 problem. These sets of results confirm the findings of the blade-ground friction dampers and strongly suggest the application of these concepts to more complex damper models.

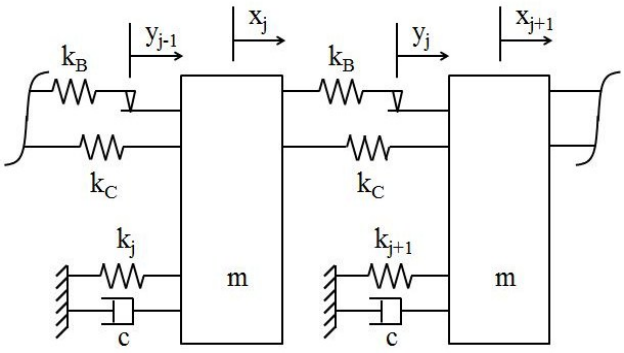

Figure 42. Model of bladed disk with blade-blade friction dampers (from [19]).

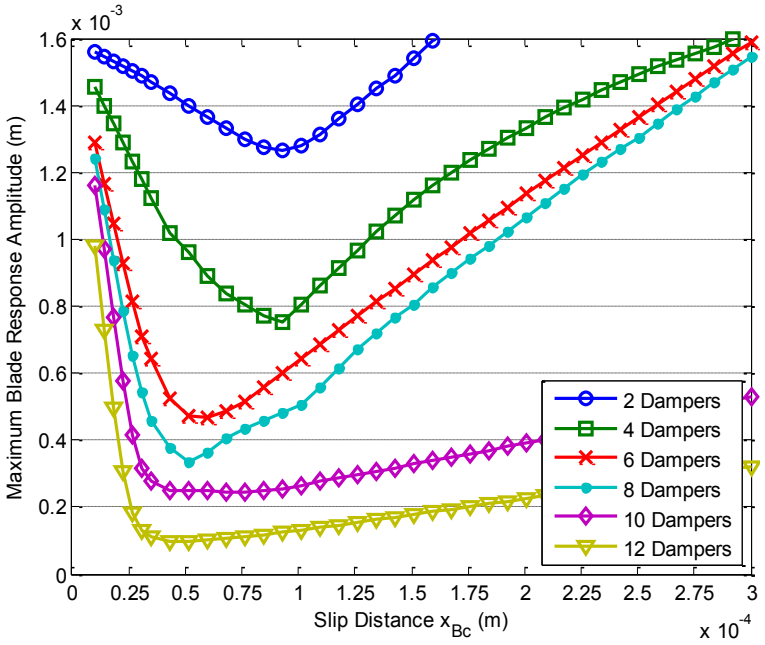

Figure 43. Optimum bucket curves as a function of the number of blade-blade friction dampers.

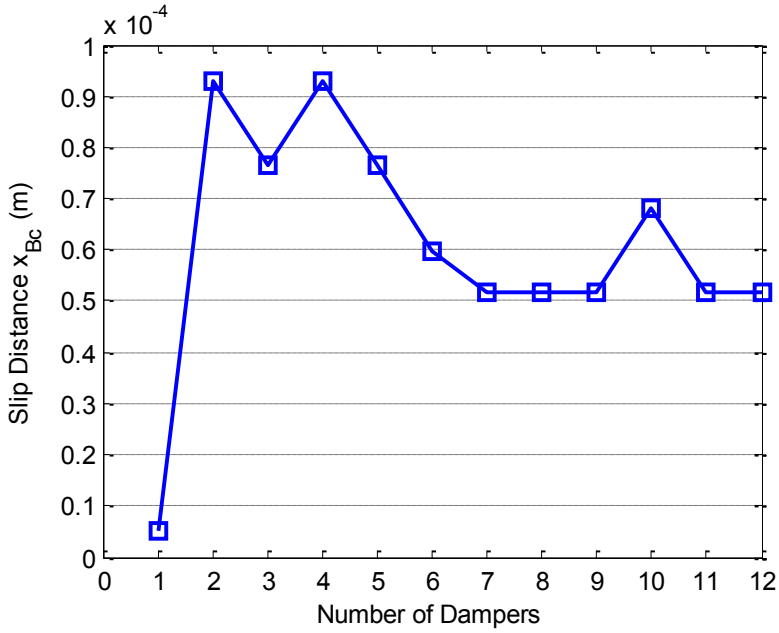

Figure 44. Optimum slip distances $\mu_F F_N / K_B$ as a function of the number of blade-blade friction dampers.

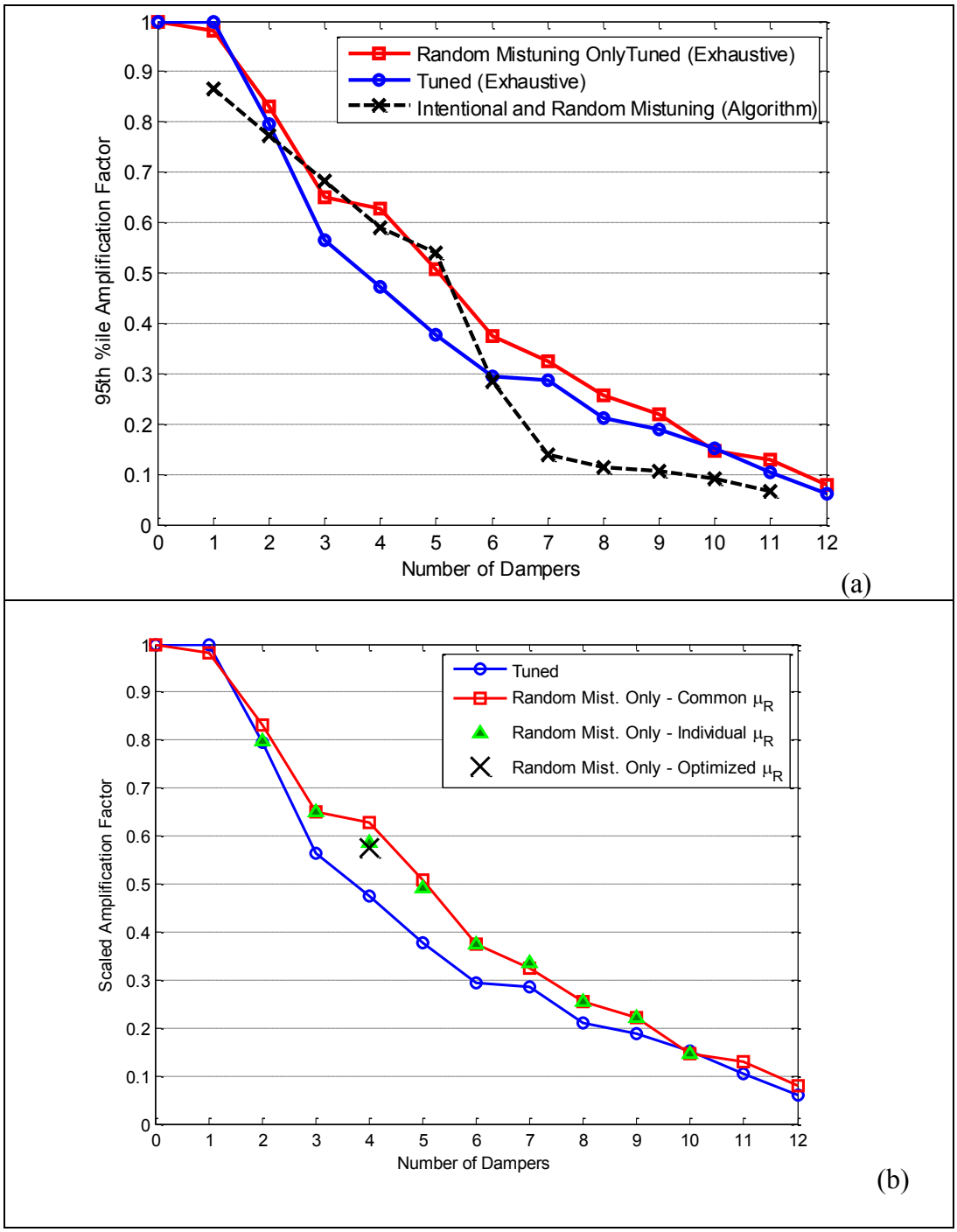

Figure 45. Normalized peak response vs. number of blade-blade friction dampers (a) for different options single degree of freedom per sector model, engine order 2 excitation, (b) for different options with individual and optimized friction coefficients μ_R.

There appears to be a noticeable feature in the scaled amplification factor of the P2 and P3 problems around the vicinity of 3-4 dampers, where the reduction in the blade response does not seem to follow the smooth decrease observed in previous cases. Since both the P2 and P3 optimizations were carried out using the optimum damper properties identified form the P1 problem, i.e. the "common μ_R", an assessment of the effect of optimizing the damper properties was carried out. As an initial assessment, the response of different number of dampers on the bladed disk was recomputed using the optimum friction coefficient values corresponding to each unique damper position obtained at the end of the previous optimization, i.e. the P1 problem – this result can be seen in Figure 45 and corresponds to the "individual μ_R" cases. Finally, a particular location (at 4 dampers) was chosen and the optimization was carried out including the friction coefficient as a parameter in the optimization process. The single point marked by the black cross and labeled "optimum μ_R" corresponds to the resulting blade response. It is evident from the smaller amplitudes of blade response obtained in both the "individual μ_R" as well as the "optimum μ_R" cases that the optimization process needs to include the friction damper parameters as variables in addition to the damper locations and the intentional mistuning pattern.

Further, the optimum bucket curves for the three cases of friction coefficient were plotted – optimization with optimum μ_R from the P1 problem, optimization with "individual μ_R" for the P2 problem, and optimization with "optimum μ_R" for the P2 problem, see Figure 46. Observe that indeed, when there is no random mistuning of the blades' stiffness, the damper friction coefficient

μ_R obtained in the P1 problem leads to a much smaller level of blade response than either the "individual μ_R" or the "optimum μ_R" obtained from the P2 problem optimization. However, in the presence of random mistuning, we observe a noticeable increase in the response of the optimum obtained from the P1 problem, whereas the optima obtained from the P2 problem (i.e. "individual μ_R" and "optimum μ_R" respectively) are considerably more robust to the presence of random mistuning. This observation indeed confirms that the optimization of the placement of friction dampers on a bladed disk must be accompanied by an optimization of the friction damper properties as well.

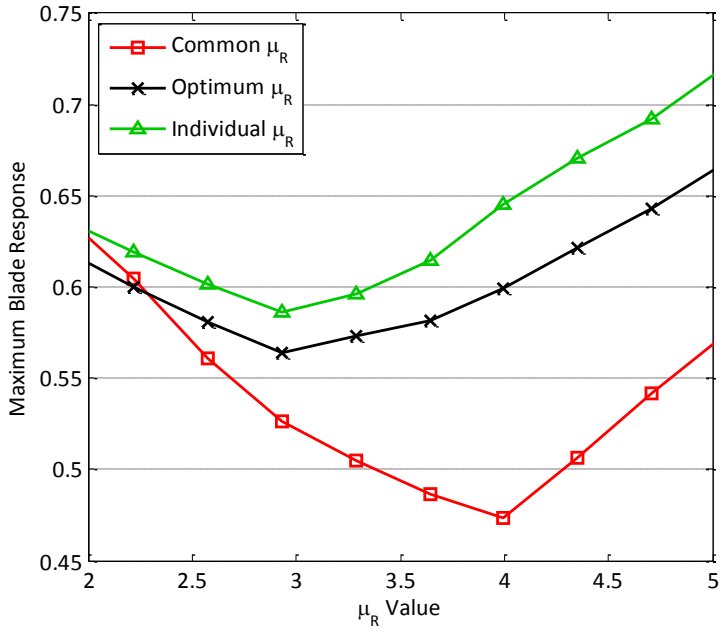

(a)

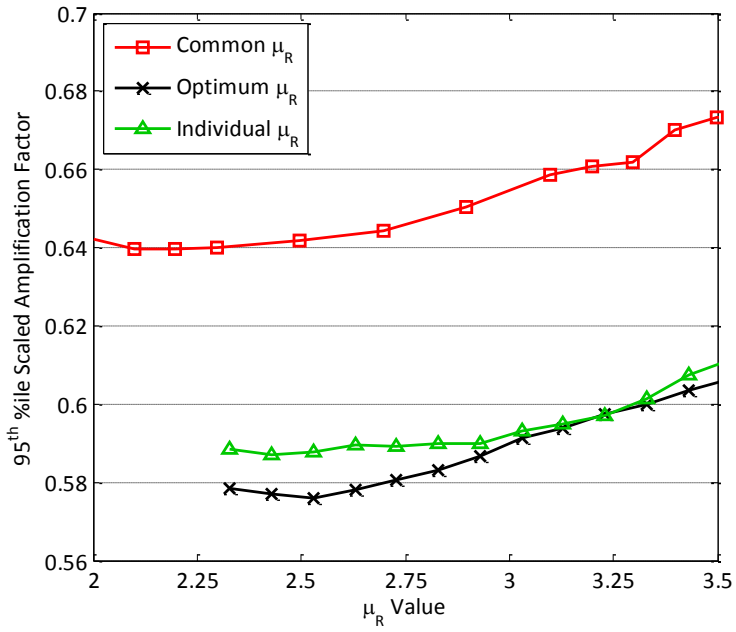

(b)

Figure 46. Bucket curves for P1 optimum, P2 “individual”, and P2 optimum damper locations on (a) tuned disk, and (b) tuned disk with random mistuning in blades’ stiffness.

5 – INTENTIONAL MISTUNING OF FRICTION DAMPERS

5.1 Introduction

Mistuning has traditionally been considered an undesirable feature in bladed disks as it leads most notably to an amplification of the forced response as compared to the tuned disk. Yet, some past investigations, e.g. [14, 43-46], have shown that a well selected (intentional) mistuning of the blades on a disk can lead to some decrease of the peak blade response and to a significant increase of the robustness of this forced response to additional, random, mistuning. Practical implementations of such a scheme are important to consider. In this context, it has first been proposed that the intentional mistuning be achieved through the combination around the disk of only two types of blades, A and B say, having different vibrational properties. Then, the desirable intentional mistuning can be obtained by optimizing the pattern of A and B blades around the disk to yield the smallest maximum amplitude of blade response in critical excitation conditions. In fact, an efficient algorithm to perform this specific optimization has been devised [46] and numerous validation cases have repeatedly confirmed the benefits of intentional mistuning.

Another important practical aspect of this problem is how the blades A and B will differ. Mindful of aerodynamic constraints, much of the literature on this topic [43-46] has assumed that these two blade types would have the same geometry but would differ by mechanical properties. More specifically, stiffness properties, e.g. different Young's modulus, have been proposed to avoid the balancing issues involved in blade to blade changes in their masses.

Unfortunately, varying these stiffness properties is not an easy task and this recognition has led some investigators to tackle the consideration of the more difficult blade geometry-based intentional mistuning [47].

One other possibility for intentional mistuning that has received very little attention is underplatform friction dampers when they exist. Not being effectively part of the blades and being away from the flow, they would represent an excellent intentional mistuning option if designed variations of their properties, e.g. their mass, around the disk can provide the desired reduction in blade response. A first indication of this potential has recently been provided in [48], reporting a reduction by about 2% of the maximum amplitude of blade response when using an alternate intentional mistuning pattern of the friction dampers, i.e. friction dampers with properties A and B arranged around the disk as ABABA... While 2% is only a small benefit, the observation demonstrates that a reduction in blade response can be achieved. Past investigations of intentional mistuning of blades have demonstrated that it is of key importance to optimize the pattern of A and B friction dampers around the disk to get its full benefit as many patterns may result in only a small reduction, or in fact an increase, of blade response.

In this light, the focus of this investigation is on assessing the full benefits which can be obtained by optimizing the intentional mistuning patterns of friction dampers on bladed disks as well as the masses of the two types of dampers.

5.2 Bladed Disk Models & Optimization Strategy

The present effort is one of discovery vs. application to a particular hardware. Accordingly, the bladed disk models used are simple ones, i.e. single degree of freedom blade models with blade-ground, see Figure 47(a), and blade-blade, see Figure 47(b), dampers with the common properties of Table 5.

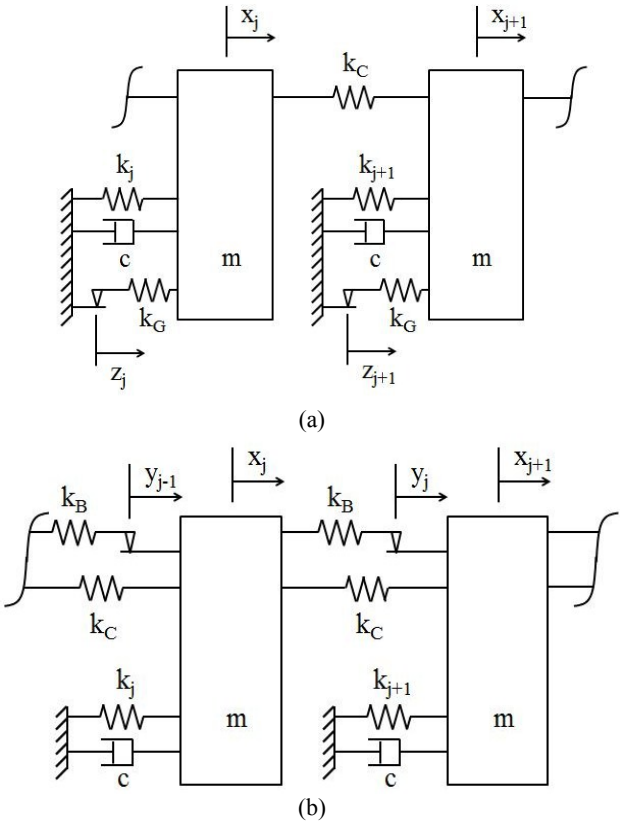

Figure 47. Model of bladed disk with (a) blade-ground and (b) blade-blade friction dampers. from [19])

Table 5. Parameters values of the model of Figure 47.

Property	**Value**
Number of Blades (*N*)	6 or 12
Blade Mass (*m*)	0.0114 Kg
Damping coefficient (*c*)	0.143 Ns/m

Blade-Disk Stiffness (k_i)	430300 N/m
Blade-Blade Coupling Stiffness (k_C)	10000 N/m
Blade-Disk Friction Damper Stiffness (k_G) Blade-Blade Friction Damper Stiffness (k_B)	43000 N/m
Friction Damper Normal Force ($\mu_f F_N$)	1.505 N
Forcing Amplitude (F_0)	1 N

The system was subjected to an engine order 2 excitation and its response was determined using a single harmonic balance method following [19]. To provide the baseline data, an optimization effort was first undertaken to determine the damper mass yielding the smallest response for each tuned disk, i.e. with identical friction dampers. This analysis is most easily conducted through the determination of the bucket curves, see Figure 48.

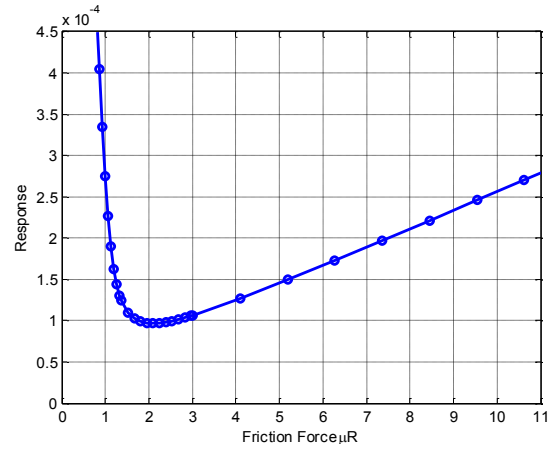

(a)

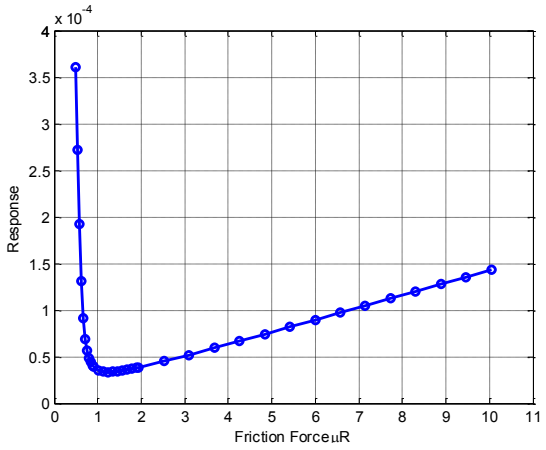

(b)

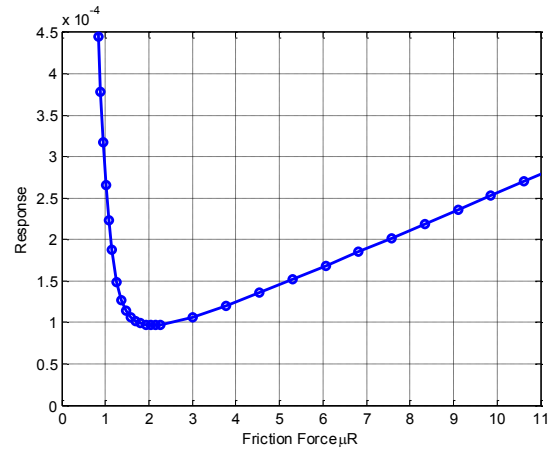

(c)

Figure 48. Bucket curves for the disks of Figure 47. 6-blade disk with (a) blade-ground and (b) blade-blade dampers. (c) 12-blade disk with blade-ground dampers.

Once the optimum damper mass was determined, patterns of A and B friction dampers were considered with the damper mass of A smaller than the optimum, i.e. $\mu Ra = m_A/m_{opt} < 1$, and the one of B larger than optimum, i.e. $\mu Rb = m_B/m_{opt} > 1$. For each pair of values of μRa and μRb, the response in sweep of each of the possible A/B patterns, 14 for 6 blades and 352 for 12 blades, was evaluated to yield the corresponding maximum amplitude of blade response. The lowest value of this maximum over the set of patterns was then identified and plotted vs. μRa and μRb.

Such an analysis was conducted in three different situations:

(a) Tuned Blades – Intended Friction Dampers. The blades are all the same and the friction dampers have indeed the properties of Table 5.

(b) Mistuned Blades – Intended Friction Dampers. While the friction dampers still have the properties of Table 5, the blade are no longer identical, they exhibit mistuning in their stiffness.

(c) Mistuned Blades and Friction Dampers – Both blades and the friction dampers have properties that vary from blade to blade although with mean values reflecting the A/B pattern.

The optimization results corresponding to these situations are described in the ensuing sections.

The optimization problem can be summarized as below, with the primary design variable being the locations of the A and B type friction dampers on the bladed disk. In the effort to introduce intentional mistuning in the system with friction dampers, the range of variation of the friction coefficient was set to between 0.9 times and 1.1 times the optimum friction coefficient obtained when using a single type of damper optimized on all blades of the disk.

The objective is then the minimization of the 95th percentile of the maximum blade response amplitude in a frequency sweep (as determined by the resonance and excitation conditions on the bladed disk) in the presence of random mistuning.

Design Variables

(1)	Locations of N dampers	d_i	$i = 1, 2, \ldots N$
(2)	Optimum pattern of friction dampers	$f_i = 0 - damper\ type\ A$ $f_i = 1 - damper\ type\ B$	$i = 1, 2, \ldots M$

Objective

$$\min_{\substack{d_i \\ f_i}} 95\text{th percentile} \left\{ \max_{\omega \in \Omega} \left[\max_{j} \left(\text{response of blade } j \text{ at freq } \omega \right) \right] \right\}$$

Constraints

(1)	Frequency range of interest	$\Omega_{\text{lower}} \leq \Omega \leq \Omega_{\text{upper}}$ Ω_{lower} and Ω_{upper} defined according to resonance excitation condition on bladed disk

(2)	Friction coefficient (continuous)	$0.9\mu_{opt} \leq \mu_i \leq 1.1\mu_{opt}$ $i = 1, 2, \ldots, N$ where μ_{opt} is the optimum friction coefficient with the same type of friction damper on all blades

5.3 Tuned Blades – Intended Friction Dampers

As a starting point to the investigation of the benefits of using different types of dampers on disks, it was assumed that the blades were all identical (tuned disk) and that the properties of the friction dampers were exactly as intended, i.e. type A or B. The results of these optimization efforts are shown in Figure 49 and Figure 50 for the blade-ground configurations and Figure 51 for the disk with blade-blade dampers.

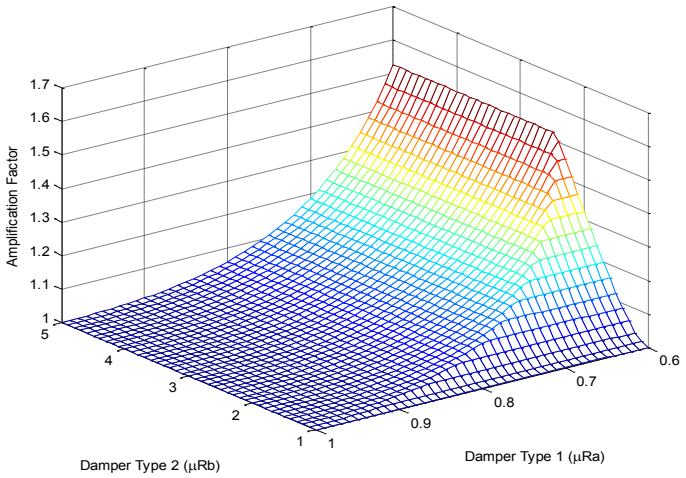

Figure 49. Amplification factor vs. A and B damper masses, 6-blades with blade-ground dampers.

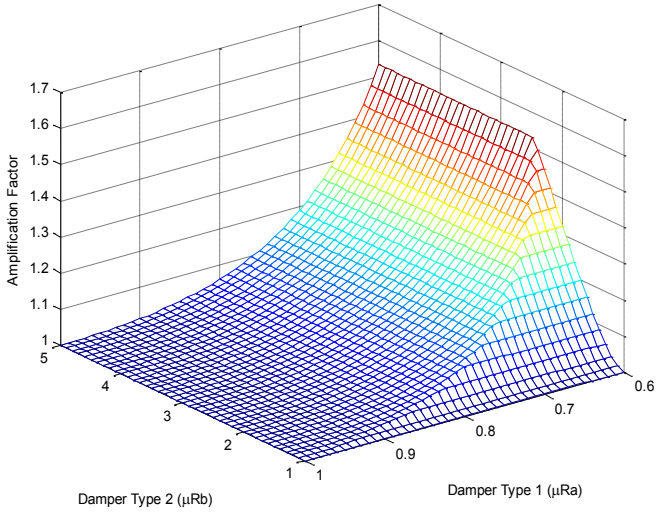

Figure 50. Amplification factor vs. A and B damper masses, 12-blades with blade-ground dampers.

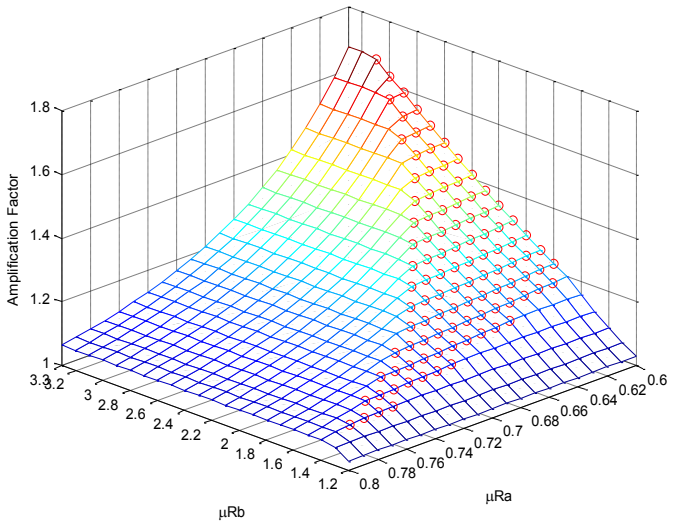

Figure 51. Amplification factor vs. A and B damper masses, 6-blades with blade-blade dampers.

A first observation to be drawn from these figures is that the lowest maximum amplitude of blade response occurs in the tuned configuration, i.e. when all friction dampers are identical with the optimum mass obtained from the bucket curves of Figure 48. The pattern of response that leads to the small maximum response for a particular pair of damper masses, i.e. µRa and µRb, was found to be all A or all B for the blade-ground dampers. For blade-blade dampers, however, alternate mistuning of the dampers was found as a third possible optimum, in the part of the damper mass space marked with semicircles on Figure 51. Note in this regard that alternating A and B friction dampers was the pattern observed in [48] to lead to a reduction in the response and that the dampers were of blade-blade type.

5.4 Mistuned Blades–Intended Friction Dampers

It would seem from the above first analysis that there is no value to intentionally mistuning friction dampers. Such a conclusion could however be somewhat hasty since the true benefits of intentional stiffness mistuning of blades are revealed only when considering the response of mistuned disks with intentional mistuning of the blades' stiffness inducing a significant increase in robustness with respect to random mistuning. To assess whether such a benefit could be obtained here, the optimization effort carried out in the previous section was repeated but with random mistuning in the blades' stiffness. Specifically, a population of 1,000 disks was generated with the blades' stiffness modeled as independent random variables with a uniform distribution and a standard deviation of 1% of the mean value of Table 5. The computation of the disk response was achieved for every disk, every A/B pattern of friction dampers and the combinations of the two damper masses as before. The 95th percentile of the maximum blade response was considered as the representative amplitude of response.

Then, shown in Figure 52 is the three-dimensional plot of the tuned amplitude divided by lowest representative amplitude over the entire set of patterns for a 6-blade disk with blade-ground dampers as a function of μRa and μRb. This figure demonstrates that a slight benefit can be obtained by selecting μRa=0.95 and μRb=1.10.The corresponding pattern of A and B friction dampers is ABABBB. The small benefit, approximately 3.4%, of using this configuration of dampers is also visible in Figure 53 which displays the 95th percentile of the

amplification factor vs. the level of blade mistuning. Note that other patterns also provide a similar benefit at different mistuning levels, see Figure 53.

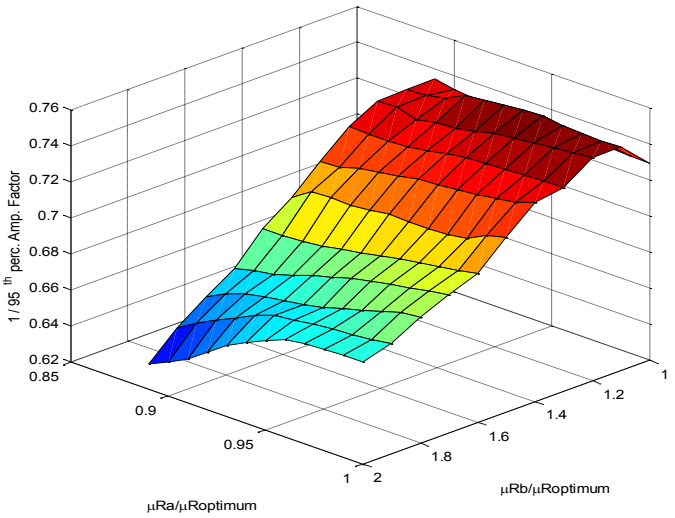

Figure 52. Tuned amplitude divided by lowest representative pattern over the entire set of patterns vs. A and B damper masses, 6-blade disk with blade-ground dampers with blade-blade coupling stiffness kC = 10,000.

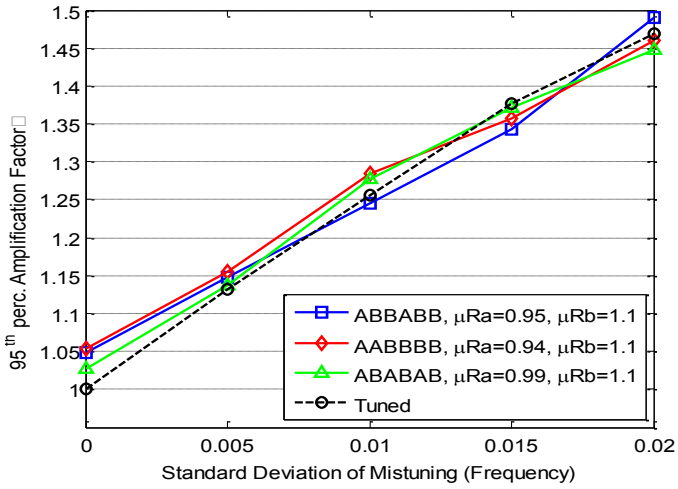

Figure 53. 95th percentile amplification factor vs. blade mistuning level, 6-blade disk with blade-ground dampers with blade-blade coupling stiffness kC = 10,000.

The physics of random and intentional mistuned disks is known to dependent strongly on the blade-disk or blade-blade structural coupling. In this light, the above analysis was also repeated with the larger value kC = 45,430N/m and the corresponding results are shown in Figure 54 and Figure 55. The results are quite similar leading to a small benefit.

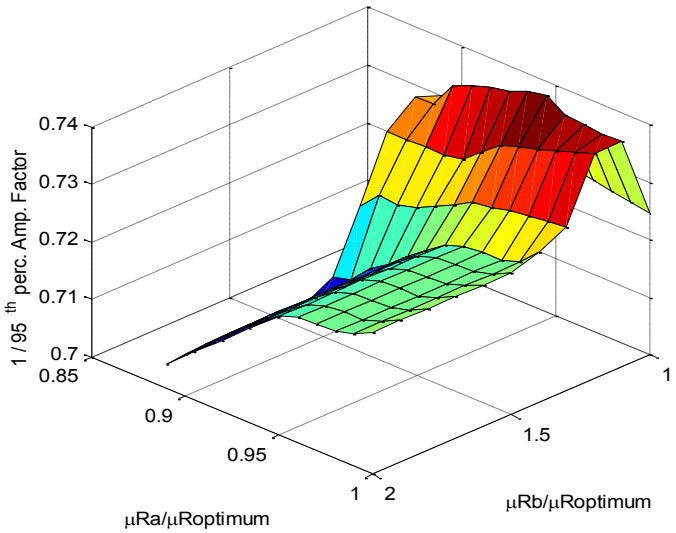

Figure 54. Tuned amplitude divided by lowest representative pattern over the entire set of patterns vs. A and B damper masses, 6-blade disk with blade-ground dampers with blade-blade coupling stiffness kC = 45,430.

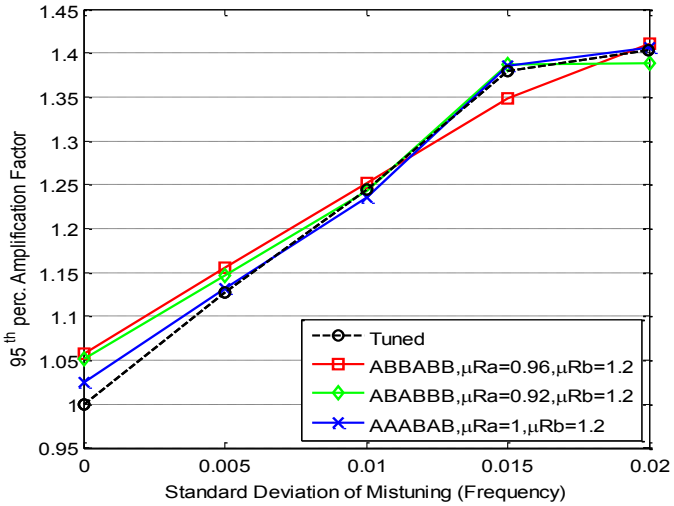

Figure 55. 95th percentile amplification factor vs. blade mistuning level, 6-blade disk with blade-ground dampers with blade-blade coupling stiffness kC = 45,430.

Finally, the analysis was repeated for the 6-blade disk blade-blade damper of properties given in Table 5 and the corresponding results, shown in Figure 56 and Figure 57, confirm the above observations of small benefit.

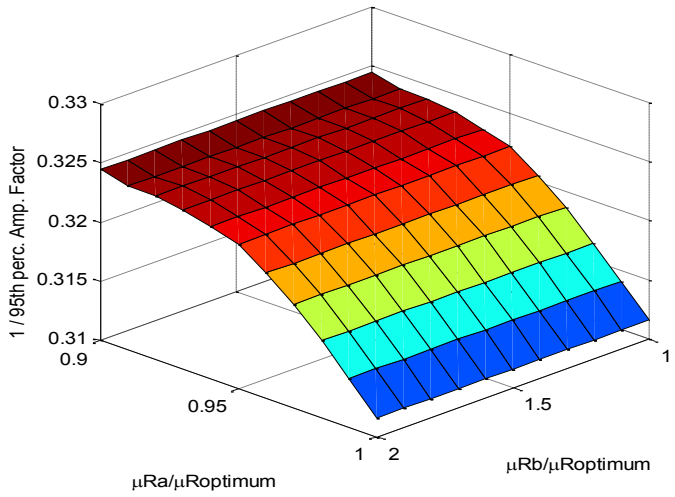

Figure 56. Tuned amplitude divided by lowest representative pattern over the entire set of patterns vs. A and B damper masses, 6-blade disk with blade-blade dampers with blade-blade coupling stiffness kC = 10,000.

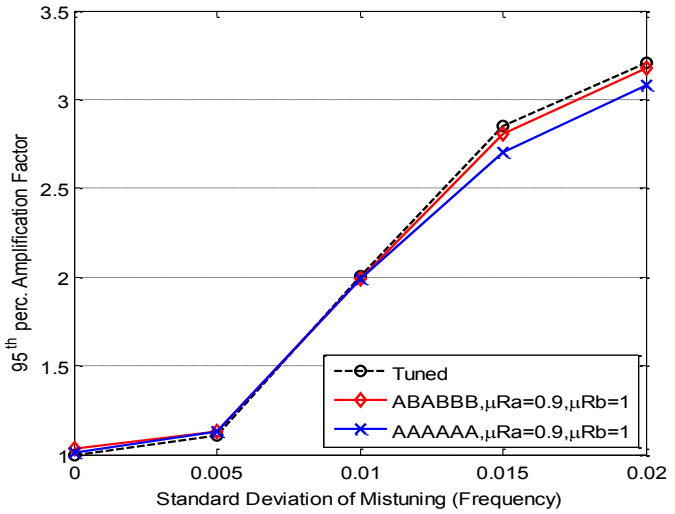

Figure 57. 95th percentile amplification factor vs. blade mistuning level, 6-blade disk with blade-blade dampers with blade-blade coupling stiffness kC = 10,000.

5.5 Mistuned Blades and Friction Dampers

The manufacturing and in-service sources of variability of the blades' stiffness will also induce variability in the properties of the dampers. To include this aspect in the analysis, the Monte Carlo study was performed with independent variations of the normal force of the dampers. These quantities were modeled as Gamma distributed random variables with mean equal the values μRa and μRb and with standard deviations equal to half of these values, recognizing the large spread of friction properties expected in practice. As in the previous section, the 95th percentile of the maximum blade response was considered as the representative amplitude of response.

Shown in Figure 58 is the three-dimensional plot of the tuned amplitude divided by lowest representative amplitude over the entire set of patterns for a 6-blade disk with blade-ground dampers as a function of μRa and μRb, with variability in the damper properties. This figure demonstrates that a slight benefit can be obtained by selecting μRa=1 and μRb=1.3. The corresponding pattern of A and B friction dampers is ABBABB, and a small benefit, approximately 3.1%, of using this configuration of dampers is obtained. This is shown along with some other patterns showing similar benefit in Figure 59, which displays the 95th percentile amplification factor vs. the level of blade mistuning with variability in dampers considered.

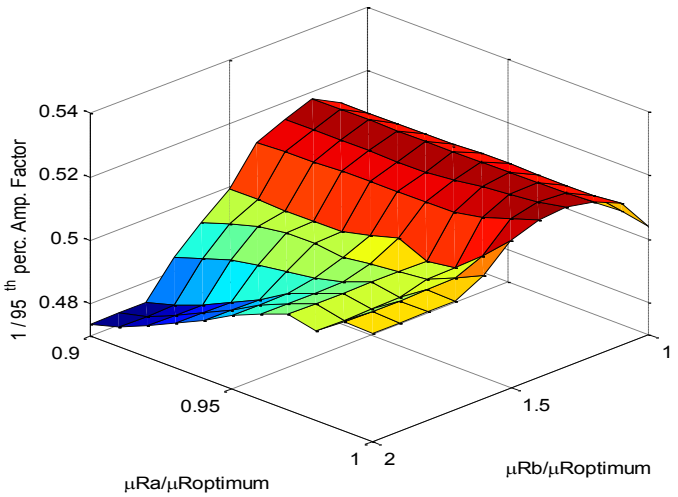

Figure 58. Tuned amplitude divided by lowest representative pattern over the entire set of patterns vs. A and B damper masses with damper mistuning. 6-blade disk with blade-ground dampers with blade-blade coupling stiffness kC = 45,430.

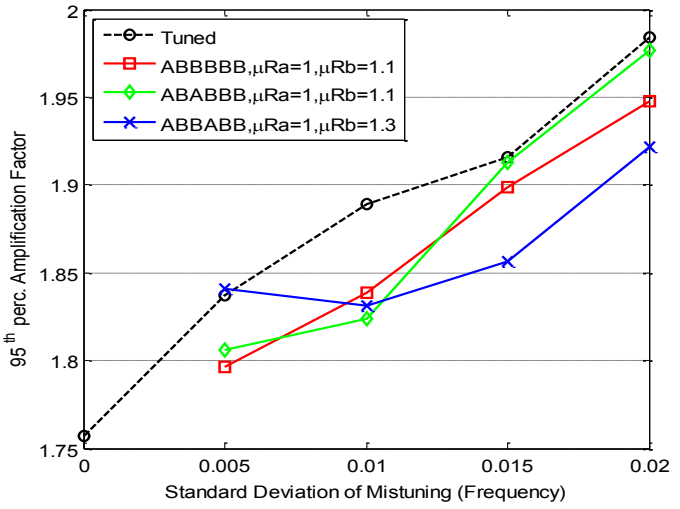

Figure 59. 95th percentile amplification factor vs. blade mistuning level, with damper mistuning, 6-blade disk with blade-ground dampers with blade-blade coupling stiffness kC = 45,430.

6 – SUMMARY

The present effort focused on the optimal positioning of a few dampers, i.e. fewer than the number of blades, on a bladed disk to induce the smallest possible amplitude of blade response with or without involuntary, random mistuning. Intentional mistuning corresponding to the use of two types (A and B) of blades was also considered as an option to reduce the amplitude of blade response.

The optimization of the damper locations and, when appropriate, the intentional mistuning pattern was found to exhibit a large number of local optima of varying bladed disk response. This finding coupled with the expensive cost of a function evaluation led to the formulation of dedicated strategies to solve this optimization problem. These algorithms involve two steps, the first one of which is the selection of approximate solutions from which, in the second step, a local search is carried out until convergence. Three rules were proposed for the sequential construction of the initial damper locations while the starting intentional mistuning patterns could be in particular obtained through the "subspace" algorithm in which constraints were imposed on the blade types of two consecutives sectors to minimize the search space. The validation of these algorithms was accomplished on both a single degree of freedom per sector model and the reduced order model of a blisk by comparison with a limited set of optimum solutions obtained by an exhaustive search. A very good to excellent match of these exhaustive search results was obtained at a computational cost

which was shown to be dramatically smaller than that of the corresponding exhaustive search.

Recognizing the possibility of damper failure, the optimization algorithm was then modified to allow for a non-zero probability of failure of the dampers introduced. Three different probabilities of failure (0.01, 0.03 and 0.10) were analyzed, and their effect on the response of the system was shown. The sensitivity of the intentional mistuning pattern as well as the locations of the dampers was also studied and the system found to be quite robust for small probabilities of damper failure.

Next, the optimization of the damper locations and, when appropriate, the intentional mistuning pattern was first repeated with linear blade-blade dampers. The observations made in connection with blade-alone dampers were again found to hold.

Further, the sensitivity of the optimum configuration of dampers (blade-only or blade-blade) and intentional mistuning pattern to random variations of the damper coefficients was assessed to evaluate the potential effects of in-service/manufacturing damper variability. Quite surprisingly, it was found that the optimum solutions of the P2 and P3 problems were very robust with respect to these variations and thus that they need not be considered in the optimization process, although their inclusion was demonstrated to be straightforward.

Further, the extension of these concepts to nonlinear dampers was initiated by considering friction dampers. The nonlinearity of these dampers implies that the effective damping they provide depends on the bladed disk response and thus

implicitly on the number of dampers present. This observation demonstrated that an optimization of the damper properties, the normal force was selected here, should be carried out for each number of dampers on the disk. A process to accomplish this task was demonstrated which relies on the exhaustive solution of the P1 problem. The results obtained for both blade-ground and blade-blade friction dampers with optimized normal force were found to be in close agreement with those obtained with linear dampers.

Finally, an investigation of the potential benefits resulting from using two different types of friction dampers on a bladed disk was carried out. Every blade or platform was equipped with a damper of either type A or B with these two types differing by their masses. The benefit of this strategy was measured in comparison with using identical dampers of optimized mass on every blade or platform, and is found to be dependent on the pattern of A/B dampers around the disk as well as the damper masses.

The optimization was accomplished through an exhaustive search for all patterns on a grid of values of the two damper masses. As this was a discovery effort vs. application to a particular damper geometry, these were carried out on single-degree-of-freedom per sector models of both blade-ground and blade-blade friction dampers with small blade counts of 6 and 12 blades. In all cases considered, the benefit of this intentional mistuning of friction dampers is either zero or small, of the order of a few percent, consistently with a single data point reported in the literature.

REFERENCES

[1] Avalos, J., and Mignolet, M.P., "On Damping Entire Bladed Disks through Dampers on only a few Blades," Journal of Engineering for Gas Turbines and Power, Vol. 132, No. 9. 2010.

[2] Nashif, A., "Modeling of the Linear and Nonlinear Behavior of Ceramic Coatings," Proceedings of the 10th High Cycle Fatigue (HCF) Conference, New Orleans, Louisiana, Mar. 8-11, 2005.

[3] Kielb, J., Weaver, M., Mesing T., Turner, A., and Moritz, R., "A Robust High Cycle Fatigue Analysis and Durability Testing of a Constrained Layer Viscoelastic Damping System," Proceedings of the 8th National Turbine Engine High Cycle Fatigue (HCF) Conference, Monterey, California, Apr. 14-16, 2003.

[4] Garay, G., Schorr, D., Turner, A., Weaver, M., McCormick, M., "Design and Subcomponent Testing of a Viscoelastic Constraint Layer Damping System for Fan Airfoils," Proceedings of the 9th National Turbine Engine High Cycle Fatigue (HCF) Conference, Pinehurst, North Carolina, Mar. 16-19, 2004.

[5] Nashif, A., Henderson, J., Justice, J., Johnson, P., Runyon, B., "High Temperature Rim Dampers for IBR System Modes," Presented at the Propulsion - Safety and Affordable Readiness (P-SAR) Conference, Jacksonville, Florida, Mar. 28-30, 2006.

[6] Shen, H., "Free Layer Blade Damper by Magneto-Mechanical Coupling - Phase II," Presented at the Propulsion - Safety and Affordable Readiness (P-SAR) Conference, Jacksonville, Florida, Mar. 28-30, 2006.

[7]Henderson, J.P., Torvik, P.J., Willson, R.M., Justice, J.A., "Recent Progress on Modified Plasma Sprayed Damping Coatings for Titanium Airfoils," Presented at the Propulsion - Safety and Affordable Readiness (P-SAR) Conference, Jacksonville, Florida, Mar. 28-30, 2006.

[8] Henderson, J.P., Zabierek, D.W., Justice, J.A., and Willson, R.M., "Preliminary Investigations of Modified Plasma Sprayed Damping Coatings for Titanium Coatings," Proceedings of the 10th High Cycle Fatigue (HCF) Conference, New Orleans, Louisiana, Mar. 8-11, 2005.

[9] Patsias, S., Byrne, A., and Shipton, M., "Hard Coatings: Optimisation of Damping Effectiveness by Controlling the Deposition Parameters," Proceedings of the 9th National Turbine Engine High Cycle Fatigue (HCF) Conference, Pinehurst, North Carolina, Mar. 16-19, 2004.

[10] Patsias, S., and Gent, J., "Hard Coatings: Effect of Powder Morphology on Damping Effectiveness," Proceedings of the 10th High Cycle Fatigue (HCF) Conference, New Orleans, Louisiana, Mar. 8-11, 2005.

[11] Bladh, R., Castanier, M. P., and Pierre, C., "Component-Mode-Based Reduced Order Modeling Techniques for Mistuned Bladed Disks—Part I: Theoretical Models," Journal of Engineering for Gas Turbines and Power, 123(1), pp. 89–99, 2001.

[12] Castanier, M.P., Ottarson, G., and Pierre, C., "A Reduced Order Modeling Technique for Mistuned Bladed Disks," Journal of Vibration and Acoustics, 119, pp. 439-447, 1997.

[13] Kiflu, B., "Analysis of Mistuned Bladed Disks by a Reduced Order Technique: Validation, Identification, and Stochastic Modeling," M.S., Arizona State University, May 2005.

[14] Han, Y., and Mignolet, M.P., "Optimization of Intentional Mistuning Patterns for the Mitigation of the Effects of Random Mistuning," Turbo Expo 08, Berlin, Germany, June 9-13, 2008. Paper GT-2008-51439.

[15] Joshi, A.G.S., and Epureanu, B.I., "Reduced Order Models for Blade-to-Blade Damping Variability in Mistuned Blisks," Turbo Expo 11, Vancouver, Canada, June 6-10, 2011, Paper GT-2011-45661.

[16] Mignolet, M.P., and Choi, B-K., "Robust Optimal Positioning of Strain Gauges on Blades," Journal of Turbomachinery, Vol. 125, No. 1, pp. 155-164, 2003.

[17] Lin, C. C., and Mignolet, M. P., "Effects of Damping and Damping Mistuning on the Forced Vibration Response of Bladed Disks". Journal of Sound and Vibration, Vol. 193, pp. 525–543, 1996.

[18] Joshi, A.G.S., and Epureanu, B.I., "Reduced Order Models for Blade-to-Blade Damping Variability in Mistuned Blisks," Turbo Expo 11, Vancouver, Canada, June 6-10, 2011, Paper GT-2011-45661.

[19] Sinha, A., Griffin, J.H., "Effects of Friction Dampers on Aerodynamically Unstable Rotor Stages", AIAA Journal, Vol. 23, No. 2, Feb. 1985, pp. 262-269.

[20] Cha, D., Sinha, A., "Statistics of responses of a mistuned and frictionally damped bladed disk assembly subjected to white noise and narrow band excitations," Probabilistic Engineering Mechanics, Vol. 21, Issue 4, pp. 384-396, 2006.

[21] Cha, D., Sinha, A., "Computation of the Optimal Normal Load for a Mistuned and Frictionally Damped Bladed Disk Assembly Under Different Types of Excitation," Journal of Computational and Nonlinear Dynamics, Vol. 6, Issue 2, 2011.

[22] Chen, S., Sinha, A., "Probabilistic Method to Compute the Optimal Slip Load for a Mistuned Bladed Disk Assembly With Friction Dampers," Journal of Vibration and Acoustics, Vol. 112, Issue 2, pp. 214-221, Apr. 1990.

[23] Griffin, J. H., Sinha, A., "The Interaction Between Mistuning and Friction in the Forced Response of Bladed Disk Assemblies," Journal of Engineering for Gas Turbines and Power, Vol. 107, Issue 1, pp. 205-211, 1985.

[24] Petrov, E. P., "A Method for Use of Cyclic Symmetry Properties in Analysis of Nonlinear Multiharmonic Vibrations of Bladed Disks," Journal of Turbomachinery, Vol. 126, Issue 1, pp. 175-183, Jan. 2004.

[25] Petrov, E. P., Ewins, D. J., "Method for Analysis of Nonlinear Multiharmonic Vibrations of Mistuned Bladed Disks With Scatter of Contact Interface Characteristics," Journal of Turbomachinery, Vol. 127, Issue 1, pp. 128-136, Jan. 2005.

[26] Popp, K., Panning, L., Sextro, W., "Vibration Damping by Friction Forces: Theory and Applications," Journal of Vibration and Control, Vol. 9, Issue 3-4, pp. 419-448, Mar. 2003.

[27] Sextro, W., Popp, K., Krzyzynski, T., "Localization in Nonlinear Mistuned Systems with Cyclic Symmetry," Nonlinear Dynamics, Vol. 25, Issue 1-3, pp. 207-220, Jul. 2001.

[28] Griffin, J. H., "Friction Damping of Resonant Stresses in Gas Turbine Engine Airfoils," Journal of Engineering for Power – Transactions of the ASME, Vol. 102, Issue 2, pp. 329-333, 1980.

[29] Csaba, G., "Forced Response Analysis in Time and Frequency Domains of a Tuned Bladed Disk with Friction Dampers," Journal of Sound and Vibration, Vol. 214, Issue 3, pp. 395-412, 1998.

[30] Firrone, C. M., Zucca, S., Gola, M. M., "The effect of underplatform dampers on the forced response of bladed disks by a coupled static/dynamic harmonic balance method," International Journal of Nonlinear Mechanics, Vol. 46, Issue 2, pp. 363-375, Mar. 2011.

[31] Berruti, T., Filippi, S., Goglio, L., Gola, M. M., Salvano, S., "A test rig for frictionally damped bladed segments," Journal of Engineering for Gas Turbines

and Power – Transactions of the ASME, Vol. 124, Issue 2, pp. 388-394, Apr. 2002.

[32] Berruti, T., Firrone, C. M., Gola, M. M., "A Test Rig for Noncontact Traveling Wave Excitation of a Bladed Disk with Underplatform Dampers," Journal of Engineering for Gas Turbines and Power – Transactions of the ASME, Vol. 133, Issue 3, Mar. 2011.

[33] Sanliturk, K. Y., Ewins, D. J., Stanbridge, A. B., "Underplatform Dampers for Turbine Blades: Theoretical Modeling, Analysis, and Comparison With Experimental Data," Journal of Engineering for Gas Turbines and Power, Vol. 123, Issue 4, pp. 919-929, Oct. 2001.

[34] Cameron, T. M., Griffin, J. H., Kielb, R. E., Hoosac, T. M., "An Integrated Approach for Friction Damper Design," Journal of Vibrations and Acoustics – Transactions of the ASME, Vol. 112, Issue 2, pp. 175-182, Apr. 1990.

[35] Sanliturk, K. Y., Imregun, M., Ewins, D. J., "Harmonic Balance Vibration Analysis of Turbine Blades with Friction Dampers," Journal of Vibration and Acoustics – Transactions of the ASME, Vol. 119, Issue 1, pp. 96-103, Jan. 1997.

[36] Moré, J. J., "The Levenberg-Marquardt Algorithm: Implementation and Theory," Numerical Analysis, ed. G. A. Watson, Lecture Notes in Mathematics 630, Springer Verlag, pp. 105-116, 1977.

[37] Thomas, D. L., "Dynamics of Rotationally Periodic Structures," International Journal for Numerical Methods in Engineering, Vol. 14, pp. 81-102, 1979.

[38] Wei, S. T., and Pierre, C., "Localization Phenomena in Mistuned Assemblies with Cyclic Symmetry – Part I: Free Vibrations," Journal of Vibration, Acoustics, Stress, and Reliability in Design, Vol. 110, No. 4, pp. 429-438, 1988a.

[39] Wei, S. T., and Pierre, C., "Localization Phenomena in Mistuned Assemblies with Cyclic Symmetry – Part II: Forced Vibrations," Journal of Vibration, Acoustics, Stress, and Reliability in Design, Vol. 110, No. 4, pp. 439-449, 1988b.

[40] Rivas-Guerra, A.J., and Mignolet, M.P., "Local/Global Effects of Mistuning on the Forced Response of Bladed Disks," Journal of Engineering for Gas Turbines and Power, Vol. 126, No. 1, pp. 131-141, 2004.

[41] Ewins, D. J., "The Effects of Detuning Upon the Forced Vibrations of Bladed Disks," Journal of Sound and Vibration, Vol. 9, pp. 65-79, 1969.

[42] Whitehead, D. S., "Effect of Mistuning on the Vibration of Turbomachines Blades Induced by Wakes," J. Mech. Eng. Sci., Vol. 8, pp. 15-21, 1966.

[43] Castanier, M.P., and Pierre, C., 1998, “Investigation of the Combined Effects of Intentional and Random Mistuning on the Forced Response of Bladed Disks,” AIAA paper, No. AIAA-98-37200.

[44] Castanier, M.P., and Pierre, C., 2002, “Using Intentional Mistuning in the Design of Turbomachinery Rotors,” AIAA Journal, Vol. 40, No. 10, pp. 2077-2086.

[45] Kenyon, J.A., and Griffin, J.H., “Intentional Harmonic Mistuning for Robust Forced Response of Bladed Disks,” 5th National TurbineEngine High Cycle Fatigue (HCF) Conference, Chandler, AZ, Mar.7–9, 2000.

[46] Choi, B.-K., Lentz, J., Rivas-Guerra, A.J., Mignolet, M.P., 2003, “Optimization of Intentional Mistuning Patterns for the Reduction of the Forced Response Effects of Unintentional Mistuning,” Journal of Engineering for Gas Turbines and Power, Vol. 125, No. 1, pp. 131-140

[47] Mbaye, M., Soize, C., and Ousty,J.-P., 2010, "A Reduced-Order Model of Detuned Cyclic Dynamical Systems With Geometric Modifications Using a Basis of Cyclic Modes," Journal of Engineering for Gas Turbines and Power-Transactions of the ASME Volume: 132 Issue: 11

[48] Götting, F, Sextro, W.,Panning, L, and Popp, K., “Systematic Mistuning of Bladed Disk Assemblies With Friction Contacts,” Proceedings of ASME Turbo Expo 2004, Jun. 14-17, 2004, Vienna, Austria, GT2004-53310.

APPENDIX A

CONVERGENCE ANALYSIS OF NUMBER OF MONTE CARLO SIMULATIONS

The effects of random mistuning were considered in this study by carrying out Monte Carlo simulations to simulate statistics of the response of the bladed disk. As a general rule, 10000 Monte Carlo simulations were chosen for the single-degree-of-freedom system, and 1000 Monte Carlo simulations were chosen for the blisk reduced order model to be a reasonable number of simulations to accurately represent the statistical parameter used to quantify the response of the system, i.e. the 95th percentile of the maximum blade response amplitude.

The need for computationally quick and efficient algorithms brings up the question of whether it is possible to accurately quantify this 95th percentile with a smaller number of Monte Carlo simulations. In addition, the effect of other system parameters such as the intentional mistuning pattern or the damper locations may have an effect (positive or negative) on the number of Monte Carlo simulations necessary for a quantitative analysis. In order to study this, the 12 blade blisk model of [11] was chosen and an analysis of the convergence of the amplification factor was carried out. The ensemble of all intentional mistuning patterns was considered and 10000 Monte Carlo simulations were carried out at each intentional mistuning pattern in the presence of random mistuning. From these results, the average and standard deviation of the number of simulations required for convergence of the amplification factor to within $\pm 1\%$ of the value of the 95^{th} percentile at 10000 simulations was then evaluated. Figure 60 and Figure 61 show scatter plots of the values of the averages and standard deviations as a function of the amplification factor for engine orders of excitation 1 and 2. This convergence analysis was repeated for engine order 1, for a few cases with

dampers present on the blisk in addition to the intentional and random mistuning, and these points are plotted as the black crosses in Figure 60.

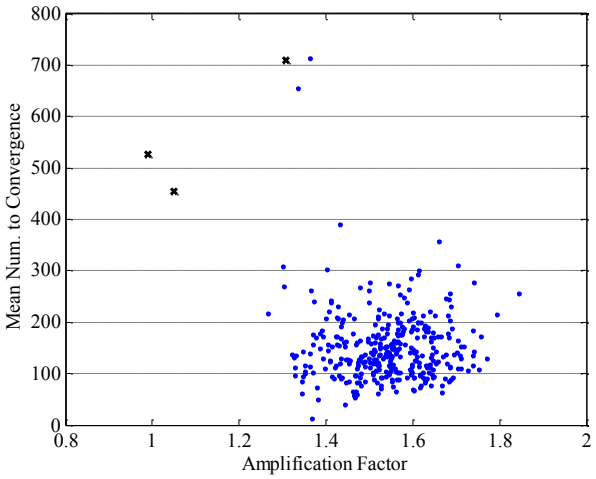

(a)

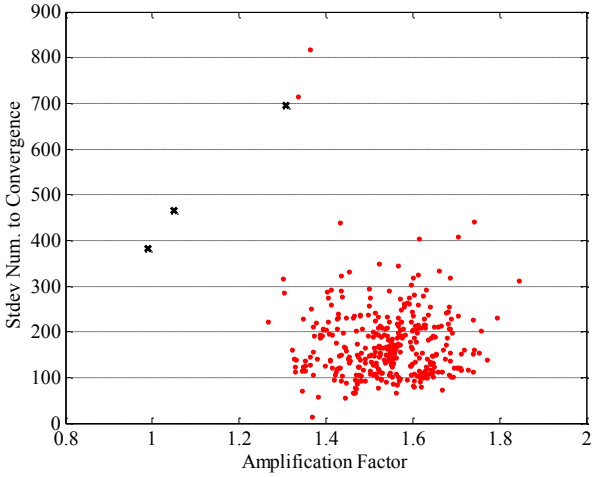

(b)

Figure 60. Scatter plots for (a) mean number of simulations to convergence and (b) standard deviation of number of simulations to convergence vs. amplification factor. Blisk model, engine order 1.

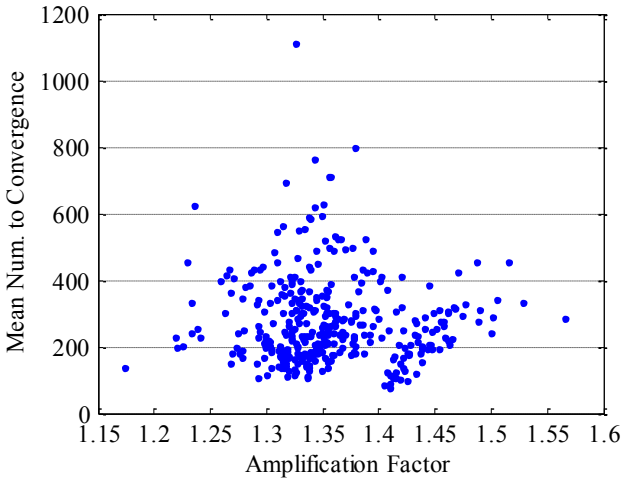

(a)

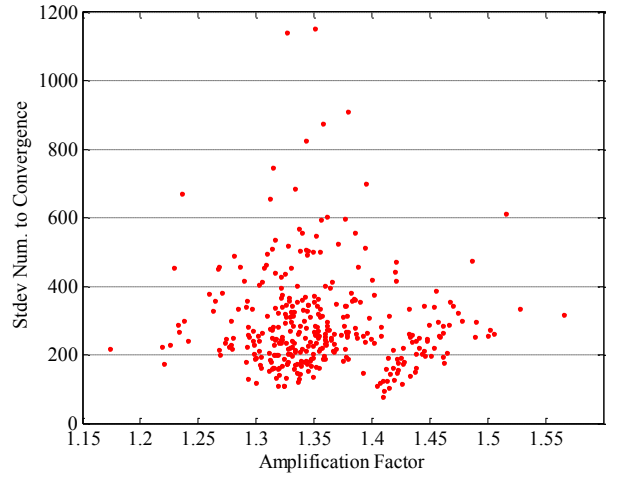

(b)

Figure 61. Scatter plots for (a) mean number of simulations to convergence and (b) standard deviation of number of simulations to convergence vs. amplification factor. Blisk model, engine order 2.

There seems to be no clear trend in the data of either the averages or standard deviations of the number of simulations required for convergence. However, it can be noted that the average number of simulations as well as the respective standard deviations are usually well below the value of 1000 simulations that was used for the various cases investigated in this work, making the choice of 1000 simulations a reasonable one in this application. Further, there

are differences observed between the two engine order cases which shows that the resonance condition at which the evaluations are carried out can have a significant effect on the number of simulations required to capture the 95^{th} percentile well. The addition of dampers to the optimization also seems to show a need for an increased number of simulations compared to the addition of just intentional mistuning, while still keeping below the 1000 simulations that were used in the simulations in this work.